A Design Approach for Compressed Air Energy Storage in Salt Caverns

by

Arjun Tharumalingam

A thesis

presented to the University of Waterloo

in fulfilment of the

thesis requirement for the degree of

Master of Applied Science

in

Civil Engineering

Waterloo, Ontario, Canada, 2019

Author’s Declaration

I hereby declare that I am the sole author of this thesis. This is a true copy of the thesis, including any required final revisions, as accepted by my examiners.

I understand that my thesis will be electronically available to the public.

Abstract

This thesis develops a first order design approach for compressed air energy storage. The objectives of this thesis are to inform geomechanical design with specific energy delivery needs and mechanical constraints. Often aspects of CAES design can be divorced from each other, this thesis attempts to provide a design framework that better integrates the disciplines associated with energy storage design. The geomechanical design will be based on CAES in salt caverns, as they are the best medium, and can be dissolution mined to adapted to specific design needs.

The first chapter offers the motivation and necessary background on CAES. Introducing the CAES configurations and discussing existing facilities. The second chapter discusses the methodology behind volume calculations and the state-space model used to characterize the loads the cavern experiences. The third chapter provides an overview of salt caverns; describing the mineralogy of rock salt and its behaviour. The operational failure criteria are discussed, which govern the geomechanical feasibility of the cavern. Three possible cavern shapes are established, describing the 2-D approximations and how they are created. The fourth chapter discusses the numerical modelling methodology with which caverns will be assessed for stability. The chapter details the first order assumptions made to simplify modelling. The fifth chapter describes the design algorithm developed, which serves as the basis for first order assessment. In the sixth chapter, the design algorithm is applied in two case studies.

The main purpose of this study was to synthesize design components of a facility into a first order algorithm. This design algorithm can be applied to any site and is simplified to accommodate a range of energy storage requirements. The initial stage of design entails an understanding of salt extent and characteristics such as depth and thickness. With a geographic constraint, one may determine the energy needed, as far as delivery requirements. The site's energy needs will be a design constraint, and appropriate mechanical equipment can be selected which will yield the characteristics of necessary volume, pressure limitations, and discharge times. An energy consumption and production profile can be produced. From here one may assess the cavern's stability to determine a factor of safety. Upon several iterations to fine tune the shape and operability of the cavern, one may proceed into a cost benefit analysis and more rigorous technical design.

To demonstrate the design algorithm, two energy storage applications were developed at the same site location. One application was a small-scale energy storage case, and the other was for a much larger grid scale case. The small-scale case could be achieved with a single cavern of 6000 m^3, the cavern would have operating pressures between 5 and 10 MPa. It could provide 30 MWh of energy storage. The cavern was cylindrical, and dimensions made for geomechanically sound design. The other cavern was for 1160 MWh application, the mechanical equipment selected required 270,000 m^3 of storage. The operating pressures of the cavern were 4.6 and 7.2 MPa. A cylindrical cavern would not have enough salt thickness, to achieve the necessary volume, an ellipsoid was modelled alternatively. It was determined that the ellipsoid would not provide suitable stability. It is recommended to develop four cylindrical caverns instead.

Acknowledgements

The author would like to express gratitude to Dr. Maurice Dusseault for patient guidance, and useful critique of the research. Special thanks to Mr. Roman Bilak for industry expertise and insight throughout.

The author would like to acknowledge the help of Siddharth Kakodkar of the CAES research group at the University of Waterloo for assistance in understanding turbomachinery. The author would also like to thank Fraser Lord, Jai Duhan, Wayne Park, and Li Li, for their assistance in geomechanics.

Finally, the author would like to acknowledge the support of the Natural Sciences and Engineering Research Council of Canada (NSERC), which invests annually over $1 billion in people, discovery and innovation. The author would also like to acknowledge the support of Ontario Centres of Excellence (OCE), which invests in innovation and entrepreneurship on behalf of the Province of Ontario.

Nous reconnaissons l’appui des Centres d’excellence de l’Ontario (CEO), qui investissent dans l’innovation et l’entrepreneuriat pour la Province de l’Ontario.
We acknowledge the support of Ontario Centres of Excellence (OCE), which invests in innovation and entrepreneurship on behalf of the Province of Ontario.

Cette recherche a été financée par le Conseil de recherches en sciences naturelles et en génie du Canada (CRSNG), qui investit chaque année plus d’un milliard de dollars pour soutenir les gens, la découverte et l’innovation.
We acknowledge the support of the Natural Sciences and Engineering Research Council of Canada (NSERC), which invests annually over $1 billion in people, discovery and innovation.

Dedication

To my fiancée,

For her endless love and support

Table of Contents

List of Figures

1.0 Introduction

This chapter introduces the need for Compressed Air Energy Storage (CAES) and the solutions it can offer to the energy market. This chapter will also cover the basic concepts of compressed air energy storage. The two major configurations of CAES, adiabatic and diabatic, will be discussed. The chapter will also discuss existing CAES facilities and the services they offer.

1.1 Motivation

Renewable energy is recognized as the future of energy production in the global effort to reduce greenhouse gas emissions. According to the BP Energy Outlook, renewable energy is the fasting growing source of energy, contributing half of the growth in global energy supply. Renewables are poised to become the largest source of power by 2040 (BP, 2019). In a national context, according to Natural Resources Canada, renewable energy (including hydro) accounts for 18% of Canada's total primary energy supply. Ontario currently has the highest capacity of wind power and is home to the largest solar farms in Canada. Ontario's total wind and solar generating capacity is expected to meet 23% of electrical power needs by 2025(National Energy Board, 2016).

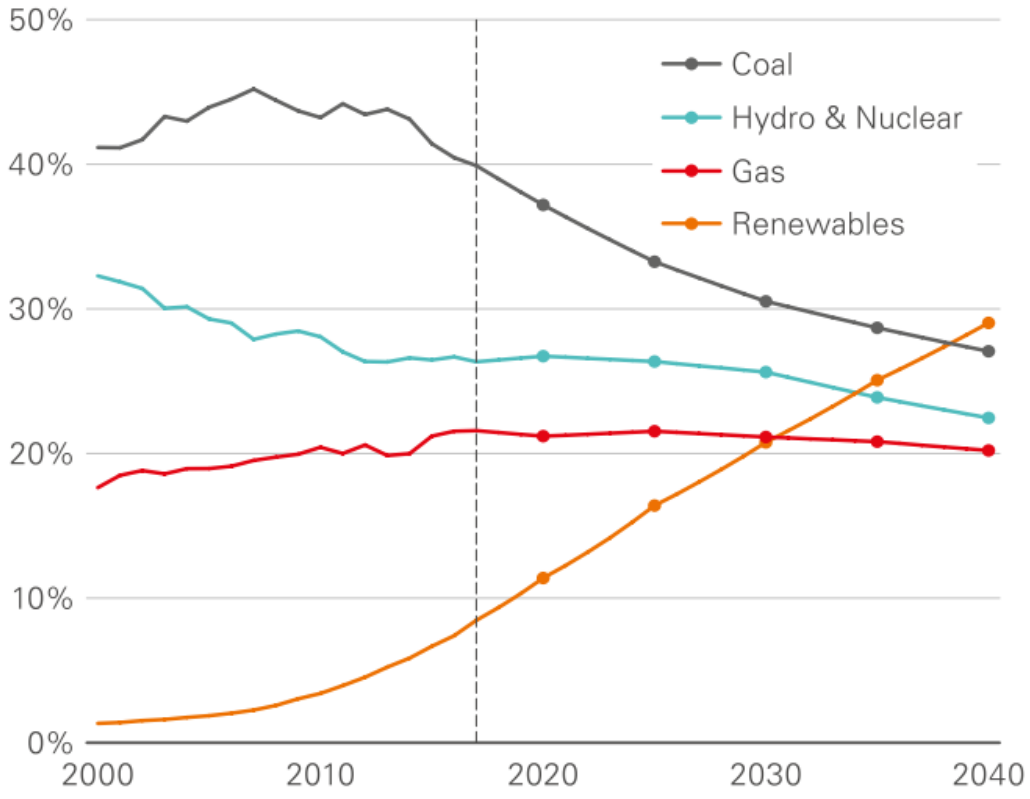

Figure 1.1 Global Energy Supply Projections (BP Energy Outlook, 2019)

Renewables are not without their drawbacks. It is crucial that renewable sources are paired with energy storage, as they are often subject to intermittency and variability. Clean energy sources such as wind and solar are dependent on fluctuating conditions, meaning that alone they are not effective in providing energy to meet grid demand. These renewable energy sources require

"balancing" and "smoothing" to provide reliable and affordable energy. With energy storage one may smooth out variations and intermittency of renewable energy sources, allowing more intelligent energy management decisions.

Batteries of various types and sizes are considered one of the most suitable approaches to energy storage. Batteries have a high efficiency and high energy density than CAES. Environmental impacts of large-scale batteries are not negligible, however. Environmental liabilities exist for batteries throughout their design life and decommissioning: mining, manufacturing, recycling and waste management all present a liability to the environment. Batteries are subject to a shorter shelf life than other energy storage systems, lithium ion batteries for example have a life span of seven years. Batteries are also four to five times more expensive than CAES per kilowatt hour (Deghani-Sanij *et al.*, 2019).

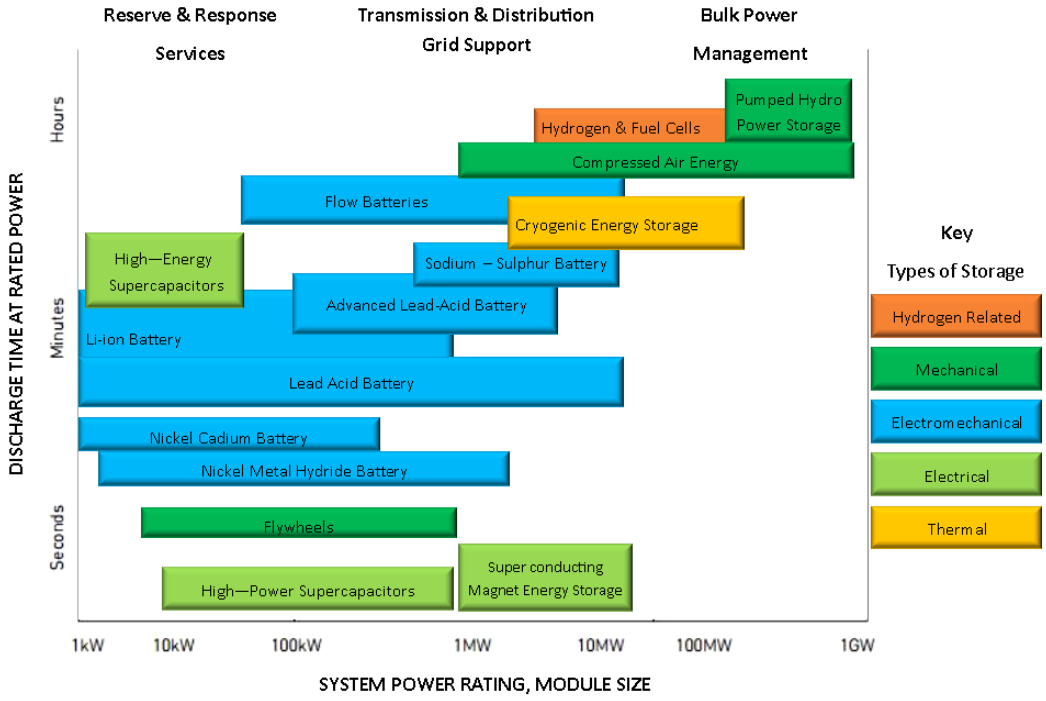

Figure 1.2 Power to Discharge Time of Energy Storage Technologies (After University of Birmingham Energy Storage Report)

Several services may be provided using CAES system. CAES can be used to smooth inputs of variable power sources to improve the power quality so that it can be integrated into the grid at a large scale. CAES has the potential to do peak shaving for base load optimization, meaning that peak demand can be met with power provided from storage. CAES may even be used to provide storage for microgrids, storing renewable energy locally.

1.2 Background on Compressed Air Energy Storage

CAES is a mechanical form of energy storage, where electricity is converted into the mechanical compression of air. When it is desirable, compressed air is then converted back into electricity with the use of turbomachinery. CAES is traditionally thought of as a large scale (>10 MW) storage option. It is a mature technology, with a design life of 30 years, large power capacity, low capital and operating cost per unit of energy (Aneke & Wang, 2016).

Table 1.1 Comparison of Energy Storage Technologies (After Das & Mccalley, 2012)

	NaS Batteries	**Lead Acid Batteries**	**Flywheels**	**Fuel Cells**	**Thermal Storage**	**SMES**	**Supercapacitors**	**Pumped Hydro**	**CAES**
Power Density	Good	Good	Very Good	Very Good	Excellent	Excellent	Very Good	Very Good	Very Good
Energy Density	Excellent	Very Good	Fair	Very Good	Excellent	Fair	Good	Very Good	Very Good
Life Time	15 years	3-12 years	20 years	<20 years	20 years	>20 years	8-10 years	30 years	30 years
Recharge Time	Very good	Good	Excellent	Fair	Very Good				Fair
Dynamic Response	ms	ms	ms	1s	mins	ms	<min	< 3 mins	<10 mins
Maintenance Cost	Moderate	High	Moderate	Low	Low	Low	High	High	Low
Environmental	Benign	Toxic	Benign	Benign	Benign	Adverse Health Impact	Benign	Adverse effects	Benign
Cost/kW	$1800	$120	$100-300	$4000	$600	$975	$120	$1000	$400
Round Trip Efficiency %	89-92	75	85-90	59	Depends on storage medium	90-95	95	70-85	50-70+

A CAES system is comprised of a compressor, turbine/expander – generator set, an air vessel and gas generator (in some cases a thermal storage system). Electricity is consumed by the air compressor when there is a need for energy storage. The air compressor converts electrical power into compressed air, storing energy mechanically. The compressed air will flow from the air compressor into an air vessel where it can be safely stored. The compressed air may be stored for minutes, hours or days depending on the energy storage needs. When it is time to produce power, the flow of pressured air passes through a turbine-generator set where the air pressure will drive turbomachinery and produce electricity.

There are several options for the storage vessel. Selection of the storage vessel is dependent on economic and geological conditions; its selection is often determined by the capacity of power needed as well.

For large scale, bulk power management, one would expect a vessel with a large volume. Salt caverns are the best large-scale option. However, sites are largely constrained by salt strata availability. Porous media may also be used, this would include reef structures and other traps with a cap rock. Underground hard rock mines may also be feasible if they are safely sealed so as not to allow the escape of air.

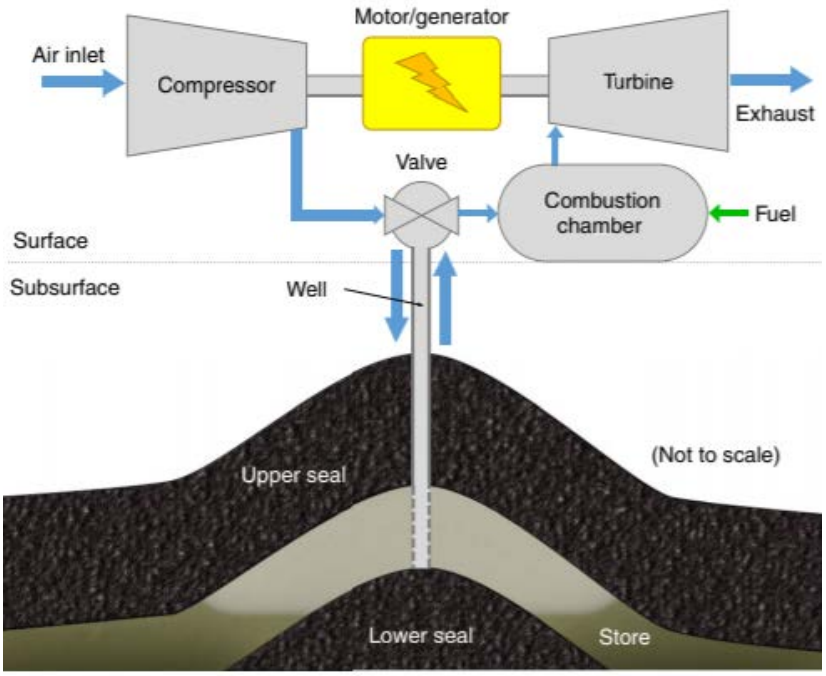

Figure 1.3 Porous Media Compressed Air Energy Storage (Mouli-castillo et al., 2019)

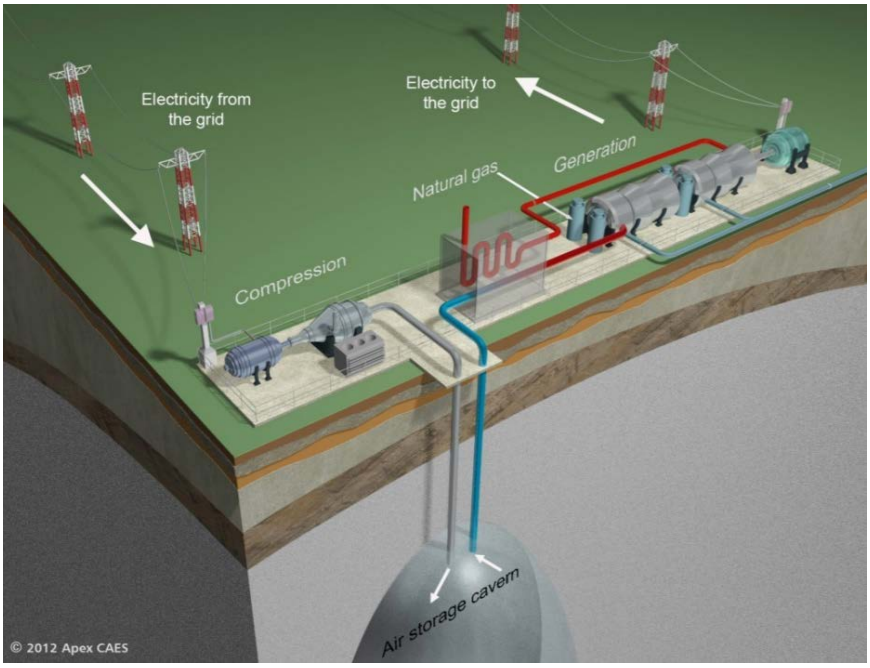

Figure 1.4 CAES in underground caverns (Image from: http://www.apexcaes.com/caes accessed 20/05/19)

For smaller scale energy storage. One may simply use smaller salt caverns, or porous media. If geological conditions are unfavourable it is possible to use steel cased boreholes. Surface vessels where air is stored in a metal tank are also an option.

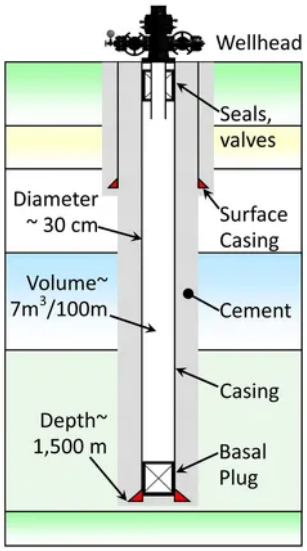

Figure 1.5 Cased Wellbore Compressed Air Storage (Image from: Cleantechgeo.com accessed 20/05/19)

1.3 CAES Configurations

Compressed air energy storage can be classified into two configurations, diabatic and adiabatic, based on how heat is managed. When energy is first being stored, the air compressor will take ambient air and pressurize it. The pressurized air will have a much higher temperature as a result. The storage vessel is limited in how much temperature and pressure it can safely store, meaning that air from the compressor should be cooled prior to entering the storage vessel. When it is time to regenerate energy from storage, the air is usually too cold for the turbine, as a sufficiently high inflow temperature at the turbine is critical for machine operation. Heat must be reintroduced prior to entering the turbine, and even in the intermediary zone of the turbine sets (Succar & Williams, 2008). As the turbines produce electricity the air temperature and pressure can be lowered dramatically leading to icing of the machinery and inefficiency. How this heat of compression and expansion is managed is where the classification between diabatic and adiabatic CAES occurs.

1.3.1 Diabatic CAES

Diabatic CAES is the most mature configuration to date. A diabatic CAES system charges the vessel by pressurizing ambient air with a single compressor or multiple compressors in series. The air is cooled using intercoolers prior to entering the storage vessel and in between compressors if needed. The heat extracted from compression is not re-used in the process and is thus considered waste heat. The heat loss enables safe storage of the compressed air inside of the vessel. When it is time to regenerate energy, the air is discharged from storage into a combustion chamber with the help of a fuel source such as natural gas. The air is heated using a certain amount of fuel and can now be used to drive a turbine that is connected to a generator. The turbines may also be in series, where the outlet temperature after the first turbine may be too low and will require heating once more. Diabatic CAES has a low round trip efficiency of 54% (Succar & Williams, 2008), but offers a simple solution to large scale energy storage.

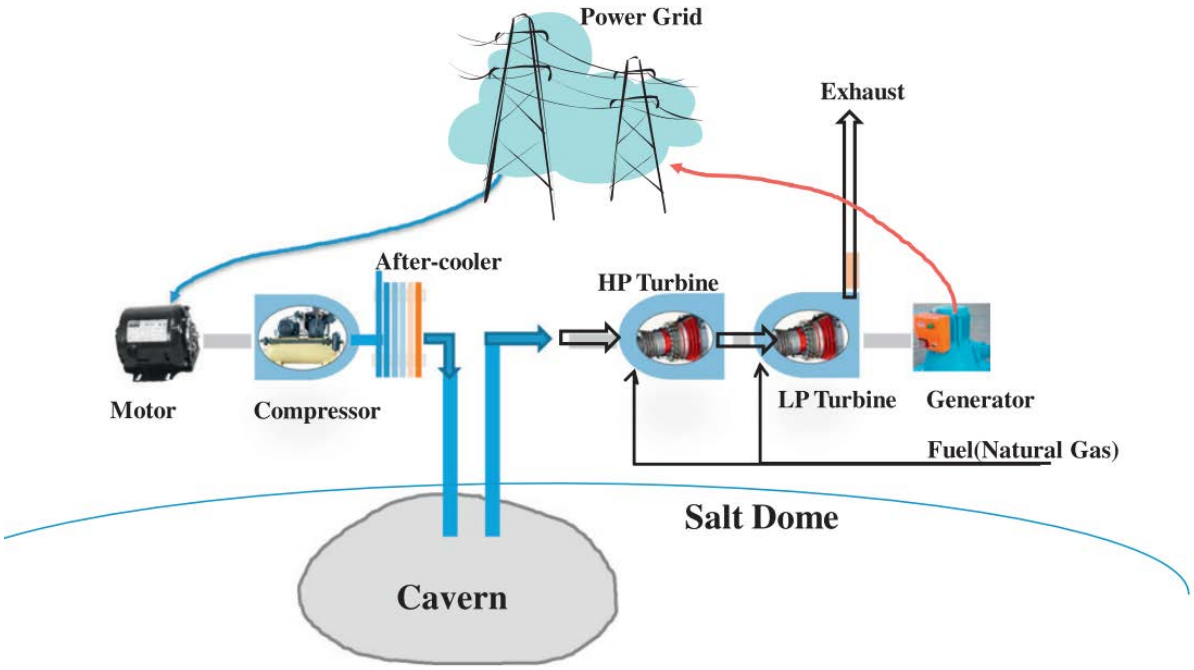

Figure 1.6 Diabatic CAES Components(Das & Mccalley, 2012)

1.3.2 Adiabatic CAES

An adiabatic system is very similar to a diabatic system. In an adiabatic system, the heat from compression is stored for later use. The heat stored is used to reheat air before expansion in the turbine and used again in between turbines, meaning that there is little to no need for fuel combustion. If no fuel is consumed the round-trip efficiency of the system is much higher, at approximately 70% (Das & Mccalley, 2012; Succar & Williams, 2008). There is also the opportunity to introduce waste heat from elsewhere, for instance a nearby industrial plant. The heat can be used in the power production stage and there would be no need for storage.

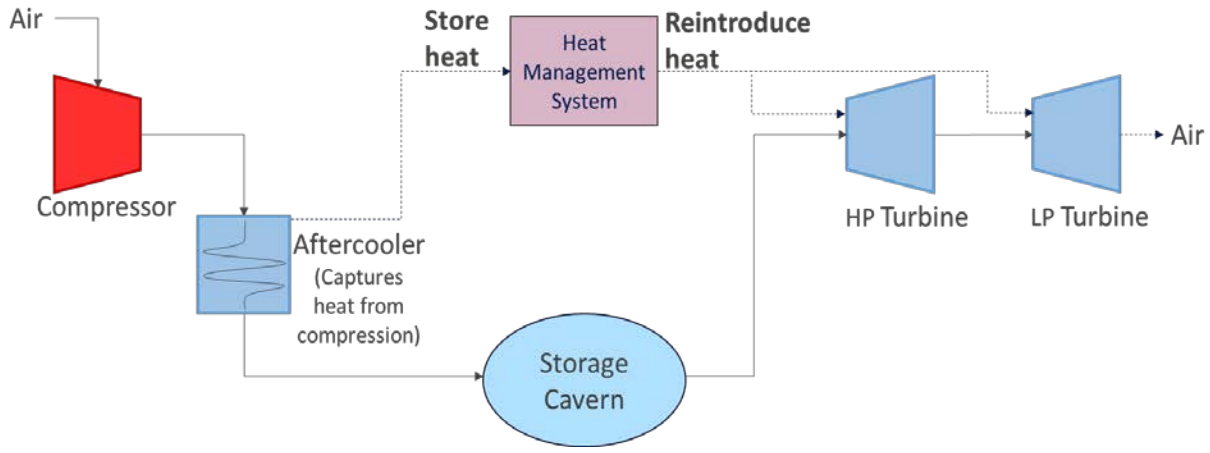

Figure 1.7 Adiabatic CAES Components

1.4 Existing CAES Facilities

The Huntorf plant in Germany, belonging to E.N Kraftwerke, is a diabatic CAES plant which has been in operation since 1978. It is the world's first CAES plant and initially had a generating capacity of 290 MW for 3 hours. The plant makes use of two solution mined salt caverns created in a local diapir. The expansion train was retrofitted in 2008, allowing the power capacity to increase from 290 MW to 321 MW (Budt, Wolf, Span, & Yan, 2016). After 28 years of operation the observed volume loss of the cavern was minimal. The two salt caverns which serve as the storage vessel have volumes of 140,000 m^3 and 170,000 m^3, for a total volume of 310,000 m^3 (Crotogino *et al.*, 2001). The caverns experienced pressures from 46 to 72 bar (Raju & Kumar Khaitan, 2012). The round-trip efficiency of the facility was 42%.

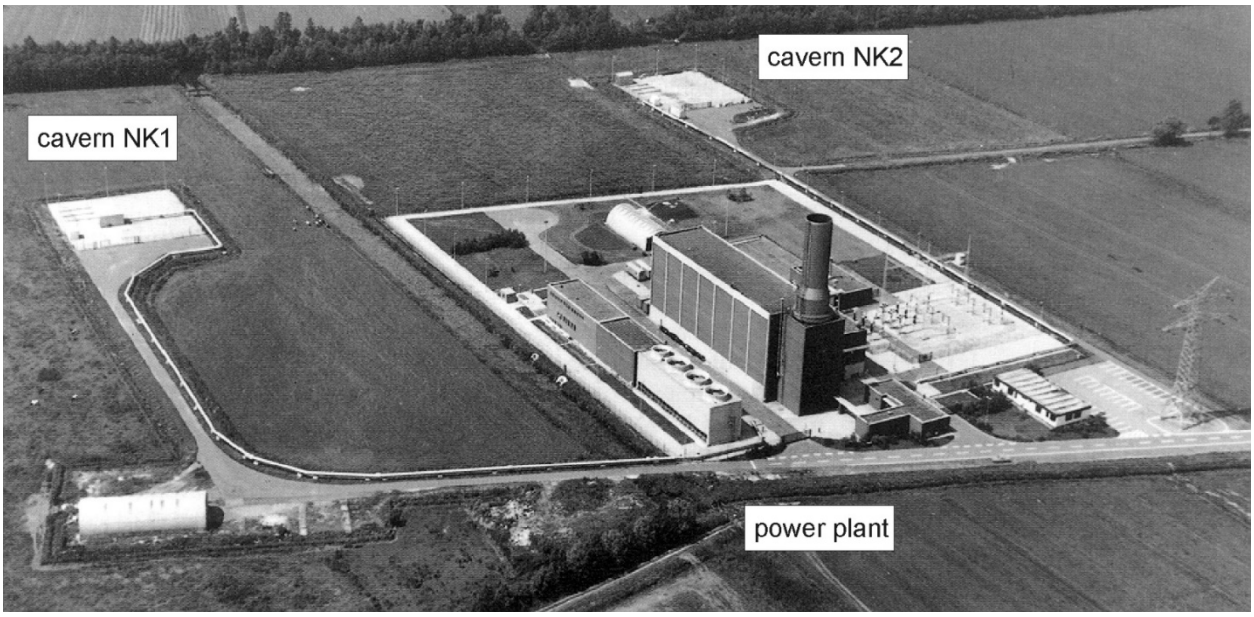

Figure 1.8 Huntorf CAES plant (Crotogino et al., 2001)

The McIntosh plant, operated by the Alabama Electric corporation, in Alabama USA has been in service since 1991. The McIntosh plant makes use of a single salt cavern, with a volume of 538,000 m^3. McIntosh has a generating capacity of 110 MW for 26 hours. The McIntosh cavern experiences pressures between 45 and 76 bar (PowerSouth Energy Cooperative, 2014). The plant has multi-stage compression with no thermal energy storage. The efficiency is much higher than Huntorf, with a round trip efficiency of 54%.

Small scale CAES projects have been developed in Ontario. Hydrostor (https://www.hydrostor.ca) has developed a 0.7 MW adiabatic CAES project in Toronto, deploying the use of an underwater bladder serving as the storage vessel. NRStor (http://nrstor.com) in collaboration with Hydrostor is developing a 1.75 MW CAES project in Goderich Ontario. This project refurbishes an existing salt cavern that was developed for salt production.

1.5 Thesis Objectives

The objective of this thesis is to develop a first order design algorithm for CAES. The algorithm will inform geomechanical design with specific energy delivery needs, and mechanical constraints. Often aspects of CAES design can be divorced from each other, this thesis attempts to provide a design framework that better integrates the disciplines associated with energy storage design. The geomechanical design will be based on CAES in salt caverns, as they are the best medium, and can be dissolution mined to adapt to specific design needs.

The first chapter offers the motivation and necessary background around CAES. The second chapter relates mechanical equipment operating parameters to energy consumption and cavern loading conditions, allowing for informed design from a geomechanics perspective. The third chapter covers the baseline geomechanical considerations for a storage cavern, providing initial cavern geometries that may be considered in first order design. The fourth chapter discusses the numerical modelling methodology in which caverns will be assessed for stability. The fifth chapter establishes the design algorithm which provides a framework for first order design. The sixth chapter exams case studies in southern Ontario, to demonstrate the effectiveness of the algorithm.

2.0 Volume Calculations

This chapter establishes the methodology behind developing the state-space representation of a CAES system. It is important to be able to relate energy supply and demand parameters to storage conditions for first order design. This chapter will describe the distinction made between adiabatic, and diabatic CAES. It will also describe the state-space model sections by detailing power consumption, power production, and volume required for energy storage. The relevant formulae will be presented, along with a range of parameter values that are relevant to CAES.

2.1 Diabatic and Adiabatic Considerations

CAES systems are classified into two configurations, adiabatic and diabatic. The distinction between the two is determined by how heat is managed. Adiabatic CAES systems preserve heat of compression, by storing it and later reintroducing it as heat for the air stream. Diabatic CAES is dependent on an external heat source to heat the air stream in the expansion phase. Adiabatic and diabatic systems differ significantly in round trip efficiency, 70% and 55% respectively. Both systems will require different equipment based on the need for external heat, or heat storage. For diabatic CAES it will be assumed that a fuel fired generator will be used to regenerate energy from storage; however, other external heat sources can be used such as industrial waste heat. It will be assumed that diabatic CAES will require a supply of natural gas, in the form of a constant mass flow rate for energy generation.

2.2 Energy Consumption

The system will draw energy ideally when it is abundant and at a low price. The system 'charges' when an air compressor, operating on electricity from the grid, compresses ambient air to the desired storage pressure (the maximum operating pressure of the storage vessel). Air exits the machine at the storage pressure, at a much higher temperature and density than at the inlet. The pressurized air will have to be cooled in order to store it safely inside of the vessel, this is done with the use of an after-cooler. Typically, compressors are purchased based on their mass flow rate and outlet pressure, however, one may determine mass flow rate using equation (2.1) (Das & Mccalley, 2012). This equation relates the consumed power of the machine to the outlet pressure. The equation is useful for first order iterations of how much energy can be stored and the time to reach maximum pressure inside of the cavern.

$$\dot{m}_{a\_in} = \frac{P_c}{c_{p1} T_{in} \left[\left(\frac{P_2}{P_1} \right)^{\frac{\gamma-1}{\gamma}} - 1 \right]} \qquad (2.1)$$

Here, $\dot{m}_{a\_in}$ is the mass flow rate of the compressor (kg/s), P_c is the input power of the compressor (kW), c_{p1} is the specific heat at constant pressure, P_2 and P_1 are outlet and inlet

pressure respectively in kilopascals. T_{in} is the temperature at the inlet of the machine (K), and γ is the ratio of specific heat at constant pressure to specific heat at constant volume.

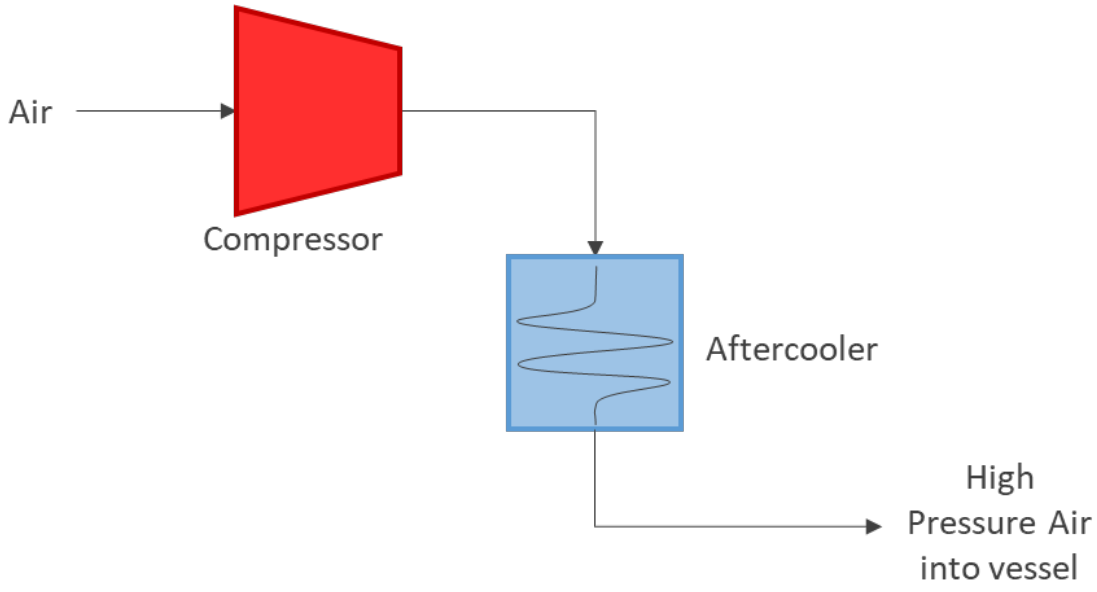

Figure 2.1 Conceptual Drawing of Compressor Operation

2.3 Energy Discharge

The system will produce energy ideally when it is in higher demand. The system 'discharges' when a series of turbines/expanders are driven by the air pressure flowing out of the storage vessel. The air enters the machines at a high inlet pressure, the expansion causes the air to flow at a lower pressure and temperature at the outlet of the machine. It is beneficial to allow expansion to occur in stages as the reduction in temperature could be dramatic. If the temperature is too low, the machinery could be subject to icing damage. It is therefore prudent to utilize two or more stages of air expansion to allow for heat recovery in between the machines as depicted in figure 2.2. The two most mature CAES projects in operation, Huntorf & McIntosh, have used two turbines in series to produce energy (Succar & Williams, 2008). The formulae described will assume two stages of expansion. The equation relates produced power generated to inlet and outlet conditions of both machines(Das & Mccalley, 2012).

$$\dot{m}_{A\_out} = \frac{P_G}{\eta_M \eta_G c_{p2} T_2 \left(1+\frac{\dot{m}_{A\_out}}{\dot{m}_{Fuel}}\right)\left(\frac{c_{p1}T_1}{c_{p2}T_2}\left[1-\left(\frac{P_2}{P_1}\right)^{\frac{k_1-1}{k_1}}\right]+1-\left(\frac{P_b}{P_2}\right)^{\frac{k_1-1}{k_1}}\right)} \quad (2.2)$$

Here, $\dot{m}_{A_o ut}$ is the mass flowrate from the storage vessel (kg/s), $\dot{m}_{Fuel}$ is the mass flow rate of fuel into the turbine set if needed, P_G is the power generated by the turbines (kW). P_1, P_2 and P_b are the pressures at the high-pressure turbine, the low-pressure turbine, and atmospheric pressure (kPa). $\eta_M$is the mechanical efficiency of the turbine, and η_G is the efficiency of the generator. k_1 is the ratio of c_{p1} and c_{v1}. T_2 is the temperature at the inlet of the low pressure turbine (k), T_1 is the temperature at the inlet of the high pressure turbine.

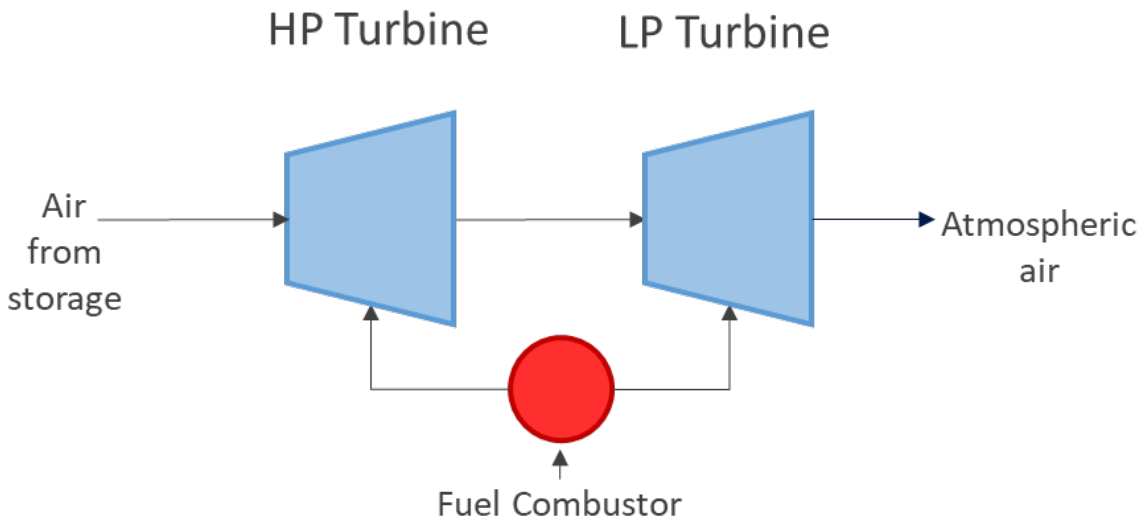

Figure 2.2 Conceptual Schematic of Expander Operation

2.4 Volumetric Assessment

This sub-section describes formulae for assessing the required volume for a CAES storage vessel. The volume is determined in part by the mechanical equipment at the time of energy regeneration. More specifically, volume is determined by the amount of energy required, and the flow parameters of the turbines. It is also dependent on the operation mode of the cavern.

The two modes of operation considered are variable turbine inlet pressure, and constant turbine inlet pressure. In both cases storage volume is fixed, and the pressure the storage vessel experiences will vary. Variable turbine pressure involves no throttling out of the storage vessel, allowing the pressure of air exiting to vary as it depletes itself. Fixed turbine pressure involves throttling as the air exits storage before entering the expander system, meaning that the cavern will deplete itself at a fixed rate.

The formulae presented are based on two stages of expansion. The volume for a constant turbine inlet pressure is given by equation (2.6), and the volume for a variable inlet pressure is given by equation (2.3) (Succar & Williams, 2008). These equations assume no heat loss during compression, expansion, and storage.

$$V_{s\_variable} = \frac{E_{GEN}}{\left[\frac{\alpha M_w p_{S2}}{RT_{S2}}\left\{(\beta+1)\left(1-\left(\frac{p_{S1}}{p_{S2}}\right)^{1/k_s}\right)-\left(\frac{p_1 p_b}{p_2 p_{S2}\varphi}\right)^{\frac{k_2-1}{k_2}}\frac{1}{k_s\left(\frac{1}{k_s}+\frac{1}{k_2}-1\right)}\left(1-\left(\frac{p_{S1}}{p_{S2}}\right)^{\frac{1}{k_s}+\frac{1}{k_2}-1}\right)\right\}\right]} \quad (2.3)$$

$V_{s\_variable}$ is the volume of storage in cubic meters, R is the universal gas constant (kJ/mol K), and M_w is the molecular weight of dry air (kg/mol). E_{GEN} is the desired energy (MWh). p_b, p_{S1}, p_{S2} are the atmospheric pressure, maximum cavern pressure, and minimum cavern pressure (kPa). T_{S2} is the temperature of the cavern at full pressure (K). k_s, $k_1$and k_2 are the ratio of specific heat at storage, at the high-pressure turbine and at the low-pressure turbine

respectively. φ is the assumed pipe friction loss. T_1 and T_2 are the average temperatures across the high-pressure turbine and low-pressure turbine (K).

$$\alpha = \eta_M \eta_G c_{p2} T_2 \left(1 + \frac{\dot{m}_F}{\dot{m}_A}\right) \quad (4)$$

$$\beta = \frac{c_{p1} T_1}{c_{p2} T_2}\left[1 - \left(\frac{p_2}{p_1}\right)^{\frac{k_1 - 1}{k_1}}\right] \quad (5)$$

$$V_{s\_constant} = \frac{E_{GEN}}{\left[\frac{\alpha M_W p_{S2}}{R T_{S2}}\left(\beta + 1 - \left(\frac{p_b}{p_2}\right)^{\frac{k_2 - 1}{k_2}}\right)\left(1 - \left[\frac{p_{S1}}{P_{S2}}\right]^{\frac{1}{k_S}}\right)\right]} \quad (6)$$

$V_{s\_constant}$ is the required storage volume assuming constant pressure at the outlet of the cavern.

With a way to calculate the volume required, one may geographically assess the potential for a CAES facility on the basis of salt availability. The volume determined does not need to be for a single cavern; multiple caverns could be created to achieve the necessary volume.

Given the operating parameters of Huntorf summarized in table 2.1, a contour of volume assessment was generated. Figure 2.3 shows the relationship between operating pressures of the cavern and the required volume of storage. The operating pressure is constrained also by the available salt, as the quality of the rock mass may determine the maximum pressure of the cavern. The ratio of the minimum cavern pressure and the maximum operating pressure plays a great role in the volume required for a certain amount of energy storage, as the ratio can compensate for volume.

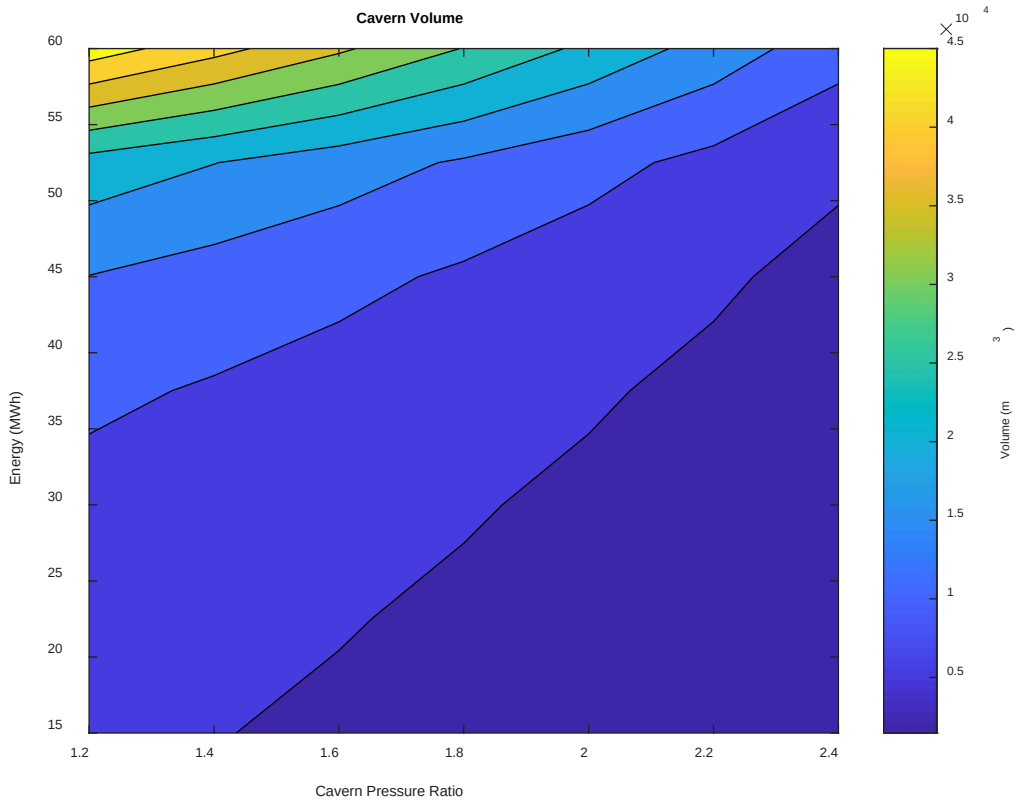

Figure 2.3 First Order Volumetric Assessment

A figure like this may be generated for a series of differing expander sets. This tool would be valuable in first order assessment of a potential CAES facility. Mechanical equipment is a more flexible design parameter than the presence of salt and its geomechanical integrity. It is therefore prudent to assess volume with a fixed machine and adjust the pressure ratio of the cavern accordingly.

Table 2.1 Huntorf Turbomachinery Parameters (Raju & Kumar Khaitan, 2012)

Gas Turbine Parameters		
Turbine Power	290	MW
Mass flow rate	417	kg/s
Inlet pressure HP turbine	42	bar
Inlet temperature HP turbine	550	Deg C
Inlet pressure LP turbine	11	bar
Inlet temperature LP turbine	825	Deg C
Compressor		
Mass flow rate	108	bg/s
Rated compressor power	60	MW
Temperature at exit of after cooler	50	Deg C
Pressure at exit of after cooler	46-72	bar

2.5 State-space Model

It is also useful to determine the operating conditions the cavern is subject to. There will be a certain energy requirement to meet in terms of power and duration of output, which will translate to the maximum pressure, volume and drawdown rate the cavern experiences. A first order model would be useful in assessing the cavern conditions at a given point of operation. The model could assess cavern conditions for a given time of power consumption and generation.

Assuming that negligible heat loss occurs in the cavern, pressure can be approximated using equation (2.7) (Das & Mccalley, 2012).

$$p = \frac{R}{V}\left(\int \dot{m}_{A\_in} T_{in} dt - \int \dot{m}_{A\_out} T_s dt\right) \quad (2.7)$$

The state space representation of the model, which relates power consumption pressure and mass, is captured in equations (2.8) and (2.9) (Das & Mccalley, 2012).

$$\begin{bmatrix} m_{A\_in}(t+1) \\ m_{A\_out}(t+1) \end{bmatrix} = \begin{bmatrix} 1 & 0 \\ 0 & 1 \end{bmatrix} \begin{bmatrix} m_{A\_in}(t) \\ m_{A\_out}(t) \end{bmatrix} + \begin{bmatrix} 1/K_C & 0 \\ 0 & 1/K_G \end{bmatrix} \begin{bmatrix} P_C(t) \\ P_G(t) \end{bmatrix} \quad (2.8)$$

$$\begin{bmatrix} m(t+1) \\ p(t+1) \end{bmatrix} = \begin{bmatrix} 1 & -1 \\ \left(\frac{RT_{in}}{V}\right) & -\left(\frac{RT_S}{V}\right) \end{bmatrix} \begin{bmatrix} m_{A\_in}(t) \\ m_{A\_out}(t) \end{bmatrix} \quad (2.9)$$

$$K_C = c_{p1} T_{in} \left[\left(\frac{P_2}{P_1}\right)^{\frac{\gamma-1}{\gamma}} - 1 \right] \quad (2.10)$$

$$K_G = \eta_M \eta_G c_{p2} T_2 \left(1 + \frac{\dot{m}_{A\_out}}{\dot{m}_{Fuel}}\right) \left(\frac{c_{p1} T_1}{c_{p2} T_2} \left[1 - \left(\frac{P_2}{P_1}\right)^{\frac{k_1-1}{k_1}} \right] + 1 - \left(\frac{P_b}{P_2}\right)^{\frac{k_1-1}{k_1}} \right) \quad (2.11)$$

Using the same parameters in table 1.1, the following results are generated using the state-space model. Illustrations of charging and discharging are in figure 2.4 and the corresponding cavern pressure is shown in figure 2.5. K_C & K_G are based on the mass inflow and outflow terms in equations 2.1 and 2.2 respectively.

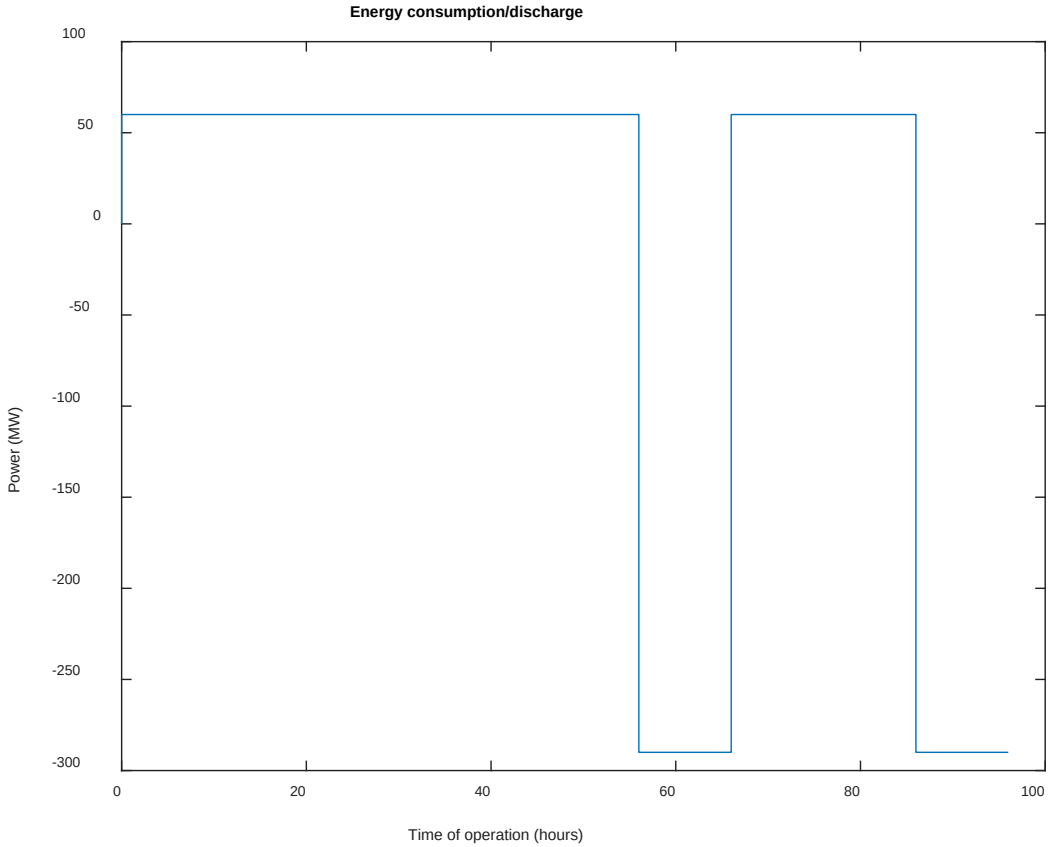

Figure 2.4 Sample Energy Consumption Based on Mechanical Equipment Selection

The assumed consumption of power is constant; the model captures constant power consumption and discharge. The compressor consumes 60 MW of power when pressurizing air to 72 bar. The cavern initially begins at atmosphere pressure, then is continuously pressurized until it reaches its maximum operating pressure of 72 bar. At this point the cavern discharges, and regenerates electricity. The cavern will discharge power until the cavern reaches its minimum operating pressure of 46 bar. The power production of the expander system is 290 MW when the inlet pressure is 46 bar.

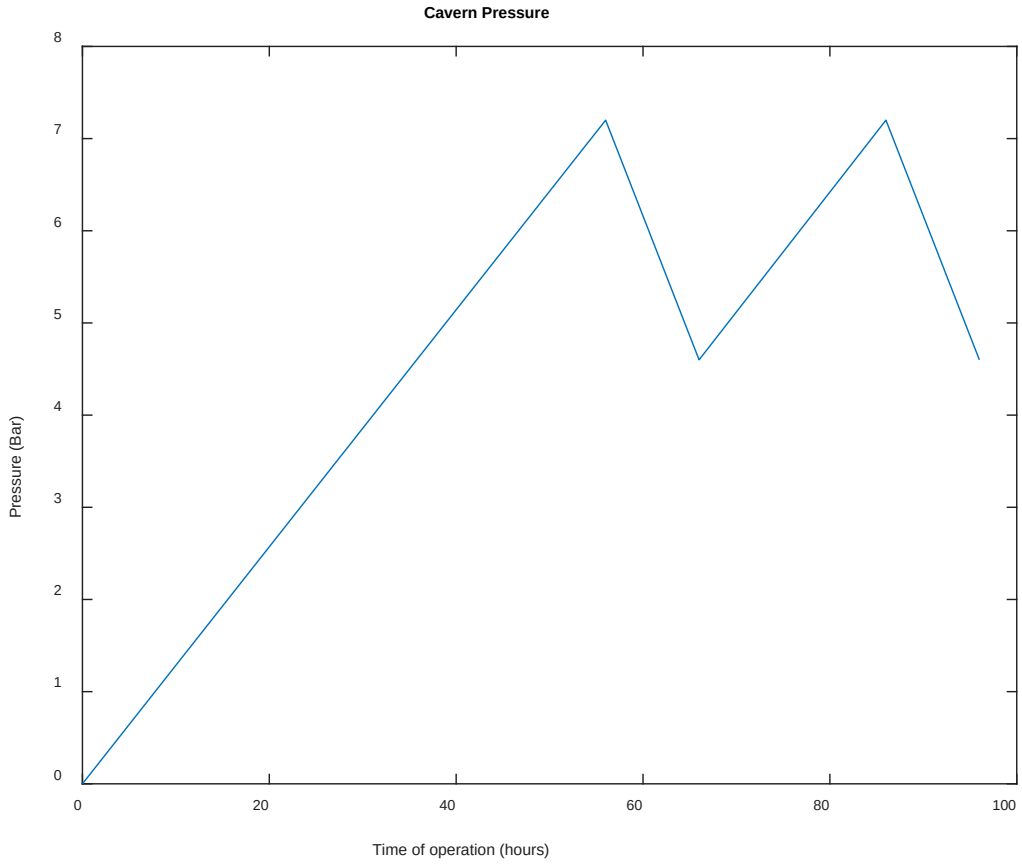

Figure 2.5 Sample Cavern Pressure Fluctuation

This simple state space model is useful for first order design. This model can capture fluctuating energy demand and turbomachinery specifications. The cavern pressure cycle can be approximated, and the model can also be used to approximate fluctuating temperature of the cavern air as well. These results allow for informed geomechanical design, where the cyclical loads can be input to attain a more accurate model, and where temperature changes can be estimated and used in rock mass behavior assessment.

3.0 Overview of Salt Caverns

Rock salt is an ideal medium for storage, as salt has advantageous properties. Rock salt has very low porosity and permeability, and salt strata can also be solution mined with ease. Salt caverns have been used for the storage of hydrocarbons since 1950 (Han *et al.*, 2006). They can also be used for the disposal of non-toxic industrial waste (Lux, 2009). This chapter will discuss rock salt in terms of mineralogy, deposition, and mechanical properties.

3.1 Background on Rock Salt

Salt deposits are formed by the evaporation of ocean waters. The most commonly found salt is halite, NaCl. Other salts might include calcium sulphates, gypsum and anhydrite, and many other halide minerals (Su, 1995). Halite is chemically stable and non-volatile, it is also highly soluble, facilitating the creation of salt caverns.

Salt can be found deposited in sedimentary beds, as diapirs, or as tectonically altered structures (salt anticlines or thrust-fault thickened sequences); each deposit type will have its own geomechanical considerations(Aubertin *et al.*, 1999). Salts are primarily deposited as laterally continuous beds as the result of evaporation of sea water in an enclosed basin. Diapirs are formed because of bedded salts experiencing different stress and temperature conditions over time. High subsurface temperatures and stresses cause salt to be driven upward due to its buoyancy(Hudec & Jackson, 2007). Bedded salts have the advantage of being laterally continuous, however diapiric structures are generally thicker and more homogeneous. Tectonic salts have experienced high tectonic activity, as the name implies. The structure of these salt deposits is complex and heterogeneous with varying thickness and folds in the deposit(Li & Urai, 2016). Tectonic salt deposits are more difficult to solution mine due to their complex structure.

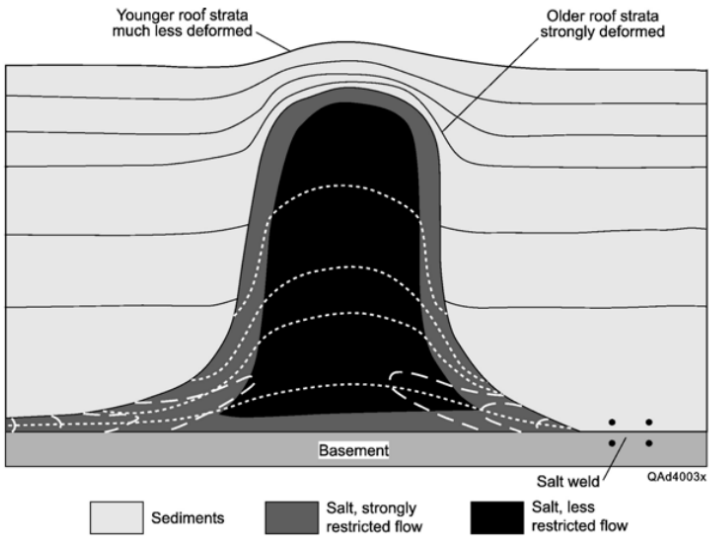

Figure 3.1 Salt Diapir Structure (Hudec & Jackson, 2007b)

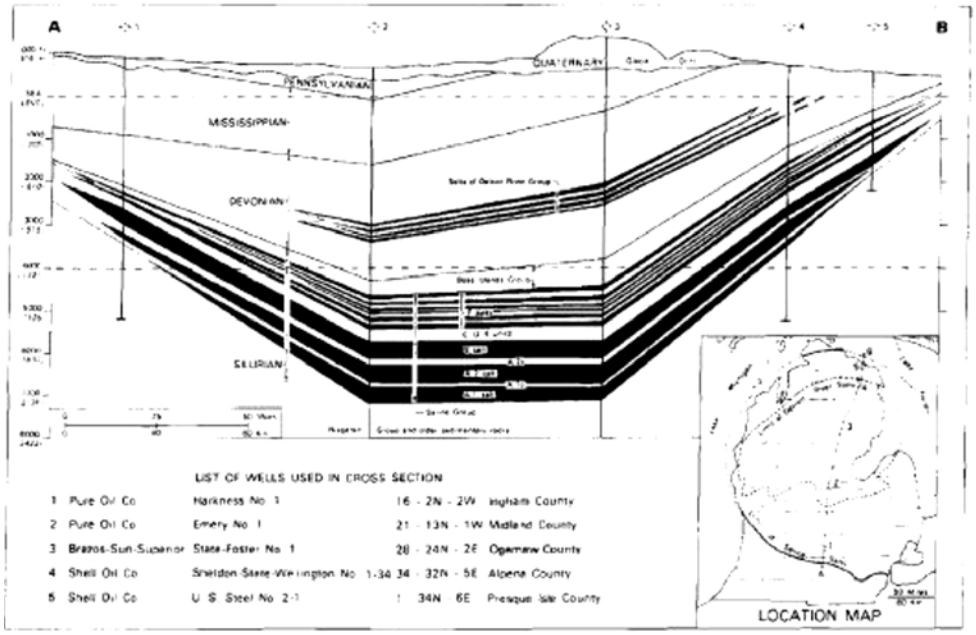

Figure 3.2 Bedded Salt Cross Section View of the Michigan Basin (Johnson & Gonzales 1978)

Rock salt must be well understood to allow proper design of caverns. Information on the strata must be gathered such as the depth, areal extent, thickness and stresses. Data collection is necessary in the form of core logging to assess geomechanical properties(Lux, 2009). This would include uniaxial compressive strength tests, triaxial compression tests, and creep tests at different stresses and temperatures. Gamma-ray geophysical logs have been used successfully to identify salt, as well as density logs and gravity methods from the surface(Su, 1995). These methods can help determine the areal extent of salt structured to guide drilling.

3.1.1 Behaviour of Rock Salt

When undergoing "instantaneous" stress changes, rock salt behaves elastically, meaning that it has recoverable deformation and can be described with Hooke's law. Hooke's law is stipulated, for isotropic materials, by the Young's modulus (E) and Poisson's ratio (ν). Under loading for a longer time period, salt will experience transient creep, steady-state creep and perhaps tertiary creep. It has self-healing capabilities because of its solubility and the presence of small amounts of interstitial moisture, which heals cracks that might develop in the rock mass, keeping it impermeable, which is ideal for storage.

There are several physical creep laws which attempt to describe the behaviour of salt. The one used to model salt behaviour in this thesis is the steady-state Norton creep law. It has very few parameters needed to model the rock's behaviour. Other behaviour models are more complex and may include transient creep expressions, such as the WIPP model and the Munson Dawson model. The Norton Creep Law is expressed as (Norton, 1929):

$$\dot{\varepsilon}_{ss} = A\left(\frac{\sigma_1 - \sigma_3}{\sigma_o}\right)^n e^{\left(\frac{-Q}{RT}\right)} \qquad (3.1)$$

where $\dot{\varepsilon}_{ss}$ is the steady-state strain, A is a material-dependent parameter, $\sigma_1 - \sigma_3$ is the deviatoric stress, , σ_o is the normalizing stress, n is the creep regime parameter, R is the universal gas constant, T is the temperature, and Q is the activation energy.

Salt caverns are subject to gradual closure as the material creeps. The volume closure rate is a key design parameter as a CAES cavern is expected to operate for more than thirty years. It is therefore necessary to operate the cavern such that minimal closure occurs. The volume loss rate of a cavern undergoing cyclical loading conditions is not possible to determine without site specific lab testing, however one may estimate the loss rate using a steady-state approximation(Shahmorad, Salarirad, & Molladavoudi, 2016).

For a spherical cavern the steady state closure rate is (Bérest *et al.*, 2001):

$$\frac{\dot{V}}{V} = -\frac{3}{2}\left[\frac{3}{2n}(P_\infty - P_i)\right]^n Ae^{\left(\frac{-Q}{RT}\right)} \qquad (3.2)$$

For a cylindrical cavern (Van Sambeek, 1990):

$$\frac{\dot{V}}{V} = -\sqrt{3}\left[\frac{\sqrt{3}}{n}(P_\infty - P_i)\right]^n Ae^{\left(\frac{-Q}{RT}\right)} \qquad (3.3)$$

Where P_∞ is the far field stress, and P_i is the internal cavern pressure.

3.1.2 General Demands

There are several design parameters to be considered when developing a salt cavern. One must create a cavern at the correct depth as the lithostatic stress and temperature are directly related to depth. The cavern geometry plays a key role, as cavern roof failure is a major issue that could impair operations. The minimum and maximum pressure inside the cavern will be determined by the cavern closure rate and rupture (hydraulic fracture) pressure. The operation pattern is also important in designing the cavern as a rapid withdrawal of air can cause tensile cracking(Brouard, 2012).

Prior to assessing the operability of caverns there are preliminary criteria that must be considered, the first being the dimensions of a salt cavern; a larger height to diameter ratio is desirable as it is more stable as demonstrated by Bruno and Dusseault (2002). The displacement in the roof of the cavern increases as the H:D ratio is lowered. It is therefore recommended that the ratio be no less than ½. Low cavern air pressure can cause failure as the internal cavern pressure supports the roof of the cavern. As cavern pressure lowers, the roof may experience tensile stress. The thickness and shape will play an important role in cavern operability, as the geometry and thickness will determine stability of the cavern. It is also recommended by Zheng *et al.* (2016) to have a roof thickness of ¼ the cavern diameter. These preliminary guidelines only serve the purpose of first order design. With strong and impermeable roof rock at a given site, the design could be much more flexible.

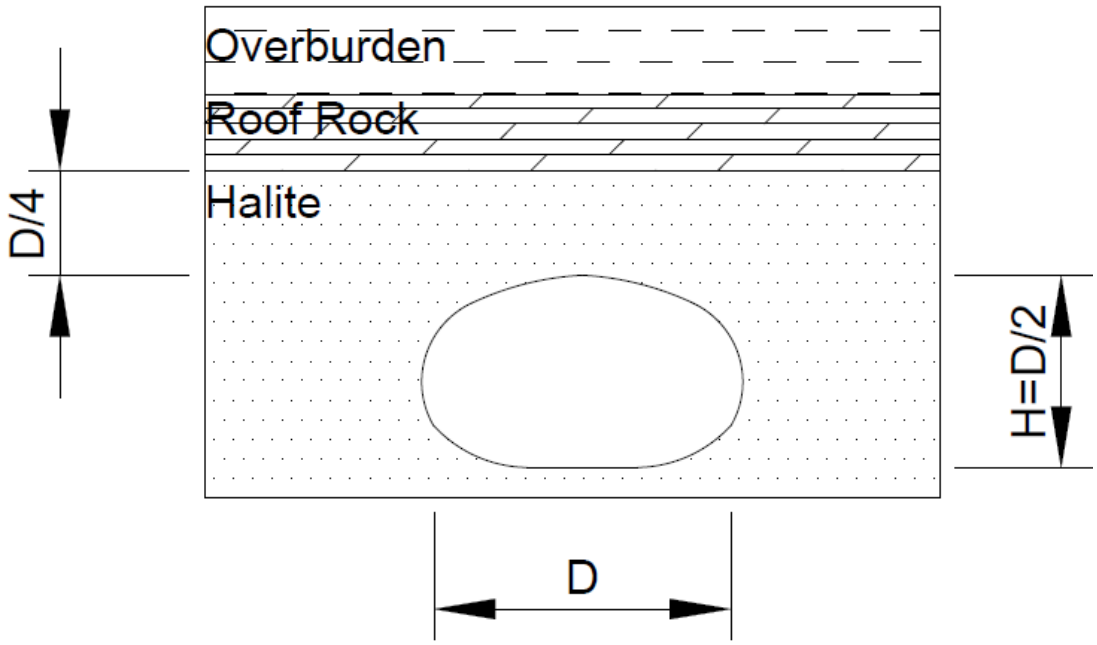

Figure 3.3 Recommended First Order Cavern Roof dimensions (Bruno and Dusseault, 2002; Zheng et al., 2016)

If multiple caverns are needed, the spacing of caverns must be taken into consideration. The caverns may be created in a thinly bedded salt deposit and could experience cyclic loading asynchronously. It is therefore necessary to separate the caverns such that they do not interact with each other. The intermediate region between two caverns must have low disturbance to ensure stability. The displacement magnitude is traditionally used to describe the interaction between two caverns. It is recommended that the spacing between two caverns is 3 times the diameter (Bruno, 2005).

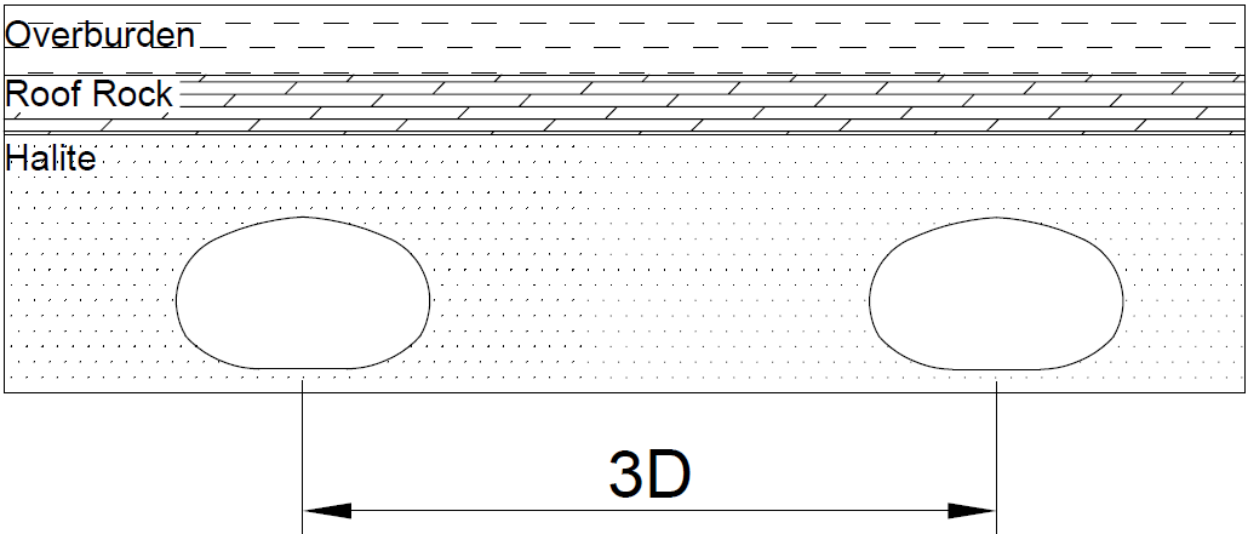

Figure 3.4 Minimum Cavern Spacing Based on Literature Guidelines

3.2 Operational Failure Criterion

During operation the cavern will undergo cyclical temperature and pressure loads. The onset of tensile stress and dilation of the cavern must be discussed. Tensile stresses at the cavern wall can lead to salt fracturing and spalling. The damage would accumulate to alter the shape of the cavern and may lead to greater instability. As per Brouard (2012), the two criteria used to assess cavern wall tension are the no tension and no effective tension condition. The no tension criterion states that no principal stress can be tensile. The no effective tension criteria states that the effective tangential stress at the wall must be compressive. When shear stresses are larger than mean stress, salt is prone to microfractures and dilation, although in the long term salt exhibits self healing. To assess dilation, the two criteria most commonly used are Ratigan's criterion (Ratigan *et al*., 1991) and DeVries's criterion (DeVries 2006) expressed in equations 3.4 and 3.5.

$$SF = -0.27 I_1 / \sqrt{J_2} \qquad (3.4)$$

I_1 is the first invariant of stress tensor, J_2 is the second invariant of deviatoric stress tensor, and *SF* is the factor of safety. When the factor of safety is less than 1, shear octahedral stress is greater than mean stress and rock dilation becomes possible.

$$\sqrt{J_2} < \frac{D_1(|I_1|/\sigma_0)^m + \bar{T}_0}{\sqrt{3}\cos\Psi - D_2 \sin\Psi} \qquad (3.5)$$

$$3\Psi = -3\sqrt{3} J_3 / 2 {J_2}^{3/2} \qquad (3.6)$$

D_1, D_2, σ_0, m, and $\bar{T}_0$ are five empirical constants. J_3 is the third invariant of the deviatoric stress tensor.

The criteria are pure stress and do not account for salt's self healing capabilities.

For a one day cycle of cavern temperature change, the heat exchange of the rock can be neglected (Berest & Brouard, 2015). However, the heating of the rock can induce additional stresses due to expansion. For simple shapes such as a spherical or cylindrical cavern, closed form solutions exist for the perfectly elastic case.

Table 3.1 Additional Stresses due to temperature variation are expressed below (Brouard, 2012)

Additional Stress	Spherical shape	Cylindrical shape
Radial $\Delta\sigma_{rr}(r)$	$-\frac{2\bar{\omega}}{r^3}I(r)$	$-\left(\frac{a}{r}\right)^2\bar{\omega}J(r)$
Tangential $\Delta\sigma_{\theta\theta}(r)$	$\frac{\bar{\omega}}{r^3}I(r)-\bar{\omega}\Delta T_{salt}(r)$	$\frac{\bar{\omega}}{r^3}I(r)-\bar{\omega}\Delta T_{salt}(r)$
Radial $\Delta\sigma_{zz}(r)$	$-\bar{\omega}\Delta T_{salt}(r)$	$-\bar{\omega}\Delta T_{salt}(r)$

$$\bar{\omega}=\frac{E_{salt}\alpha_{salt}}{(1-\nu_{salt})} \qquad (7)$$

Where E_{salt}, α_{salt}, and ν_{salt} is the Young's modulus, the coefficient of thermal expansion, and the Poisson's ratio of salt.

3.4 Pressure and Temperature Fluctuations

The cavern pressure and temperature fluctuations can be approximated using the state space model described in the second chapter. According to Bruno (2005), the operating limits can be approximated by ensuring that the maximum operating pressure is 80% of the fracture pressure of the cavern, and that minimum pressure is no more than 25% of the halmostatic pressure. The rate of load fluctuation may affect operating conditions by triggering instability; it is therefore necessary to perform numerical simulations to ensure that no dilation, or tensile stress issues arise.

Pressure cycles may have a period of several hours to a single day, or even several days, depending on energy demands. The cavern will also need to be simulated over the span of several years to determine the safety factor over time. An example of temperature penetration is illustrated in the Appendix.

3.5 Cavern Shapes

Salt caverns are created by solution mining where the salt is dissolved with the use of non-saturated water. A hole is drilled to the formation allowing the water to flow into contact with the salt. The water dissolves the salt and is then extracted in the form of brine. A single well and casing may be used for the process, but it is possible to use more than one well for fresh water injection and brine extraction. It is difficult to predict the precise shape of salt caverns as they are solution mined, however their behaviour can be approximated with simple geometries.

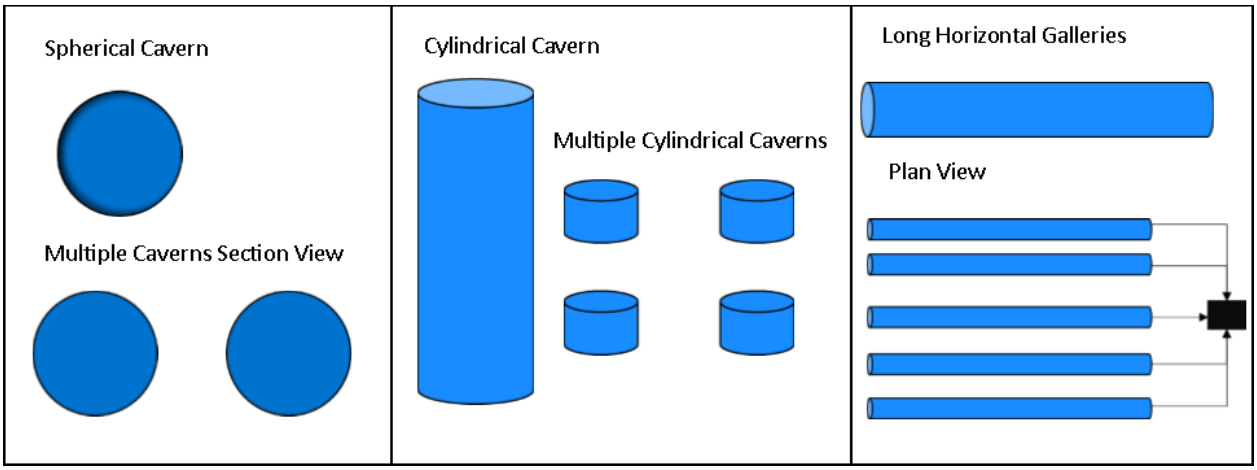

Figure 3.5 Geometric Approximations of Salt Caverns

The most simple shape of a salt cavern would be a vertical cylindrical cavern. This cavern shape is simple to solution mine, as gravity will allow the water to interact with the salt. Another simple shape would be a more spherical cavern. Storage caverns of this kind can be created with a single well and casing.

A more complicated shape would be that of a horizontal gallery, a cylinder with its long axis oriented horizontally. This would be more difficult to create and may call for two wells. Horizontal cavern creation will require a single well with tubings or two wells drilled vertically into the salt formation. Traditionally two wells are used, one well will be used to inject fresh water, and the other will serve as the extraction well for the brine. There are two methods in which these wells are connected in the salt stratum. One method requires the use of hydraulic fracturing in the injection well to allow a fracture network to be created in the salt (Liang & Zhao, 2005). The fresh water will dissolve the salt and travel through the fracture network as brine. The extraction well will remove the brine that travels through it. The fracture network will have a wide area, and it may be hard to manage the direction of fractures. Alternatively, the wells can be connected with the use of a directional drill. The dissolution would be easier to manage; however, the cost of directional drilling is not negligible. Horizontal wells would be advantageous when trying to achieve a certain storage volume, with limited salt thickness.

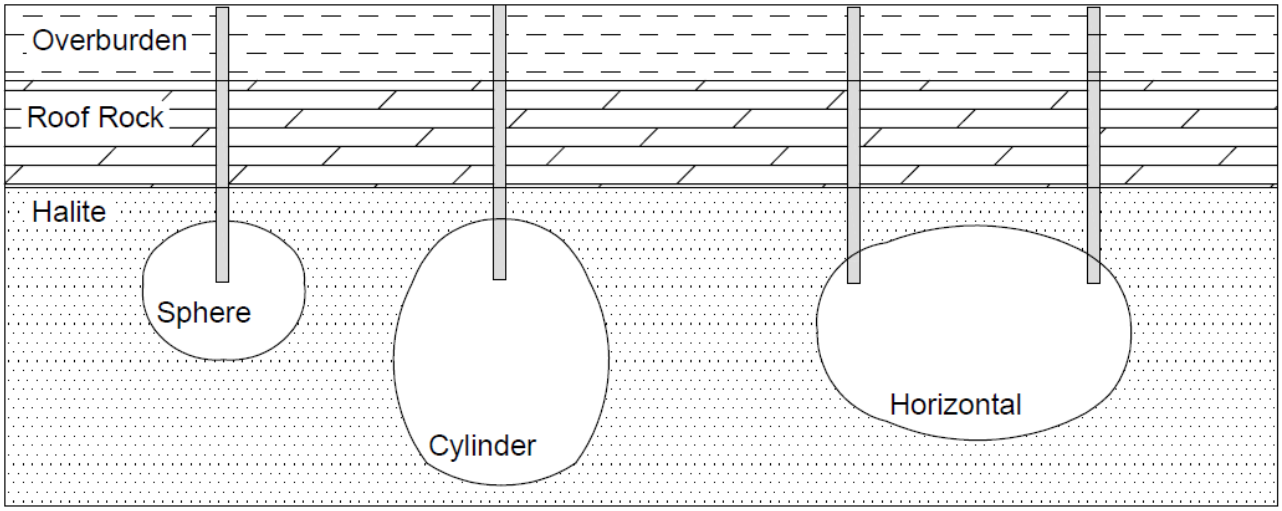

Figure 3.6 Conceptual Drawing of Solution Mined Salt Caverns

3.6 Cyclic Behaviour of Salt

Researchers have tried to understand the behaviour of salt using laboratory tests and numerical modelling. The static and cyclic creep tests show roughly the same behaviour, according to Roberts *et al.* (2014) the cyclic results match closely with the static creep test and numerical simulation in the non-dilation zone. Cyclic loading does not appear to make salt more prone to deformation than static loading. Ma *et al*. (2013) showed that loading and unloading a specimen yields linear stress-strain response, and this is more apparent with increased confining pressure. Confining pressure reduces the disparity in deformation modulus between unloading and reloading.

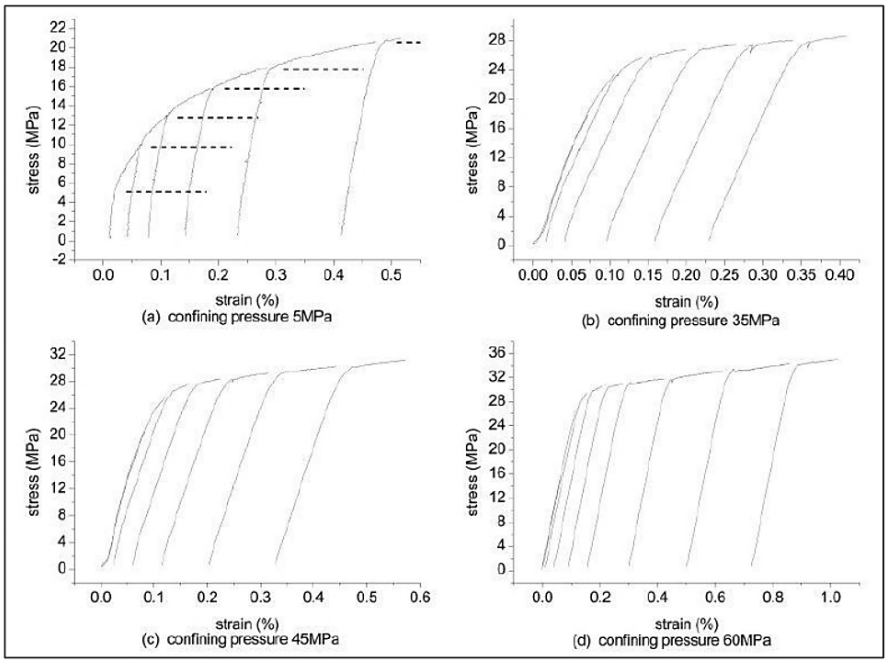

Figure 3.7 Loading and Reloading Behaviour (Ma et al., 2013)

4.0 Geomechanical Modelling Methodology

This chapter details the numerical modelling methodology used in the design algorithm. The first order numerical models are used to test geomechanical feasibility. The determination of feasibility will be based on dilation and tension. The modelling will be simplified with use of basic 2-D shapes, which allows for verification of results using an analytic solution. The first simulation will comprise assessing the elastic case of a specific cavern. The results will be evaluated and then processed. The cavern will then be assessed for long-term behaviour using the Norton creep law. The modelling will be carried out using COMSOL Multiphysics®. A cavern closure estimate will be made, using the steady-state analytic solution.

4.1 First Order Assumptions

Simplified shapes are sufficient for first-order calculations assuming that the cavern has not yet been created for a specific CAES facility. The lithologies situated above the salt layer are relevant in the final stages of design but are not critical so long as the baseline criteria discussed in chapter 3 are met. The models will largely be to estimate the deformations in the salt layer, thus the overburden effects are not examined closely.

A 2-D approximation will be used to capture the deformation behaviour of the cavern. The relevant geometries are a cylindrical, spherical and horizontal cylinder. The cylindrical and spherical cavern can easily be approximated by 2-D shapes; however, the horizontal gallery must be approximated using an ellipsoid as the cross section with a lower height to diameter ratio. Multiple caverns may be used in practice; however, it is sufficient to simulate a single cavern assuming the 3D spacing requirement is met.

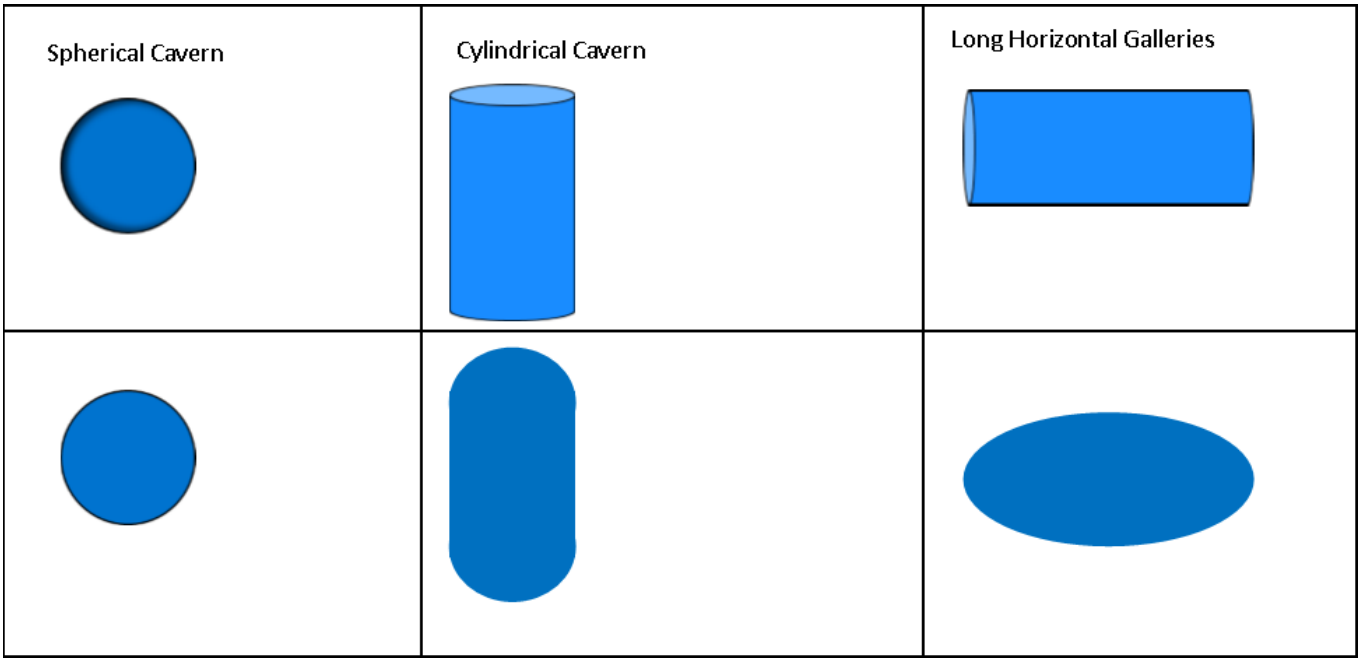

Figure 4.1 2D Approximations of Salt Cavern Shapes

4.2 Elastic behaviour

The first stage of modelling will test each cavern shape under elastic loading, with each layer as a homogenous elastic material. The material properties will vary at each site, however sample values are provided below. The initial conditions will consist of a geostatic stress applied in the form of a gravitational load, with a lateral geostatic load applied on the line of symmetry of the model. The cavern will be pressurized in a series of three steps: the initial cavern pressure will be 0, the next load step will pressurize the cavern to half of its capacity, finally the cavern will reach full pressure. The loads will be applied uniformly on the internal wall of the cavern. The model will have fixed boundaries prescribed along the bottom of the lithological model, and the top of the model.

Table 4.1 Sample Elastic Properties

Parameter	Halite
Density (kg/m^3)	2160
Young's Modulus (GPa)	37
Poisson's Ratio	0.25

The purpose of the elastic model is to test the dilation and tension criteria. Rapid pressurization can be considered to be an elastic load in the short term, and one may thus estimate the initial strain in the rock by modelling its behaviour with an elastic model.

4.3 Time Dependent Behaviour of Salt

The second stage of modelling will assess the cavern's time dependent behaviour. The loading will instead be cyclic, and with varying cavern temperature. The cavern behaviour will be the sum of the elastic and viscoplastic deformation. Creep of salt is a highly non-linear function of stress and temperature. Steady state creep is generally reached within a longer period of time and at a constant temperature and pressure. Transient creep is triggered when the stress and temperature applied are suddenly changed. The cavern will undergo a cyclic load, as discussed in chapter 3, the cyclic loading behaves similarly to static loading so long as the stress is under the dilation boundary (Ma *et al.*, 2013). The results will be evaluated at three cycles and then twenty cycles.

The time dependent behavior is modelled using the Norton law, sometimes called the power law. The model will use the COMSOL® material model behaviour built in to the software. Sample values are listed below, however the material parameters will vary from site to site.

Table 4.2 Sample Creep Parameters

Parameter	Halite
A	4.6
N	5
Q/R (K)	5750

4.4 Model Verification

To validate the model, the results produced by the computer model will be compared to an analytic solution. This verification should be done for each site selected. Van Sambeek (1986) developed closed form solutions for determining the displacement, tangential stress and radial stress of a cylindrical cavern. The values of the computer model will be compared to the analytic values.

$$\sigma_r = -p_b + p_b \left[\frac{(\frac{b}{r})^{2/n} - 1}{(\frac{b}{a})^{2/n} - 1} \right] \quad (4.1)$$

$$\sigma_\theta = -p_b + p_b \left[\frac{(\frac{2-n}{n})(\frac{b}{r})^{2/n} + 1}{(\frac{b}{a})^{2/n} - 1} \right] \quad (4.2)$$

$$u_r = -A \left(\frac{3}{4}\right)^{\frac{n+1}{2}} p_b \left[\frac{\frac{2}{n}}{(\frac{b}{a})^{\frac{2}{n}} - 1} \right]^n \left(\frac{b^2}{r}\right) t \quad (4.3)$$

Where P_b is the pressure on the outer surface of the cylinder, a and b are the inner and outer radius of the cylinder, A and n are the Norton Hoff parameters.

4.6 Cavern Closure Estimates

For cylindrical and spherical caverns, closed form solutions exist to describe the closure rate. Closure rate will govern the caverns design life; it may also affect the economic analysis. Huntorf experienced virtually no closure after thirty years of operation (Crotogino *et al.*, 2001). It is advantageous to provide a conservative estimate of closure rate. To do this the closure rate formula will be applied while the cavern is at minimum operating pressure and the minimum storage temperature.

4.7 Modelling Methodology

The modelling will begin by assessing a cylindrical cavern. This would be the simplest geometry to validate with the closed form solution. If the cylinder can not meet the baseline requirements, a spherical and then finally the horizontal cavern will be assessed. The initial loading will be a model of purely elastic deformation. Dilation will be evaluated by using Ratigan's criteria, as it is not dependent on empirical constants. The tension evaluation involves verifying the cavern does not experience tensile stress during its unloading, which can be done by ensuring that the minimum principal stress around the cavern is never tensile.

The cavern can then be assessed for one entire loading cycling, including the creep behaviour of the material. The loading will begin at atmospheric pressure inside the cavern, all the way up to its full capacity, and then to its operation cycle. To assess more long-term behaviour the model will experience 20 operation cycles.

The model will experience a gravitational load to approximate geostatic stress. A lateral load will be applied to the model approximated as equal to vertical stress in the salt layer. Before iterating

shapes, the dimensions of the cavern may be adjusted. This would include cavern depth, diameter, and height. Figure 4.2 illustrates the variations in testing.

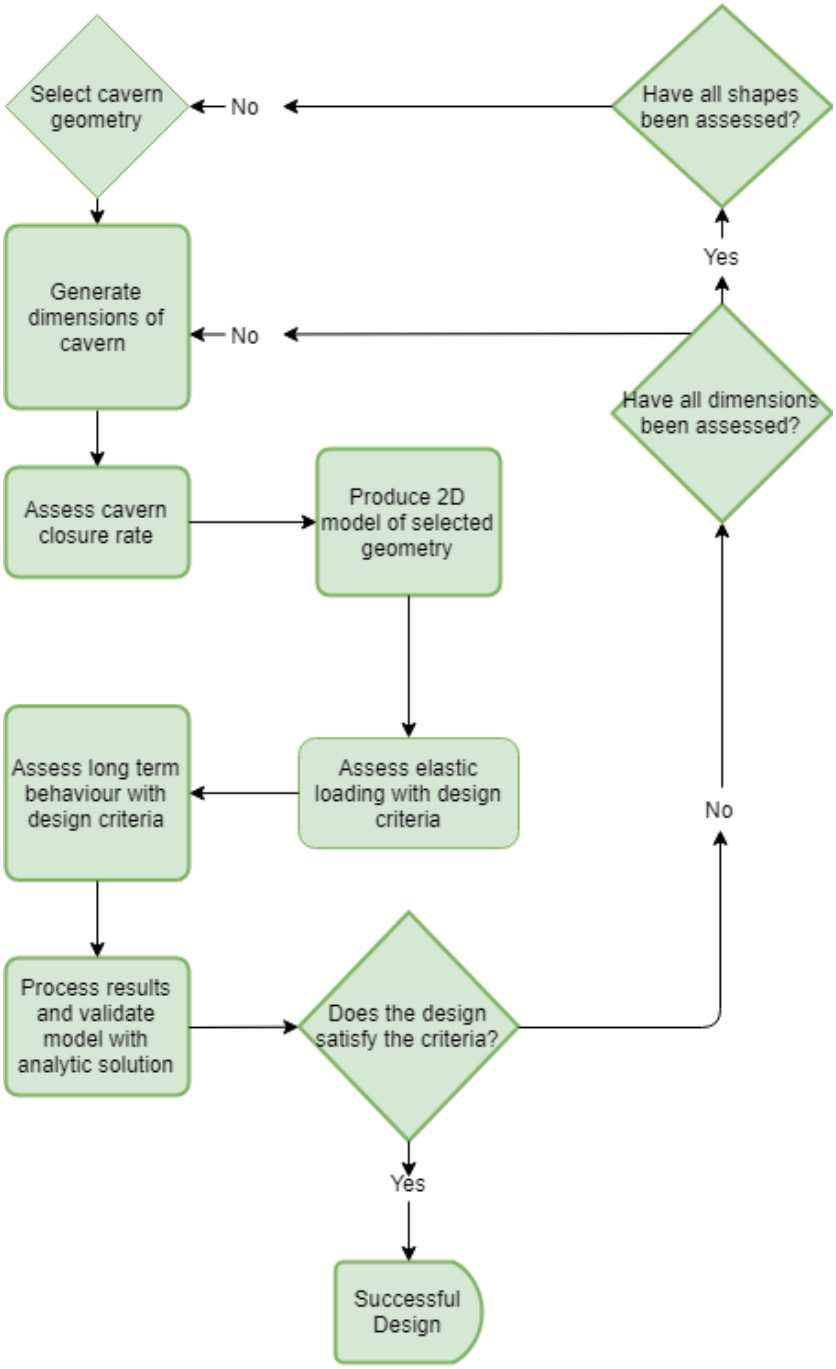

Figure 4.2 Geomechanical Design Algorithm Flow Chart

5.0 Design Algorithm Methodology

This chapter details a design algorithm which can be used to develop a first order CAES design. The parameters are simple and can be approximated with literature values if needed. The algorithm connects the otherwise separate disciplines of CAES design, to aid a more integrated design approach. This design algorithm does not include an economic analysis, but instead focuses on the first order technical feasibility of a design.

The initial stage of design entails an understanding of salt extent and characteristics such as depth and thickness. With a geographic constraint, one may determine the energy needed in terms of delivery requirements. With an initial understanding of energy needs, appropriate mechanical equipment can be selected which will yield the characteristics of necessary volume, pressure limitations, and discharge times. An energy consumption and production profile can be produced. From here one may assess the cavern's stability to determine the factor of safety against dilation and tension. The algorithm will yield a cavern design for a specific CAES facility; one may then proceed into a cost benefit analysis, more rigorous technical design, and a cavern creation program.

5.1 Geological Constraints

The availability of salt is the most rudimentary constraint of CAES design in salt caverns. An understanding of salt availability is required to initiate the design process. The existence of salt at a site must be a given, with some approximation of the lateral extent. The two most critical parameters for geomechanical feasibility are depth, and thickness of the salt formation. It is also advantageous for the proposed facility to be near transmission lines in the event of the facility being used for grid energy storage. It may also be desirable to have nearby renewable energy sources to provide power to store. It is at this point that one must know if the CAES facility will be adiabatic or diabatic. If it is diabatic, proximity to natural gas lines or a source of waste heat is necessary.

Figure 5.1 Salt Practical Limit in Ontario (Lord, 2017)

Depth is critical, shallow salt formations will be unable to handle high pressures and have more risk of fracturing the caprock of the cavern. Geostatic stress increases with depth, more depth will result in a higher maximum pressure. In general, the maximum storage pressure should be limited to 80% of the geostatic stress at the roof. However, depth is also constrained by minimum operating pressure, as a low minimum pressure could trigger rapid cavern closure or roof instability. It is recommended that the minimum storage pressure be no less than 25% of the geostatic stress (Bruno, 2005). The site geomechanical stresses should be well approximated, this also includes an understanding of the geothermal gradient which can be approximated as 25 degrees Celsius per kilometer of depth, generally.

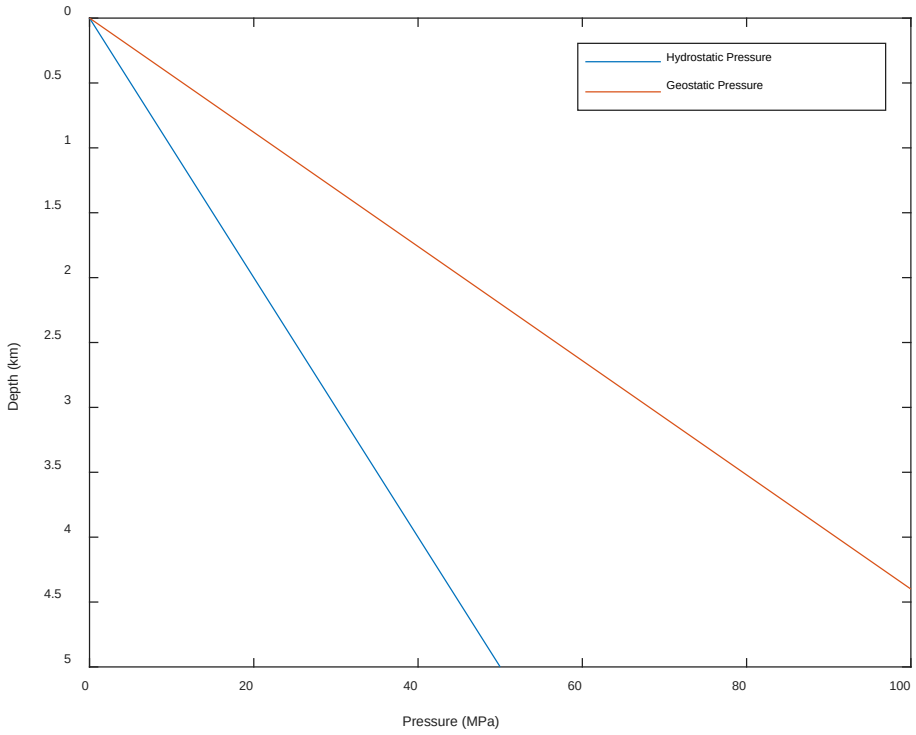

Figure 5.2 Sample Geostatic Pressure with Depth

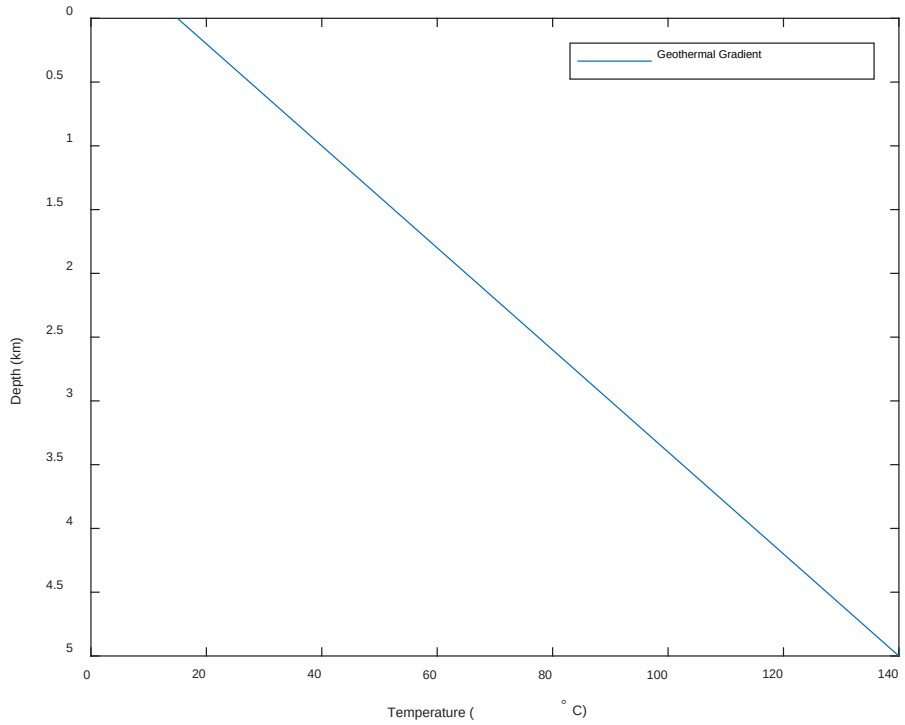

Figure 5.3 Sample Geothermal Gradient

Salt thickness and the required volume will determine the shape of the salt cavern. As mentioned in chapter 3, the thicker the salt stratum the less difficult the design of the cavern will be. If the bed is too thin, one must create multiple caverns, or a horizontal gallery. The baseline criteria of dimensions and roof thickness must also be met for first order design.

The initial stage of the design algorithm entails site selection based on the presence of salt. The salt is then deemed viable if it is at an appropriate depth and thickness. The geostatic pressure and fracture pressure of the salt formation must also be known to provide an approximation of cavern pressures. The specific cavern dimensions will be determined in the next stage of the design algorithm.

5.2 Energy Requirements

With a site location selected, one must determine the amount of energy required. Energy storage systems provide several services for different users. This can range from energy arbitrage for industrial users, or bulk energy management for the grid operator. It is most practical, in the context of first order design, to summarize the energy need in terms of power and duration required of the CAES facility. The discharge and charge profile of the system may also be considered. Although this approach may be simplistic in some circumstances, it serves to narrow the scope of geomechanical and mechanical design considerably. An understanding of the required charge time, discharge time, and power expected of the storage system is sufficient for selection of mechanical equipment.

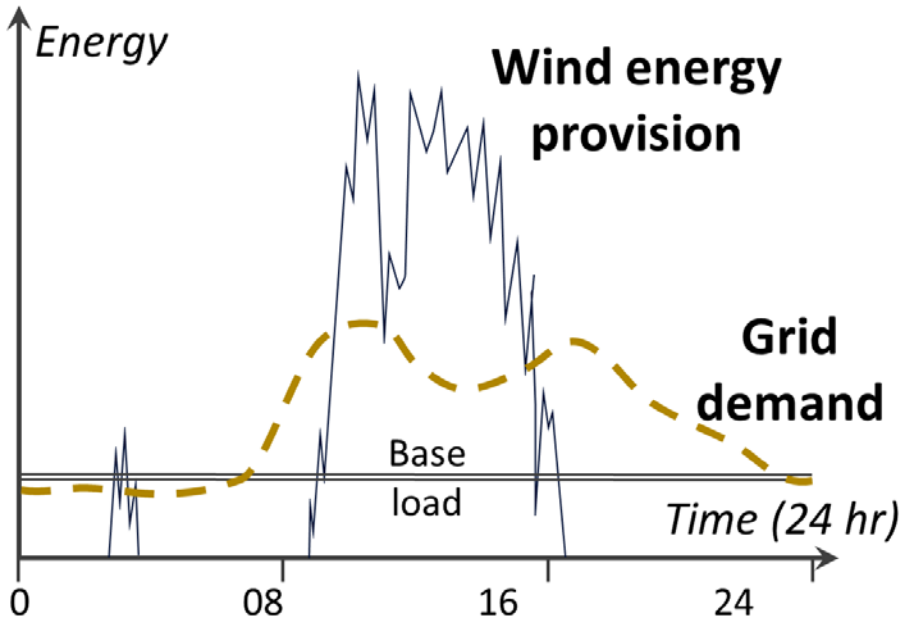

Figure 5.4 Conceptual Energy Supply and Demand

Using equation 2.1, one may select several compressor systems and assess the mass flow rate, and energy consumption. Each compressor unit will have its own rate of energy consumption, as well as its own pressurization rate. The compressor selected must have a sufficiently high outlet pressure, and an after cooler to ensure the air temperature is not dangerously high. An appropriate compressor would have an outlet pressure greater than or equal to the cavern maximum operating pressure, and an air outflow temperature no greater than 50 degrees Celsius for safe storage in a salt cavern(Berest *et al*., 2015). It is expected that several iterations are required to select the correct compressor to meet the specific energy needs; the appropriate charge times of the cavern, the power consumed, and the efficiency of the machine at the required mass flow rate.

The expander units must also be selected. This design algorithm will assume two expander units in series. The total power provided is the sum of each expander unit's power rating. The selection of expander equipment will determine the volume of the cavern as well. With the expander selected volume can be calculated to proceed to the geomechanics stage, and the energy regeneration can be assessed to see if it meets the service required. With the volume calculated one can also determine the amount of time to pressurize and depressurize the cavern.

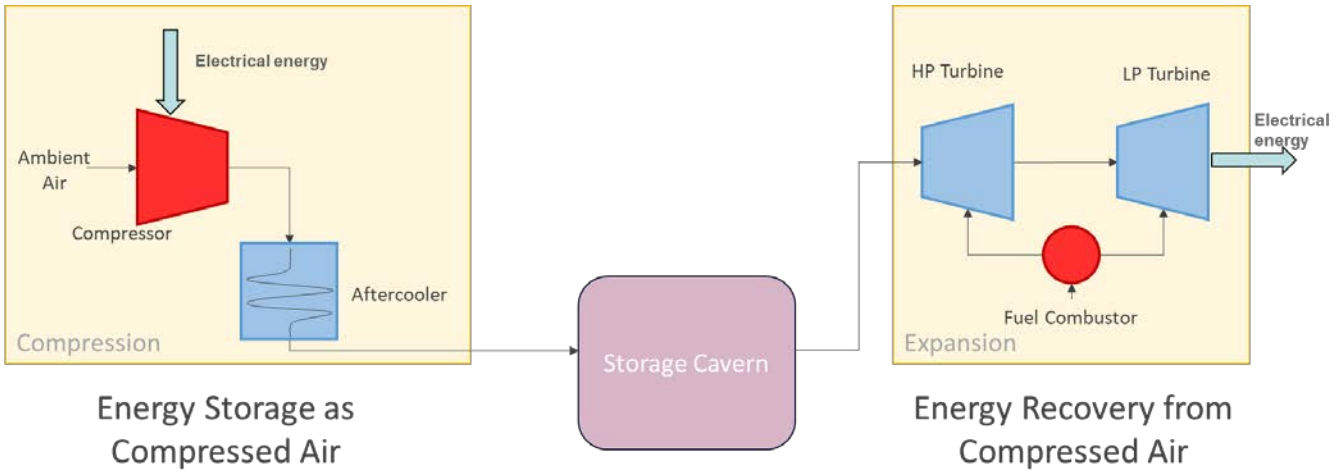

Figure 5.5 Diabatic CAES Schematic with Single Compressor and Two Expanders

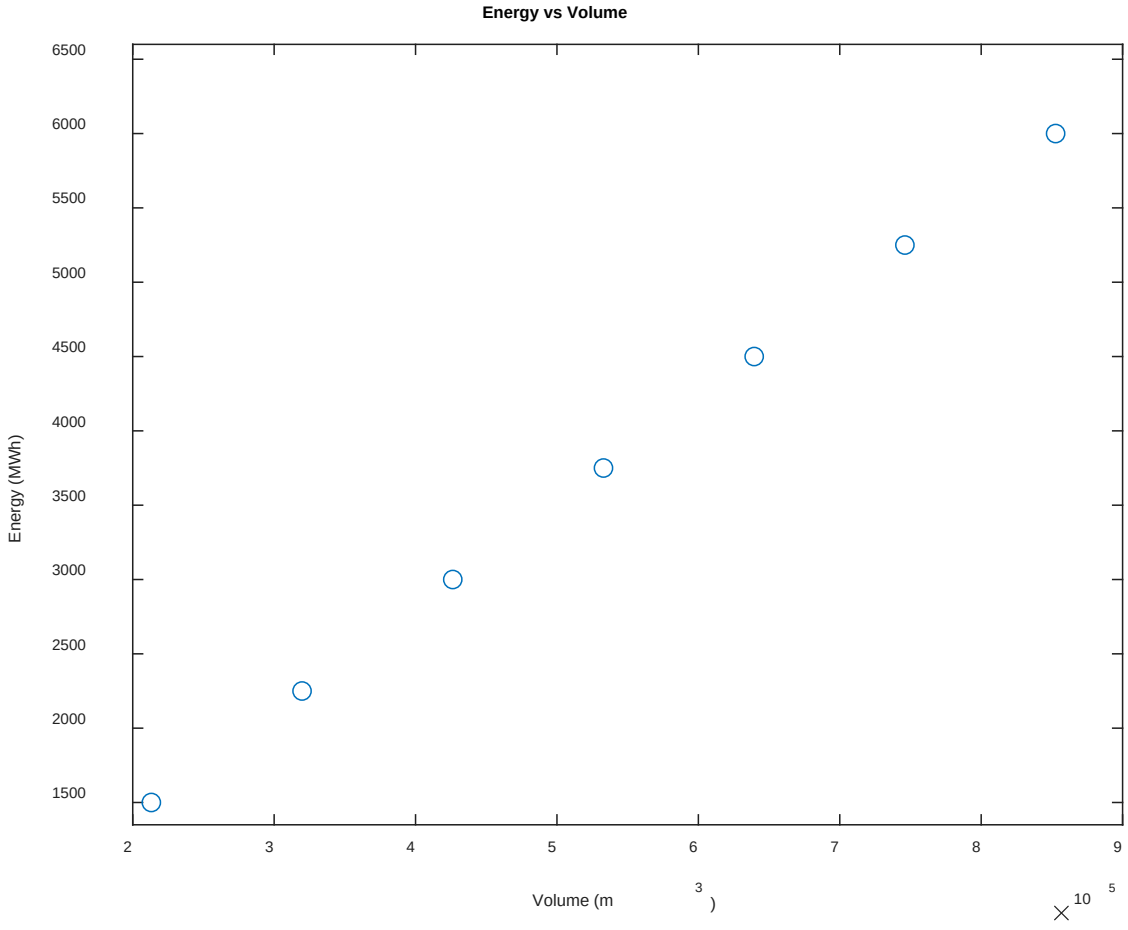

Figure 5.6 Energy vs Required Volume

5.3 Geomechanical Design

At this stage the number of input parameters required should be sufficient to begin geomechanical design. With a proposed site location the depth, thickness, and static stress of salt should be known. This yields an initial calculation for the cavern operating pressures. With an assumed storage temperature, the geomechanical assessment can begin.

Using the initial rules described in section 3.1 the cavern dimensions can be developed for a specific cavern. The minimum number of caverns is what is most desirable, as it is implicitly more cost effective. This is often constrained by the thickness of the salt. If the salt formation is too thin, multiple caverns will be developed at appropriate spacing. The cavern volume and dimensions will be also based on the shape of the cavern selected. Cavern shape selection will be based on the difficulty of shaping the cavern: the most simple is a vertically oriented cylinder, followed by the spherical cavern, and finally the horizontal gallery (horizontally oriented cylinder)(Liu *et al*., 2018).

With the cavern shape and dimensions determined, accurate values for material parameters will be inputted into the numerical model. Assessing a static, and then time dependant load will yield different results. Temperature cycling is also taken into consideration, as it affects the material behaviour and adds additional stress through expansion. With an understanding of the operating loads one can assess the cavern for the dilation and tension. This will give a factor of safety for the first order design. If the safety criteria are met, then the design is successful. If not, the cavern must be redesigned. The model must also be verified using the closed form solutions.

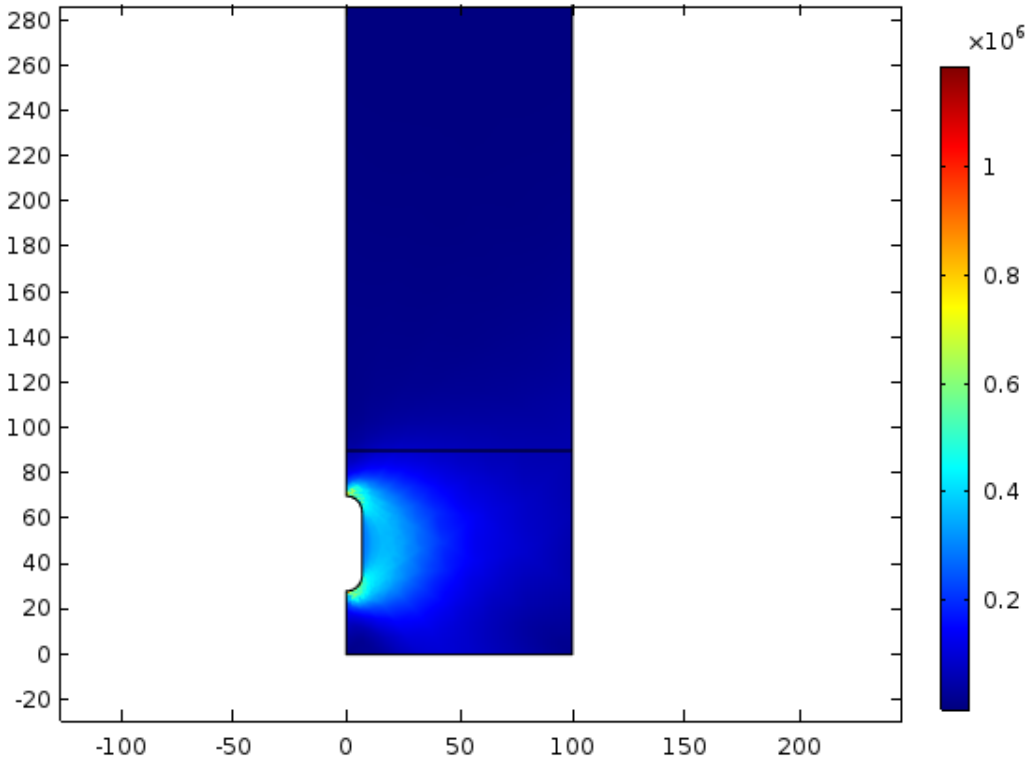

Figure 5.7 Von Mises Stress Plot of a Cylindrical Cavern

5.4 The Design Algorithm

To achieve an integrated first order design, iteration is required to ensure that all stages of design are feasible. A site is selected and assessed for proximity to energy and heating infrastructure. It is then necessary to determine if salt is even available and understand the salt properties. The properties serve as a baseline assessment of a site coloured blue, in figure 5.6.

To proceed into the mechanical design stage, in red, it is necessary to have the pressure limits and storage temperature. These values will only be estimates in the initial stage of design, however they are needed for the selection of mechanical equipment and calculating storage volume. The facility will have a desired storage capacity and the corresponding rate of charge and discharge. The demand and supply profiles will be needed, to select appropriate compressors and expanders. The charging and discharging rates of the equipment must be evaluated. If the equipment can not meet the needs of the facility, it is at this point that different equipment must be selected. With the correct equipment selected, the volume of storage can be calculated corresponding to the expander unit and the total energy required.

With the volume, pressure limits, and storage temperature the geomechanical modelling can begin. The design algorithm will iterate through each cavern shape until a feasible design is achieved. The closure rate will be calculated, to determine the life of the salt cavern. A 2-D model will be evaluated using COMSOL. The loading profiles will be used to assess the caverns stability. If no cavern geometry can be feasible, the energy storage application may be too ambitious and must be reassessed. With a more conservative energy demand, the algorithm can be applied again.

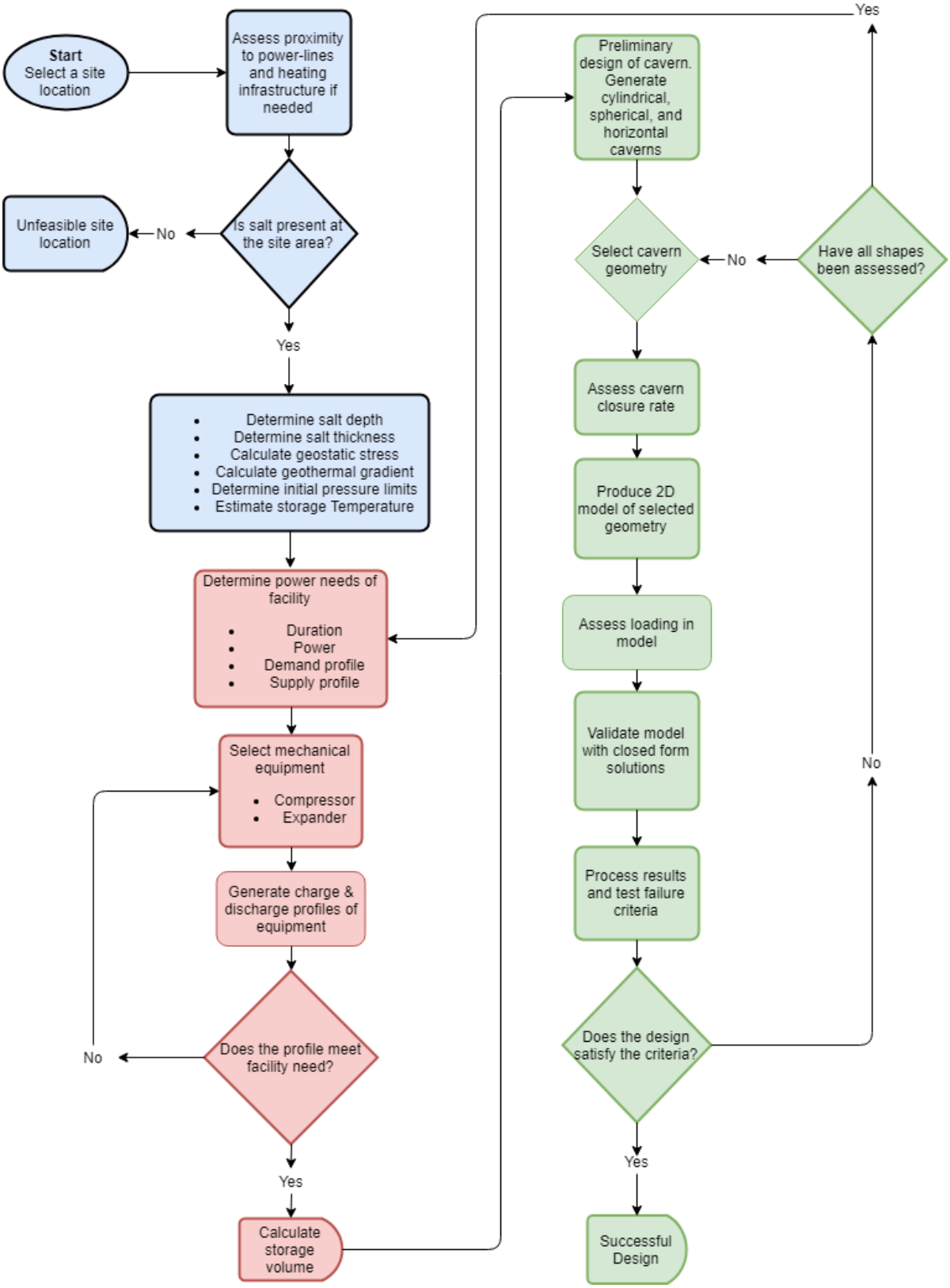

Figure 5.8 First Order Design Algorithm Flow Chart

6.0 Case Studies in Southern Ontario

This chapter will examine two case studies in southern Ontario. One will be for small scale energy storage, and the other for a much larger grid application. Both examples will be situated in southern Ontario. The design algorithm will be applied to develop a CAES facility which can meet a specific energy need. Ideally a single cavern will be used in the design.

6.1.1 Initial Site Assessment of Small-scale Storage

In southern Ontario, salt beds are part of the Michigan Basin. The sequence of salt beds is separated by shale, anhydrite and limestone. The salt deposits of interest are the unit B and the unit A. Unit B is the thickest salt unit in the sequence, it has a thickness of 90 meters. The unit B can be found at a depth of 610 meters. The unit A can also be found, it has a deposit located at a depth of 750 meters. The unit has a thickness of 40 meters(Hewitt, 1962).

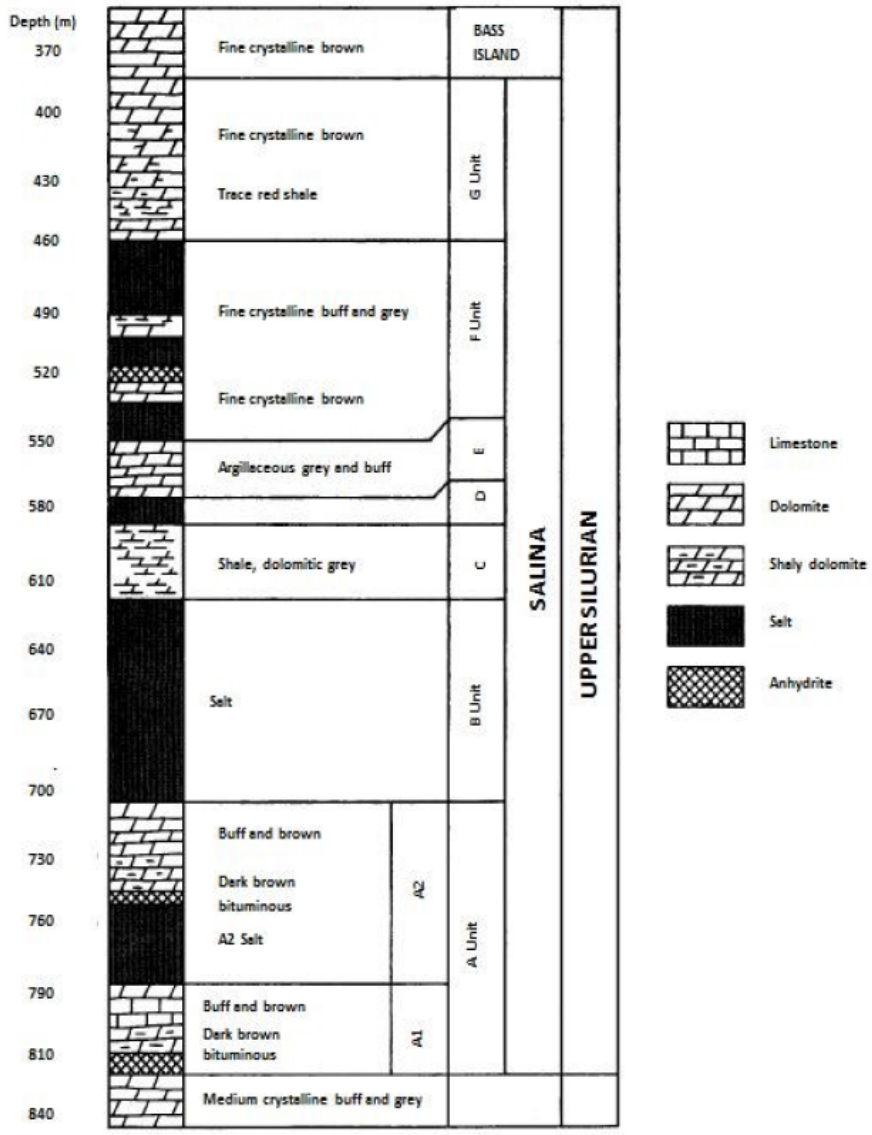

Figure 6.1 Stratigraphic Column of Southwestern Ontario (Hewitt, 1962)

For the unit B being assessed, we will assume a salt depth of 610 meters. The salt is 90 meters thick. We can expect the use of either a cylindrical or spherical cavern. It is assumed that there is proximity to transmission lines and natural gas lines. It is assumed that this system will be adiabatic.

After determining the depth of the salt, the stresses and geothermal gradient can be approximated. This will yield an initial estimate of operating pressures. The geostatic pressure is stress exerted by the overlying rock and sediment above the salt formation. The rock fracture pressure is more difficult to determine and usually involves a leak off test or a pressure integrity test(Bruno, 2005). However, it can be assumed that fracture pressure and geostatic pressure are approximately the same until a leak off test can be conducted. With the unit B in question, we can expect the average overburden density to be 2500 kg/m3; it is comprised of shale, limestone, and salt. The geostatic pressure is therefore, is 15 MPa. The upper and lower operating pressure limits will be 12 MPa and 3.75 MPa. The depth of the formation is relatively shallow; therefore, a lower storage temperature will be used. The air stored in the cavern will be no more than 50 degrees Celsius.

6.1.2 Mechanical Assessment

With the storage temperature and initial pressure limits determined, the mechanical assessment can begin. The required energy storage expected of the system must be known prior to equipment selection. To demonstrate the design algorithm's use, an assumed energy storage profile is generated for an industrial user.

In this example the customer will charge their system for 6 hours and discharge for 3 hours. The remaining time, the system will be idle. The industrial customer desires 30 MWh, 10 MW for a duration of 3 hours. The load system requirements are plotted below.

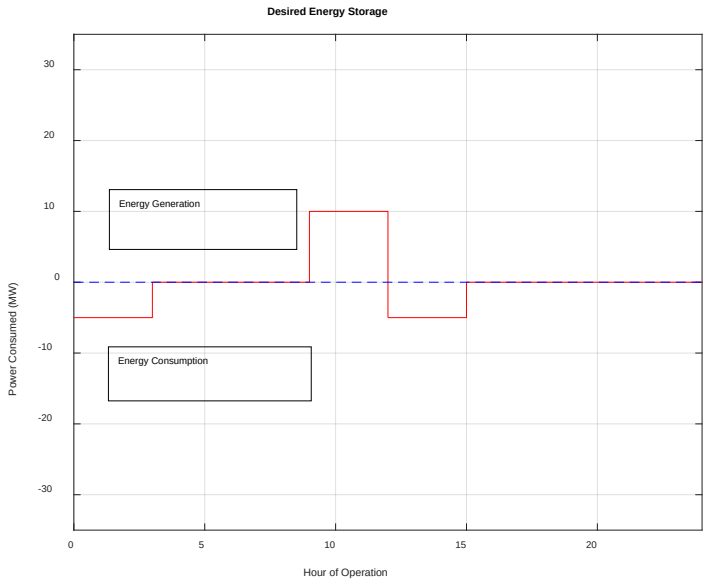

Figure 6.2 Desired Energy Storage of a Small-scale Industrial Client

To achieve the desired energy requirements a compressor will need a rated power consumption of 8.5 MW, as the system is not perfectly efficient. The expander system should have a rated power greater than or equal to 10 MW. The following table below shows equipment selected for such an application. Selecting the ideal equipment can prove quite challenging, and in some cases may require customized design of turbomachinery. Data sheets for the expander and compressor can be found in the appendix.

Table 6.1 Expander Equipment Selected for Small-scale Application

Gas Turbine Parameters		
Turbine Power	10	MW
Mass flow rate	58	Kg/s
Inlet pressure HP turbine	5	MPa
Inlet temperature HP turbine	125	Deg C
Inlet pressure LP turbine	1.2	MPa
Inlet temperature LP turbine	200	Deg C
Compressor		
Mass flow rate	25	Kg/s
Rated compressor power	8.5	MW
Temperature at exit of after cooler	50	Deg C
Pressure at exit of after cooler	10	MPa
Assumed round trip efficiency	56%	-

Figure 6.3 has been produced with the following assumptions. A single compressor unit, and two stages of expansion. Throttling will be expected at both the inlet of the expander and outlet of the compressor. An after cooler will be used on the compressor, to ensure the air being stored is at an appropriate temperature.

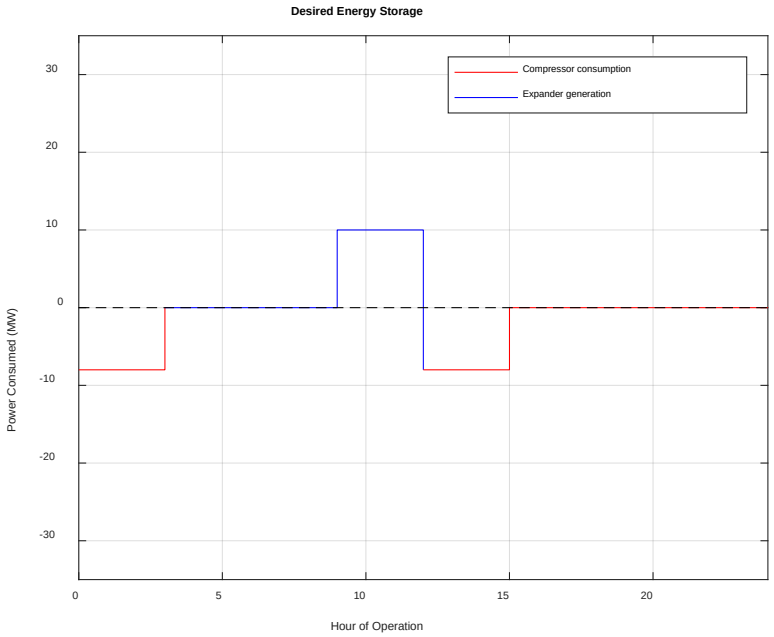

Figure 6.3 Energy Storage Provided by Equipment Selected

The profile is easy to meet with equipment if the appropriate power rating is achieved. One need only keep the machines in operation at the correct hours. The round-trip efficiency of the diabatic system is expected to be 50-60%. The assumed efficiency is 56%, the compressor must consume more power as a result. Turbomachinery has a window of efficient operation expressed in machine maps. These maps must be used to verify that the equipment is being used at its operating efficiency(Hewitt, 1962).

With the equipment selected one may calculate the storage volume required and generate a state space model to capture the behaviour of the cavern. The table below describes model assumptions. A plot is generated illustrating energy as a function of storage volume.

Table 6.2 Mechanical Model Assumptions

Turbine efficiency	0.8	-
Generator efficiency	0.9	-
Pipe friction loss	0.8	-
Desired power output	10	MW
Duration	3	hours

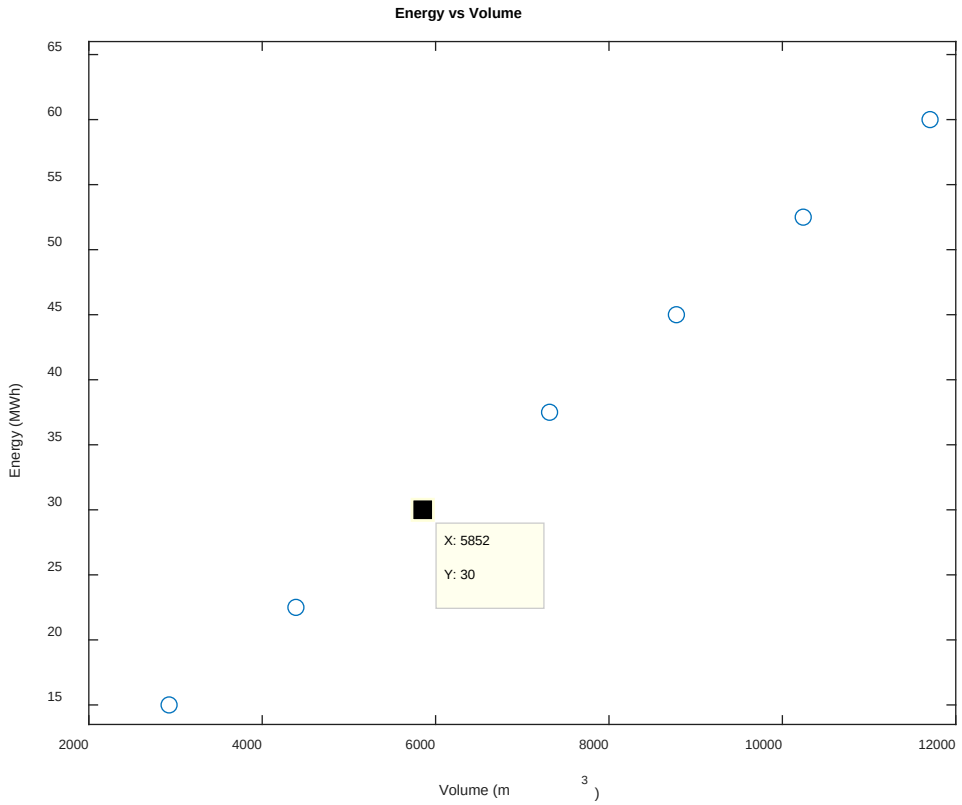

Figure 6.4 Energy vs Volume for Small-scale Application

For a single cycle the cavern pressure will rise accordingly. The pressure behaviour is approximated using the state space model. The charge time for a cavern of atmospheric pressure to a cavern of maximum pressure is 11.2 hours. The energy storage requirements can be met with 3 hours of energy discharge and 6 hours of energy charging. It will be assumed that cavern temperature fluctuates in a similar manner to Raju and Kaitan (2012) from 25°C degrees Celsius to 45 degrees Celsius.

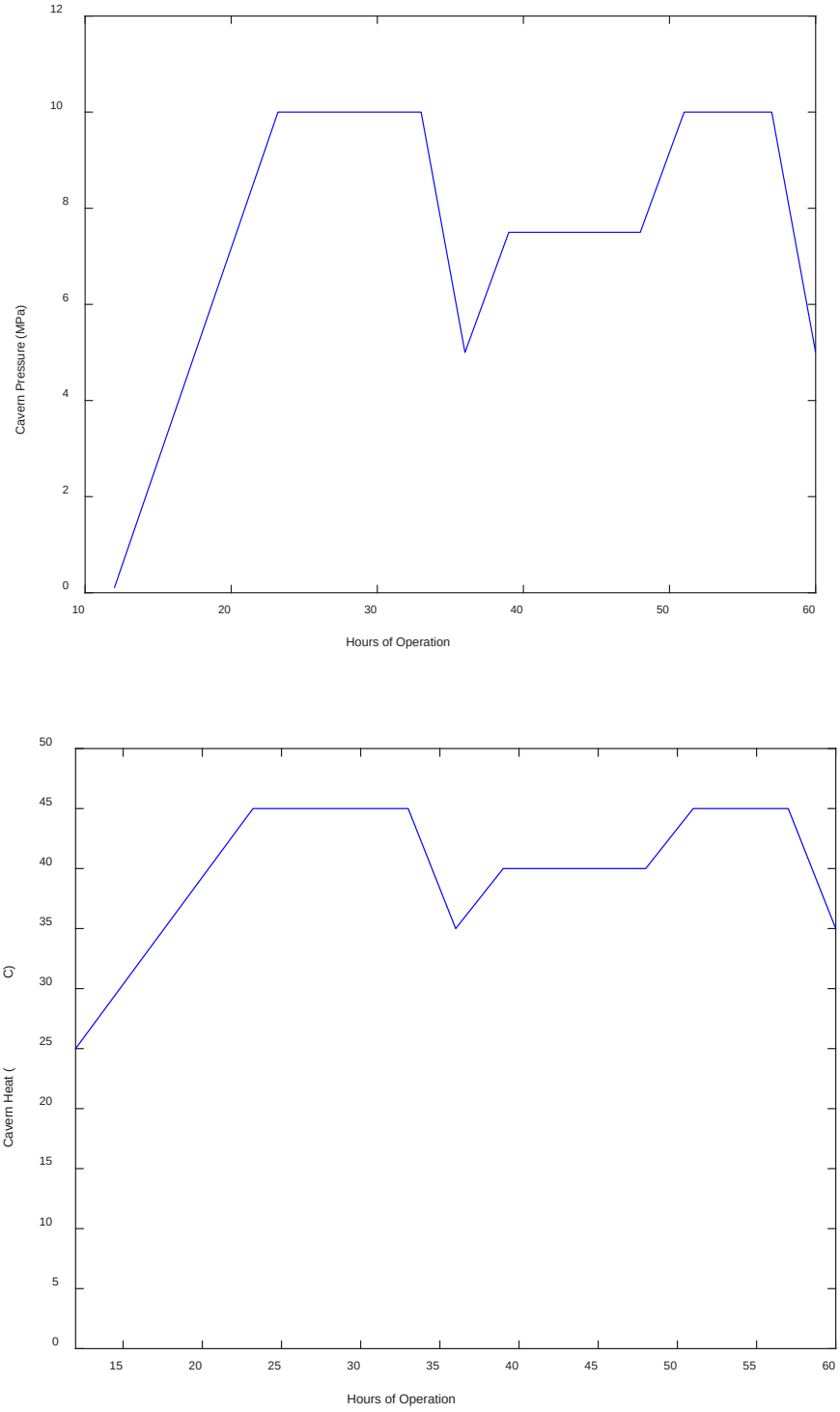

Figure 6.5 Cavern Pressure and Temperature for Small-scale Application

6.1.3 Geomechanical Assessment

With the loading pattern and required volume of 5800 m^3, the cavern assessment can begin. A 90-meter-thick deposit will be solution mined to form a cavern. The salt roof thickness must be a quarter of the diameter of the cavern, and the height to diameter ratio can be no less than 1/2. The table below describes sample geometries to meet these criteria.

Table 6.3 Cavern Dimensions for Small-scale Application

	Cylindrical cavern	Spherical Cavern	Horizontal cavern
Depth of Cavern Roof (m)	630	630	630
Diameter (m)	14	22	25
Height (m)	42	22	13

In 2D, the geometries can be modelled along its vertical symmetry. The assessment will begin by modelling a cylindrical cavern. This is the ideal cavern shape as it offers the most stability and is relatively easy to solution mine. The salt layer will be underneath a single unit of limestone, to approximate the overall overburden characteristics.

Table 6.4 Geological Material Parameters (Shahmorad et al., 2016; Wang et al., 2015)

Parameter	Halite	Average Overburden
Density (kg/m^3)	2160	2500
Young's Modulus (GPa)	25	30
Poisson's Ratio	0.25	0.3
A	4.56	-
n	3.1	-
Q/R (K)	5750	-

As the salt behaviour is dependent on temperature the model will have to be coupled with the fluctuating temperature load altering the salt creep, and the stress will vary as well. Elastic deformation will be evaluated at maximum and minimum operating pressures. Then in the time dependent analysis, the behaviour of the cavern after three loading cycles will be examined. Finally, the behaviour of the cavern can be assessed after twenty cycles.

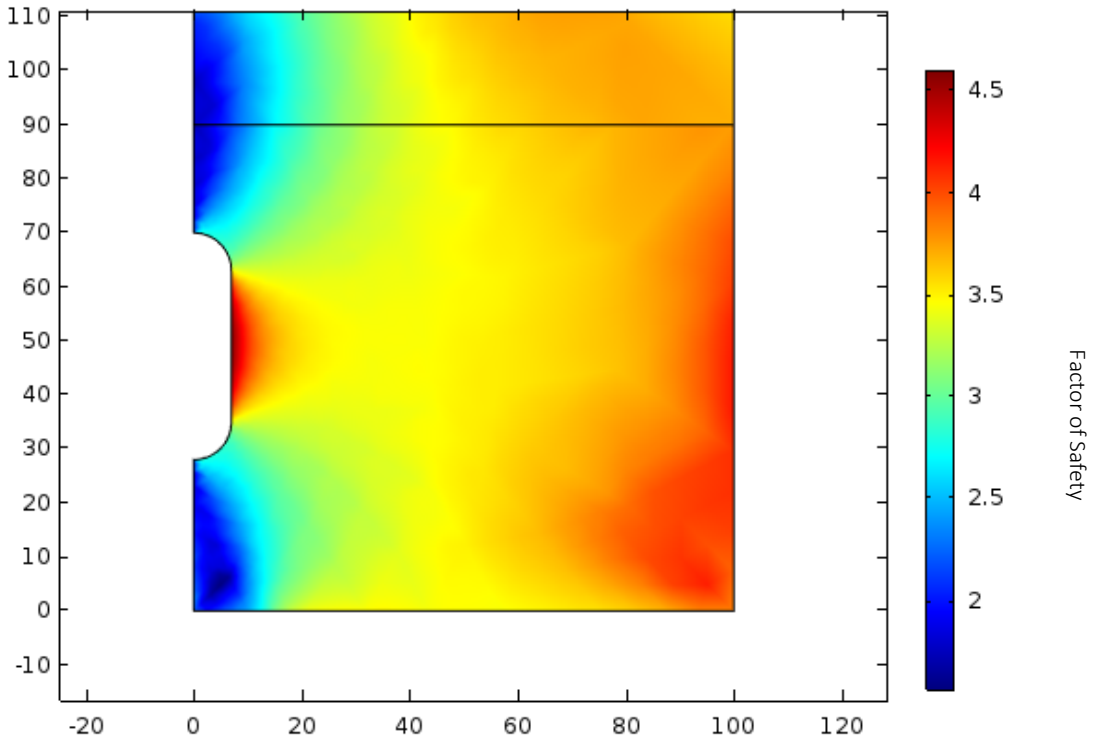

Figure 6.6 Salt Dilation Factor of Safety - Maximum Pressure

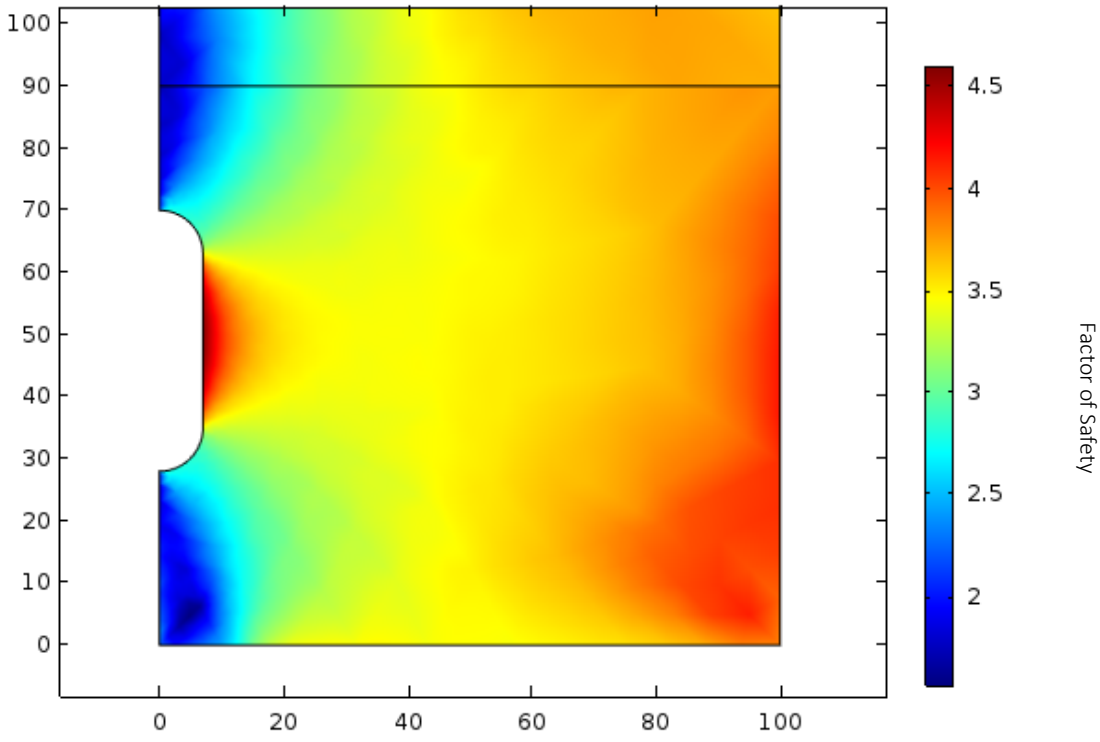

Figure 6.7 Salt Dilation Factor of Safety - Minimum Pressure

In the elastic loading scenario, it appears that the cavern satisfies the dilation criterion. In order to assess tension, the principle stress directions will be plotted. On the vertical cavern wall, the stress in the x-direction is expected to be positive. On the roof and floor of the cavern, the y-direction is expected to be positive and negative respectively.

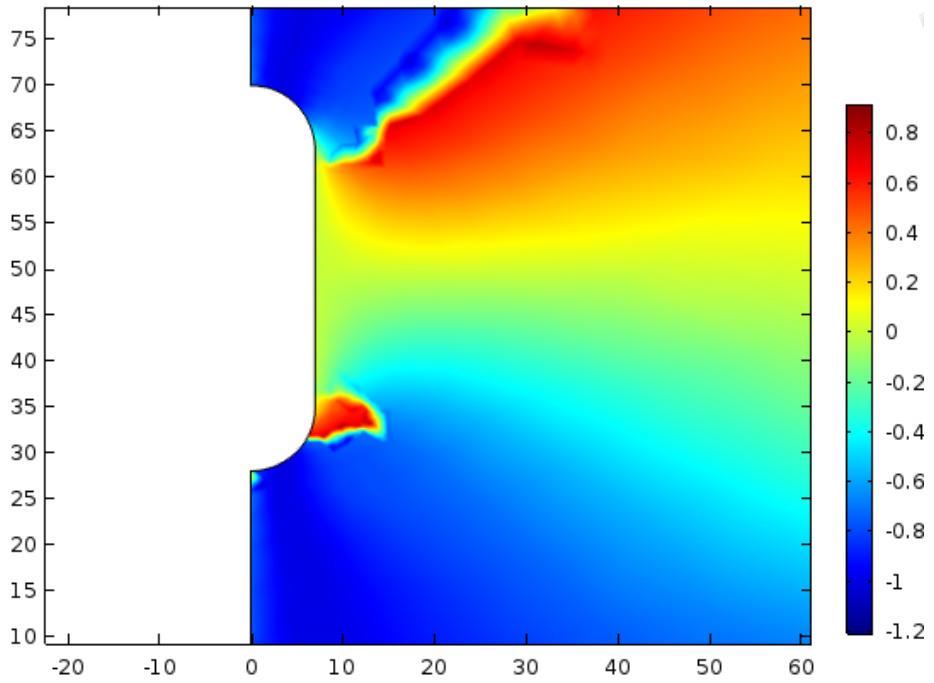

Figure 6.8 Principle Stress in X-direction

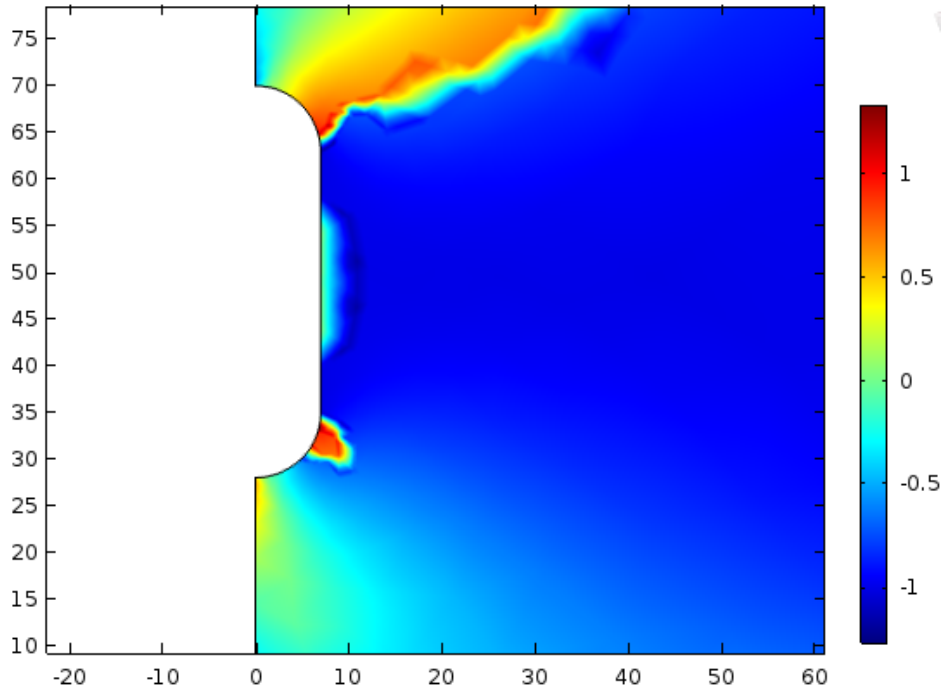

Figure 6.9 Principle Stress in Y-direction

With the elastic scenario assessed the time dependent modelling can begin. The creep model is dependent on the temperature penetration of the cavern(Bérest & Djizanne, 2010; Shahmorad et al., 2016). It will experience cyclic temperature and pressure loading, meaning that the model will be coupled. The results are presented below for this cavern design. The cavern is evaluated for dilation at its maximum and minimum pressure after three cycles, then for twenty cycles. In this scenario the cavern design is deemed feasible as it satisfies the dilative and tensile considerations. The steady state closure of the cavern at minimum pressure is 0.022%/ year. The model is validated by comparing the analytic solution to the numerical solution with 90% of the predicted analytic solution. Sample calculations for the model validation are provided in the appendix.

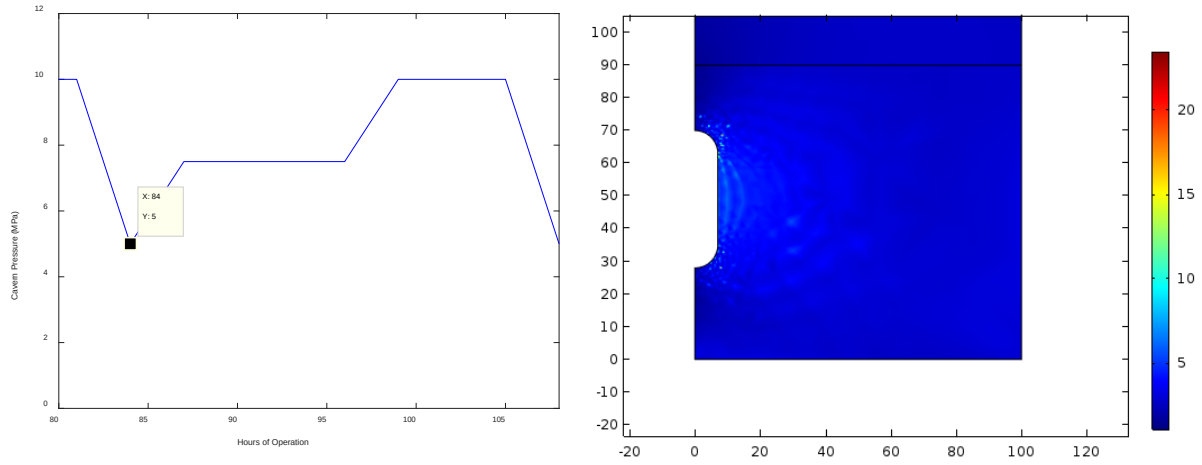

Figure 6.10 Salt Dilation at Minimum Pressure - 3 cycles – Pressure Cycle and FOS Spatial Plot

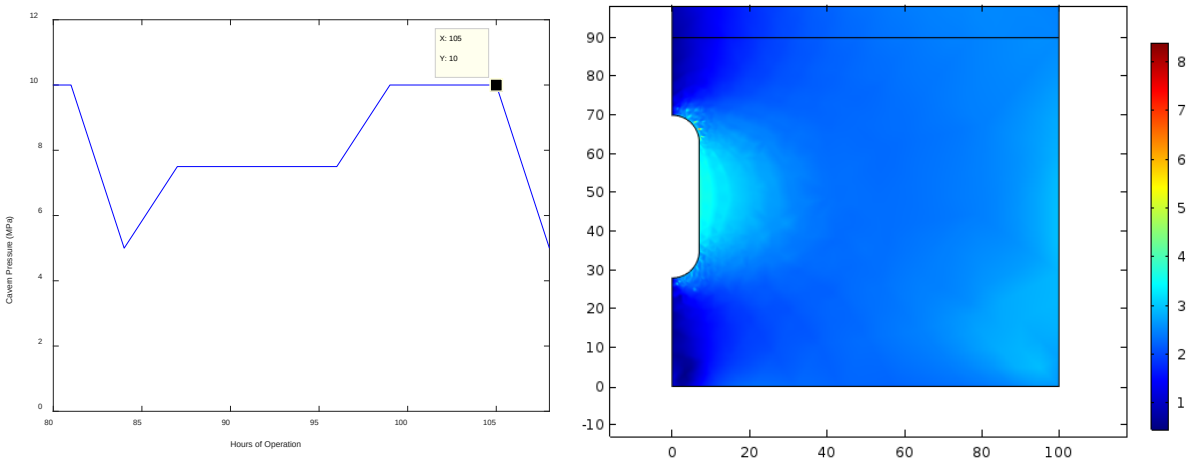

Figure 6.11 Salt Dilation at Maximum Pressure - 3 cycles – Pressure Cycle and FOS Spatial Plot

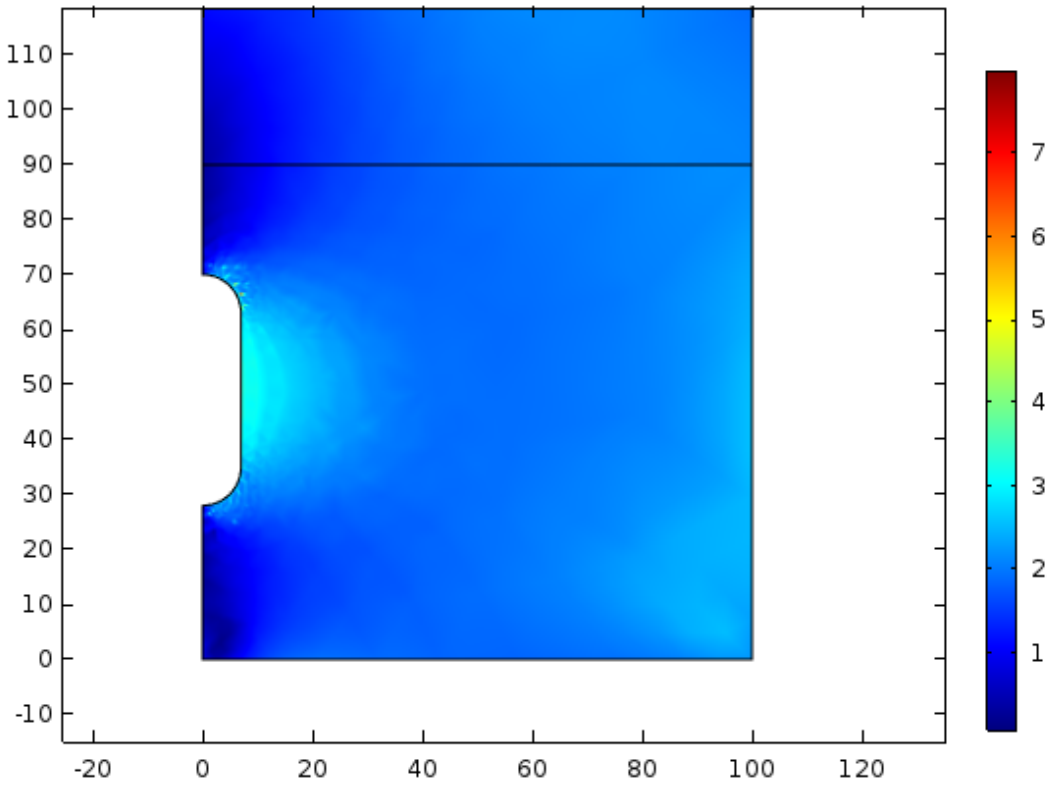

Figure 6.12 Salt Dilation at Minimum Pressure - 20 cycles

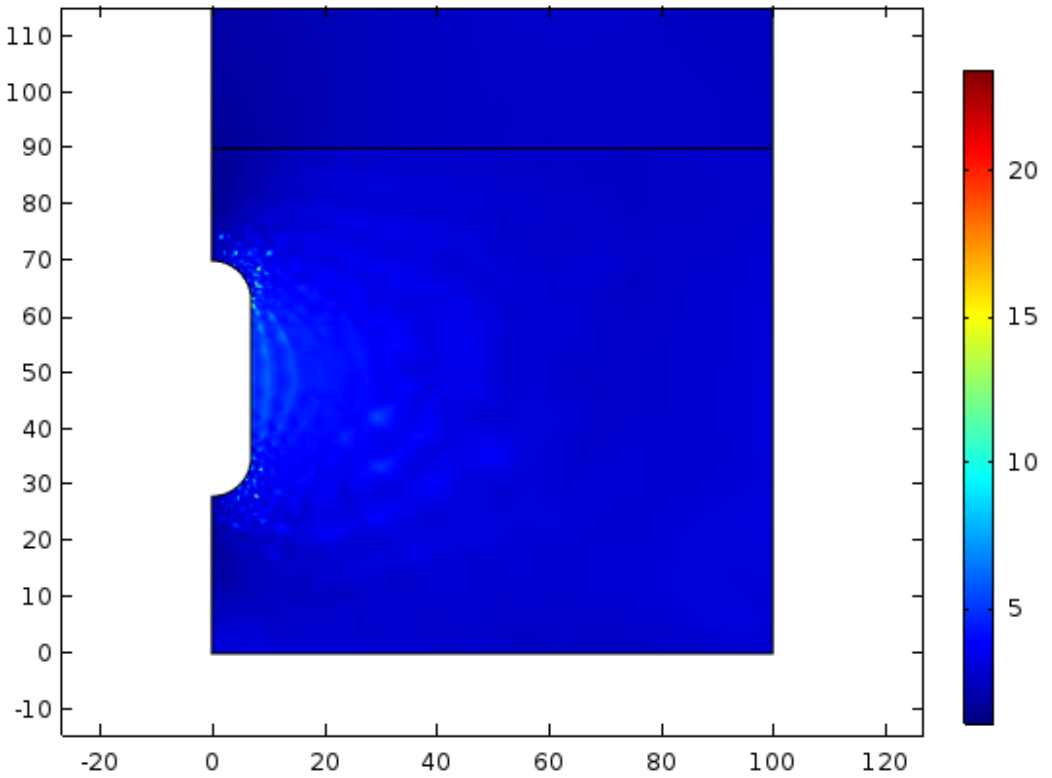

Figure 6.13 Salt Dilation at Maximum Pressure - 20 cycles

The cavern is technically feasible; after assessing the immediate and time dependent behaviour it can be determined that the cavern will be stable. The cavern volume and pressure did not need to be iterated on a geomechanical basis, however the design does not take full advantage of the pressure range the cavern is capable of. The minimum operating pressure is limited by the mechanical equipment selected. The greater the ratio of maximum to minimum pressure, the less volume is required in the cavern.

6.2.1 Grid Scale Energy Storage

In the next case study, the same site location will be used. The unit B salt will be used once more. This time the energy demand expected of the system will be much higher. The design algorithm will begin with determining the facility needs. It will be assumed that the energy storage needed is 1160 MWh, which is much more relevant to grid scale energy storage. Using the equipment selected the energy requirements can be met. It is also assumed that the system is adiabatic, yielding a round trip efficiency of 70%.

Table 6.5 Expander Equipment Selected to Meet Large-scale Storage Needs

Gas Turbine Parameters		
Turbine Power	290	MW
Mass flow rate	417	Kg/s
Inlet pressure HP turbine	42	Bar
Inlet temperature HP turbine	550	Deg C
Inlet pressure LP turbine	11	Bar
Inlet temperature LP turbine	825	Deg C
Compressor		
Mass flow rate	108	Kg/s
Rated compressor power	60	MW
Temperature at exit of after cooler	50	Deg C
Pressure at exit of after cooler	72	Bar
Assumed round trip efficiency	0.70	-

The pressure behaviour is approximated using the state space model. The time to pressurize the cavern to 7.2 MPa, is 16 hours. 4 hours will be needed to discharge the cavern to 4.2 MPa. The cavern will be idle for 4 hours at minimum pressure before being pressurized again. It will be assumed that cavern temperature fluctuates in a similar manner from 20 degrees Celsius to 45 degrees Celsius.

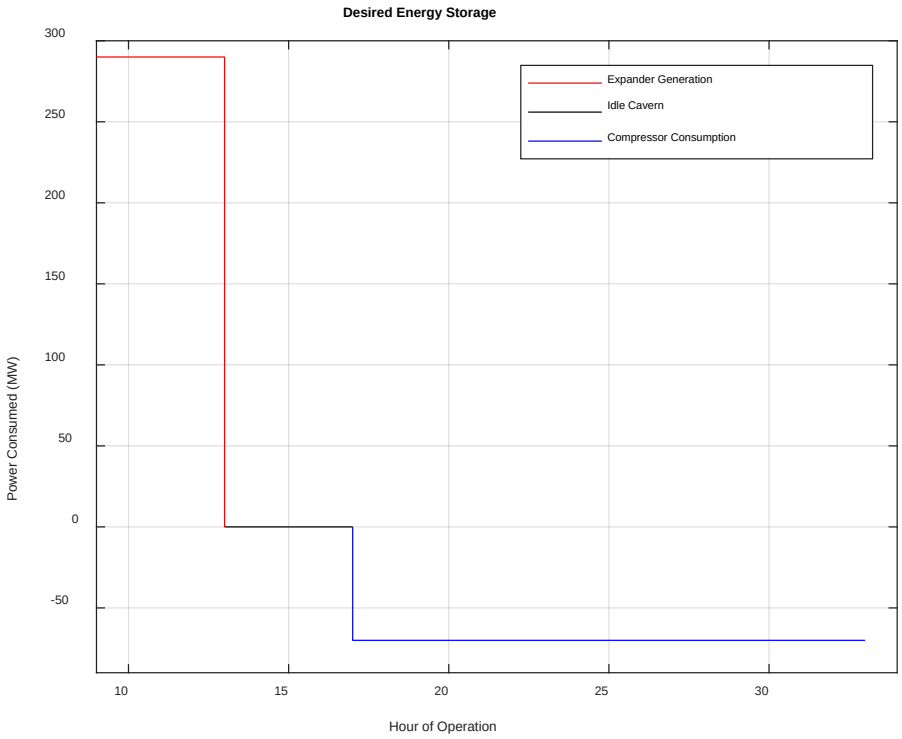

Figure 6.14 Energy Provided by Equipment – Hour of Operation vs Power

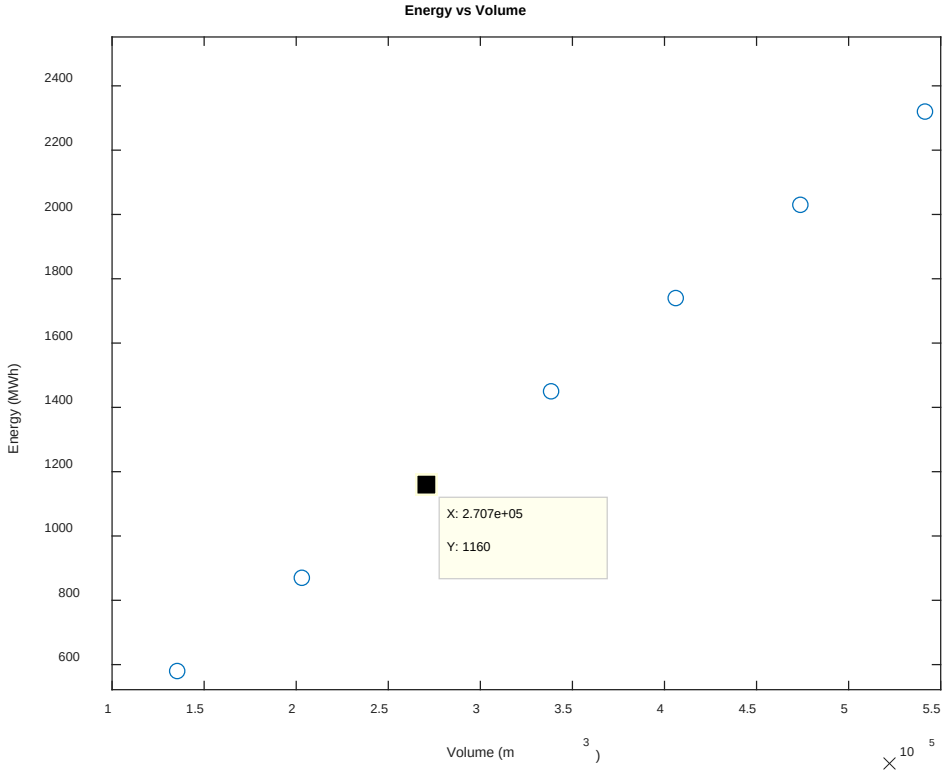

Figure 6.15 Volumetric Assessment - Energy vs Volume

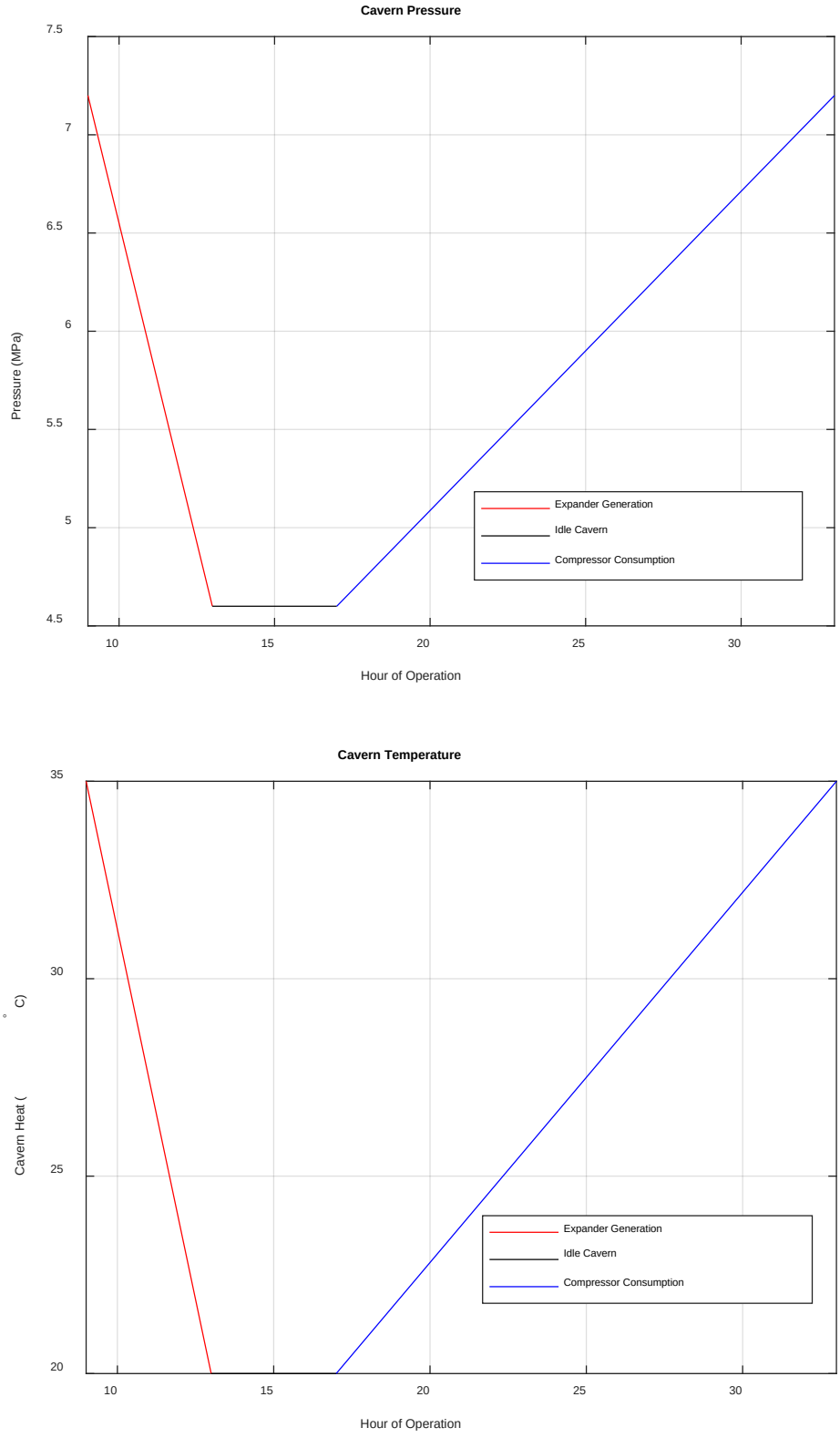

Figure 6.16 Cavern Pressure and Temperature

The volume required for such a large amount of energy is 270000 cubic meters. This a very large cavern, that would be difficult to create with single cylindrical shape in a salt layer that is only 90 meters thick. It is therefore necessary to consider other cavern geometries. The pressure is relatively conservative, so cavern stability may be achieved by adjusting the dimensions of the cavern as opposed to reassessing the mechanical equipment. If the cavern volume is too much for a cylindrical or spherical cavern, a horizontal gallery can be considered; however, it is more likely that multiple caverns will be used as opposed to the more complicated process of creating a horizontal cavern.

An ellipsoid will be created to achieve the required volume. It will be assumed that a sphere can still be used to approximate the cavern's closure rate. The same general guidelines will be used: the salt roof thickness will be at least a quarter of the diameter of the cavern, and the ratio of height to diameter must be no less than ½.

Table 6.6 Horizontal Gallery Dimensions

	Ellipsoid 1	Ellipsoid 2
Depth of Cavern Roof (m)	632	635
Diameter (m)	92	100
Height (m)	62	52

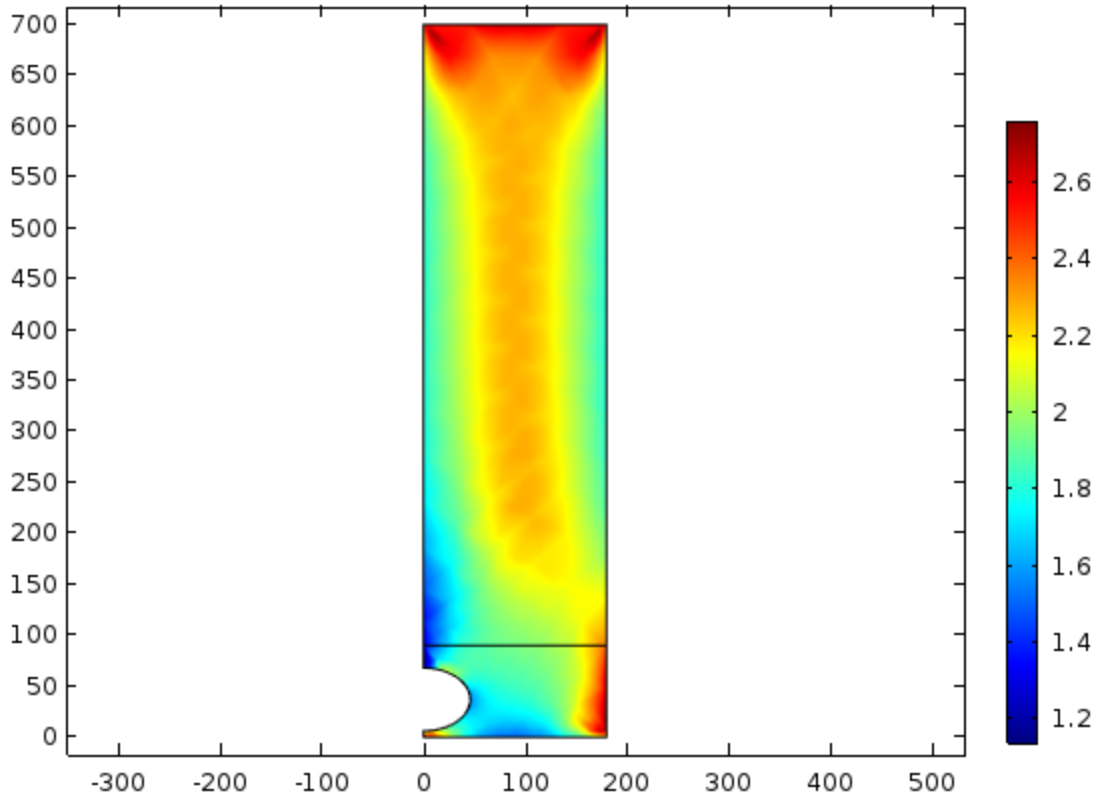

Figure 6.17 Elastic Loading at Maximum Pressure of Ellipsoid 1

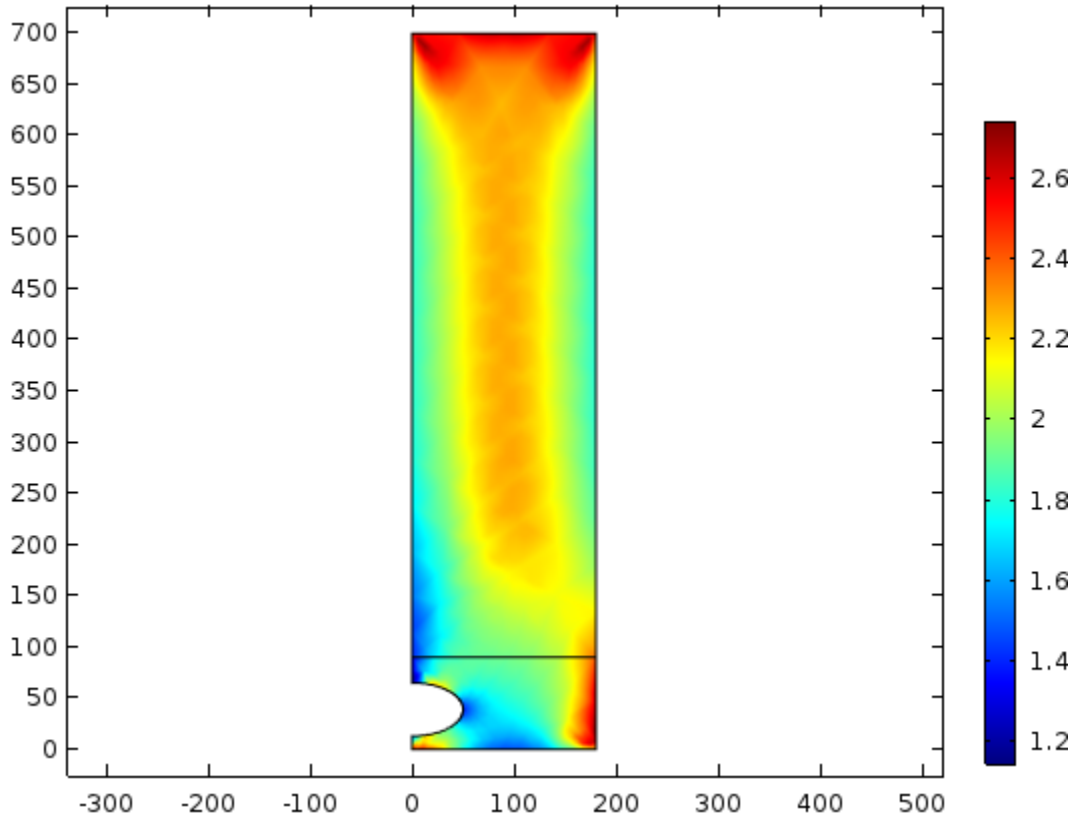

Figure 6.18 Elastic Loading at Maximum Pressure of Ellipsoid 2

In the initial comparison of elastic behavior at maximum operating pressure, it appears that the second ellipsoid is not suitable. The factor of safety against dilation in the elastic case is lower than the cylindrical cavern, as the ratio of H/D is close to ½. Further analysis was conducted on the first ellipsoid, to determine if it's time dependent behaviour would be suitable. Assessing the cavern at three cycles and twenty cycles, it was determined that this shape was not suitable. At this point multiple caverns should be assessed, to achieve the required volume. It is also possible to achieve the necessary factor of safety by lowering the maximum pressure requirements.

With four separate caverns situated at enough distance, the geomechanical assessment can be conducted for a cylindrical cavern. If each cavern is 67500 m^3, a cylindrical cavern is much easier to achieve.

Table 6.7 Suggested Cylindrical Cavern Dimensions

	Cylindrical cavern
Depth of Cavern Roof (m)	620
Diameter (m)	40
Height (m)	54
Cavern Spacing (m)	120

7.0 Conclusions

A design algorithm was developed for the first order design of Compressed Air Energy Storage in salt caverns. The main purpose of this study was to synthesize design components of a facility into a first order algorithm. This design algorithm can be applied to any site and is simplified to accommodate a range of energy storage requirements. The initial stage of design entails an understanding of salt extent and characteristics such as depth and thickness. With a geographic constraint, one may determine the energy needed, as far as delivery requirements. The site's energy needs will be a design constraint, and appropriate mechanical equipment can be selected which will yield the characteristics of necessary volume, pressure limitations, and discharge times. An energy consumption and production profile can be produced. From here one may assess the cavern's stability to determine a factor of safety. Upon several iterations to fine tune the shape and operability of the cavern, one may proceed into a cost benefit analysis and more rigorous technical design.

To demonstrate the design algorithm, two energy storage applications were developed in the same site location. One application was a small-scale energy storage case, and the other was for a much larger grid scale case. The small-scale case could be achieved with a single cavern of 6000 m^3, the cavern would have operating pressures between 5 and 10 MPa. It could provide 30 MWh of energy storage. The cavern was cylindrical, and dimensions made for geomechanically sound design. The other cavern was for 1160 MWh application, the mechanical equipment selected required 270,000 m^3 of storage. The operating pressures of the cavern were 4.6 and 7.2 MPa. A cylindrical cavern would not have enough salt thickness, to achieve the necessary volume, an ellipsoid was modelled alternatively. It was determined that the ellipsoid would not provide suitable stability. It is recommended to develop four cylindrical caverns instead.

The major contribution of this thesis was the development of an integrated design approach that synthesized mechanical and geomechanical aspects of design. The two case studies demonstrated the algorithm's effectiveness in both a large-scale and small-scale application.

7.1 Limitations

The design algorithm is simple, as its objective is to provide a first order design framework. A number of limitations are identified and are outlined below. Eliminating these limitations can lead to an improved model fidelity and provide results that are closer to real world behavior.

- The algorithm assumes energy infrastructure is sufficient at a given site. This can largely limit the amount of energy the facility can provide, as appropriate connectivity is essential for grid scale applications.
- The design algorithm assumes that heat management, and external heat are readily available. In some instances, an additional cavern may need to be created to store natural gas for reheating. It may also call for a wellbore for heat storage.
- The model assumes that an ideal gas with constant specific heat and a compressibility of 1.00. It also assumes no pressure loss during storage.
- The model also assumes no heat loss in the cavern; in reality, some amount of heat loss is expected will the cavern air is idle.

- The state-space model also assumes linear pressurizations of the cavern, in reality cavern pressure fluctuations would have slightly more curvature.
- The state-space model assumes negligible heat loss inside the cavern, when in reality heat loss should be accounted for to produce a more robust model.
- The design algorithm can account for three geometries however it is more likely that a variety of shapes could provide sufficient roof stability and satisfy the dilation criterion.
- The dilation criterion used is Ratigan's which is useful for limiting the number of empirical variables required, however it is likely that the Devries criterion could provide a more conservative estimate of safety factor.
- The model simulates heat transfer of the rock while approximating the cavern air as a flux.
- Heat expansion of the rock is not appropriately considered. It is known to cause additional stresses around the cavern.
- The salt behaviour model is not complex. The Norton-Hoff law is not dependent on many empirical variables, but it does not accurately capture the salt rebound effects. Other behaviour models have been developed that could provide a more extensive simulation.
- This numerical models exclusively consider industrial use case in the context of first order design. Extreme cases should be considered, where in pressure and temperature are rapidly depleted in the cavern.

7.2 Recommendations for Future Work

The design algorithm provides only first order technical feasibility. The algorithm would be even more useful if economic feasibility was assessed along the way. The strongest suggestion for future work is to consider economics as a factor. This would greatly influence each step of the design algorithm from equipment selection, to volume of storage, discharge and charging hours etc.

The model was only validated using analytic equations. Salt behaviour is complex and is dependent on the large-scale stresses of a location. The design algorithm should consider this in the early stages, particularly for diapiric or tectonic salt formations.

Extreme operational cases should be considered. It is possible to extract useful design suggestions if a critical pressure and temperature gradient was discovered.

It is also difficult to validate the model, as currently closed form solutions only exist for cylindrical caverns. Equations should be developed for spherical and ellipsoidal caverns.

The design algorithm should also consider greenhouse gas emissions and grid pricing factors such as global adjustment. These considerations may be important for decision making and are often the motivation for developing a CAES facility. Integration with renewable energy technologies such as solar thermal power plants can be studied.

References

Aneke, M., & Wang, M. (2016). Energy storage technologies and real life applications – A state of the art review. *Applied Energy*, *179*, 350–377. https://doi.org/10.1016/j.apenergy.2016.06.097

Aubertin, M., Julien, M. R., Servant, S., & Gill, D. E. (1999). A rate-dependent model for the ductile behavior of salt rocks. *Canadian Geotechnical Journal*, *36*(4), 660–674. https://doi.org/10.1139/cgj-36-4-660

Bérest, P., Bergues, J., Brouard, B., Durup, J. G., & Guerber, B. (2001). A salt cavern adandonment test. *International Journal of Rock Mechanics and Mining Sciences*, *38*(3), 357–368. https://doi.org/10.1016/S1365-1609(01)00004-1

Berest, P., Brouard, B., & Consulting, B. (2015). Thermo-mechanical effects in Compressed Air Storage (CAES)., (October 2010).

Bérest, P., & Djizanne, H. (2010). Effects of a rapid depressurization in a salt cavern.

Board, N. E. (2016). CANADA ' S RENEWABLE Energy Market Analysis 2016.

BP Energy Outlook 2019 edition The Energy Outlook explores the forces shaping the global energy transition out to 2040 and the key uncertainties surrounding that. (2019).

Brouard, B. (2012). Mechanical stability of a salt cavern submitted to high-frequency cycles, (2), 381–390. https://doi.org/10.1007/s12185-011-0857-0

Bruno, M. S. (2005). Geomechanical Analysis and Design Considerations for Thin-Bedded Salt Caverns (Final Report), (626), 142. Retrieved from https://www.osti.gov/scitech/servlets/purl/850502

Budt, M., Wolf, D., Span, R., & Yan, J. (2016). A review on compressed air energy storage : Basic principles , past milestones and recent developments. *Applied Energy*, *170*, 250–268. https://doi.org/10.1016/j.apenergy.2016.02.108

Crotogino, F., Gmbh, K. B. B., Mohmeyer, K., Scharf, R., & Bremen, E. O. N. K. (2001). Huntorf CAES : More than 20 Years of Successful Operation by, (April).

Das, T., & Mccalley, J. D. (2012). *Compressed Air Energy Storage*. *Iowa State*

University. https://doi.org/10.5772/52221

Deghani-Sanij, A. R., Tharumalingam, E., Dusseault, M. B., & Fraser, R. (2019). Study of energy storage systems and environmental challenges of batteries. *Renewable and Sustainable Energy Reviews*, *104*(January), 192–208. https://doi.org/10.1016/j.rser.2019.01.023

Han, G., Bruno, M., Lao, K., Young, J., & Dorfmann, L. (2006). Gas Storage and Operations in Single Bedded Salt Caverns : Stability Analyses. *2006 SPE Gas Technology Symposium*, (May), 1–10. https://doi.org/10.2118/99520-MS

Hewitt, D. . (1962). *Salt in Ontario*.

Hudec, M. R., & Jackson, M. P. A. (2007). Terra infirma : Understanding salt tectonics, *82*, 1–28. https://doi.org/10.1016/j.earscirev.2007.01.001

Li, S. Y., & Urai, J. L. (2016). Rheology of rock salt for salt tectonics modeling. *Petroleum Science*, *13*(4), 712–724. https://doi.org/10.1007/s12182-016-0121-6

Liang, W. G., & Zhao, Y. S. (2005). A new technology of controlled solution mining for salt deposits, 303–308.

Liu, W., Jiang, D., Chen, J., Daemen, J. J. K., Tang, K., & Wu, F. (2018). Comprehensive feasibility study of two-well-horizontal caverns for natural gas storage in thinly-bedded salt rocks in China. *Energy*, *143*, 1006–1019. https://doi.org/10.1016/j.energy.2017.10.126

Lord, F. D. (2017). *Identification and Estimation of Greenhouse Gas Reduction Opportunities through the Implementation of CAES in Canada*. University of Waterloo.

Lux, K.-H. (2009). Design of salt caverns for the storage of natural gas, crude oil and compressed air: Geomechanical aspects of construction, operation and abandonment. *Geological Society, London, Special Publications*, *313*(1), 93–128. https://doi.org/10.1144/SP313.7

Ma, H. L., Yang, C. H., Liu, J. F., & Chen, J. W. (2013). The influence of cyclic loading on deformation of rock salt, (June), 63–68. https://doi.org/10.1201/b14917-10

Powersouth. (2014). *Compressed Air Energy Storage*.

Raju, M., & Kumar Khaitan, S. (2012). Modeling and simulation of compressed air

storage in caverns: A case study of the Huntorf plant. *Applied Energy*, *89*(1), 474–481. https://doi.org/10.1016/j.apenergy.2011.08.019

Shahmorad, Z., Salarirad, H., & Molladavoudi, H. (2016). A study on the effect of utilizing different constitutive models in the stability analysis of an underground gas storage within a salt structure. *Journal of Natural Gas Science and Engineering*, *33*, 808–820. https://doi.org/10.1016/j.jngse.2016.06.011

Su, M. (1995). The Potential of Solution Caverns for Permanent Disposal of Solid Wastes.

Succar, S., & Williams, R. (2008). Princeton Environmental Institute PRINCETON UNIVERSITY Energy Systems Analysis Group Compressed Air Energy Storage : Theory , Resources , And Applications For Wind Power Acknowledgments. *Princeton Environmental Institute Report*, *8*(April), 81. Retrieved from http://healutah.org/files/Succar2008_Part1.pdf

Wang, L., Bérest, P., & Brouard, B. (2015). Mechanical Behavior of Salt Caverns: Closed-Form Solutions vs Numerical Computations. *Rock Mechanics and Rock Engineering*, *48*(6), 2369–2382. https://doi.org/10.1007/s00603-014-0699-1

Appendix A – Machine Datasheet

WP6550, 5 Stage Water Cooled Compressor

Quick Reference Specifications

Operating Pressure Range	2900 to 7000 psi
Flow Rate	160 to 237 SCFM
Required Power	105 to 197 hp
Stages/Cylinders	5/6
Gas/Medium	Air, Nitrogen, Natural Gas, Bio-Methane

WP6550 Data Sheet				
	Operating Pressure	Speed		UNITS
		1180 RPM (60 Hz)	1780 RPM (60 Hz)	
Flow & Power	5000 PSIG	160	236	SCFM
		117	188	HP
	6000 PSIG	160	236	SCFM
		120	192	HP
	6500 PSIG	160	236	SCFM
		123	196	HP
	7250 PSIG	160	235	SCFM
		125	197	HP
Technical Specifications	Motor rating	125	200	HP
	Current @ 460 Volts	143	230	Amps
	Weight of block and motor	8800	8800	Pounds
	Noise level @ 3 ft	94	98	dB(A)
	Heat dissipation to water	4700	7500	Btu/min
	Heat dissipation to ambient	820	1300	Btu/min
	Cooling water needed	35	53	GPM
	Residual oil content at gas outlet (without filtration)	<5		ppm
	Delta temperature (gas oultet vs. Water inlet)	< 18		°F
	Operational ambient temperature range	130		°F
	Operating pressure range	2900-7250		psig
	Oil sump capacity	13		Gallons
	Dimensions of block and motor (L x W x H)	106 x 65 x 65		Inches
	Cooling method	Water-Cooled		
	Drive type	Direct Drive		
	Stages/Cylinders	5/6		

* All data is with 5 % tolerance and is related to ambient conditions of 68 ° F and 14.7 PSIA.

Solar Turbines
A Caterpillar Company

SATURN 20
Gas Turbine Generator Set

Power Generation

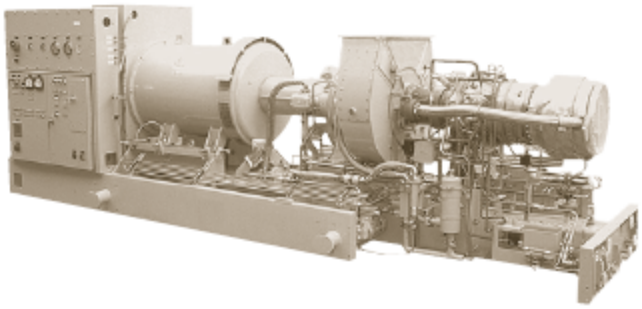

General Specifications

Saturn® 20 Gas Turbine

- Industrial, Single-Shaft
- Axial Compressor
  - 8-Stage
  - Pressure Ratio: 6.7:1
  - Inlet Airflow: 5.8 kg/sec (12.8 lb/sec)
- Combustion Chamber
  - Annular-Type
  - 12 Fuel Injectors
  - Torch Ignitor System
- Turbine
  - 3-Stage, Reaction
  - Max. Speed: 22,300 rpm
- Bearings
  - Journal: Multi-Ramp Sleeve
  - Thrust: Fixed Tapered Land
- Coatings
  - Compressor: Inorganic Aluminum
  - Turbine and Nozzle Blades: Precious Metal Diffusion Aluminide
- Velocity Vibration Transducer

Main Reduction Drive

- Epicyclic Type
- 1500 or 1800 rpm

Generator

- Type: Salient Pole, 3 Phase, 6 Wire, Wye Connected, Synchronous, with Brushless Exciter
- Construction Options
  - Open Drip Proof
- Antifriction (Ball) Bearings
- Sleeve Bearings (Option)
- Voltage Regulation
  - Solid-State Regulation with Permanent Magnet Generator
- Insulation/Rise Options
  - NEMA Class F with F Rise
  - NEMA Class F with B Rise
- Voltages: 380 to 4160 Volts
- Frequency: 50 or 60 Hz

Package

- Base Frame with Drip Pans
- 316L Stainless Steel Piping ≤4" dia
- Compression-Type Tube Fittings
- Electrical System Options
  - NEC, Class I, Group D, Div. 2
  - CENELEC, Zone 2
- Turbotronic™ Microprocessor Control System
  - Freestanding Control Console
  - Color Video Display
  - Vibration Monitoring
- Control Options
  - 24-VDC Control Battery/Charger
  - Gas Turbine and Package Temperature Monitoring
  - Serial Link Supervisory Interface
  - Turbine Performance Map
  - Historical Displays
  - Printer/Logger
  - Field Programming
- Start Systems
  - Pneumatic
  - Direct-Drive AC
- Fuel Systems
  - Natural Gas
  - Liquid
  - Dual (Gas/Liquid)
  - Alternate Fuels
- Integrated Lube Oil System
  - Turbine-Driven Accessories
- Oil System Options
  - Oil Cooler
  - Oil Heater
  - Tank Vent Separator
  - Flame Trap
- Axial Compressor Cleaning Systems
  - On-Crank
  - On-Crank/On-Line
  - Cleaning Tank
- Air Inlet and Exhaust System Options
- Enclosure and Associated Options
- Factory Testing of Turbine and Package
- Documentation
  - Drawings
  - Quality Control Data Book
  - Inspection and Test Plan
  - Test Reports
  - Operation and Maintenance Manuals

Solar Turbines
A Caterpillar Company

SATURN 20
Gas Turbine Generator Set

Power Generation

Performance

Output Power	1210 kWe
Heat Rate	14 795 kJ/kWe-hr (14,025 Btu/kWe-hr)
Exhaust Flow	23 540 kg/hr (51,890 lb/hr)
Exhaust Temp.	505°C (940°F)

Application Performance

Steam (Unfired)	4.0 tonnes/hr (8715 lb/hr)
Steam (Fired) 1536°C (2800°F)	17.7 tonnes/hr (39,130 lb/hr)
Chilling (Absorp.)	3410 kW (970 refrigeration tons)

Nominal rating – per ISO
At 15°C (59°F), sea level
No inlet/exhaust losses
Relative humidity 60%
Natural gas fuel with
LHV = 35 MJ/Nm³ (940 Btu/scf)
No accessory losses
Engine efficiency: 24.3%
(measured at generator terminals)

Available Power

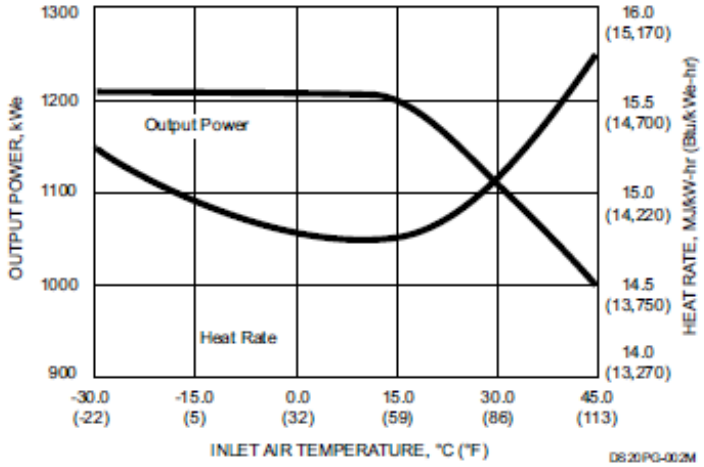

Enclosure Access and Maintenance Space

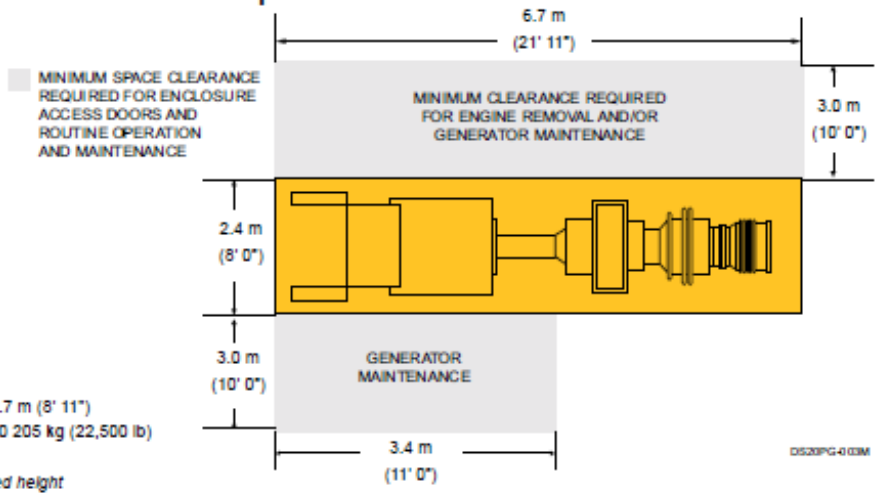

Package Height: 2.7 m (8' 11")
Package Weight: 10 205 kg (22,500 lb)

Dry weight, enclosed height

Solar Turbines Incorporated
P.O. Box 85376
San Diego, CA 92186-5376

DS20PG/1118/EO

FOR MORE INFORMATION

Telephone: (+1) 619-544-5352
Email: powergen@solarturbines.com
Internet: www.solarturbines.com

Appendix B – Matlab Code (Model Validation & Volumetrics)

```
clc
clear all
close all

p_b = 5.5e6;
b = 100;
a = 7;
n = 5;

r = 2:2:10
sigr_analytic = -p_b+p_b*((b./r).^(2/n)-
1)/((b/a)^(2/n)-1)

%Output from Comsol
sigr_numerica = [5.2e6 1.98e6 0.5e6 -0.39e6 -
1.10e6]

sigt_analytic = -p_b+p_b*(((2-
n)/n)*(b./r).^(2/n)+1)/((b/a)^(2/n)-1)

%Output from Comsol
sigt_numerica = [1.1e7 -0.90e7 -0.77e7 -0.7e7 -
0.7e7]

clc
clear all
close all
%----calculations----%

R = 8.31E-03; % Universal gas constant
Mweight = 2.90E-02; %Molecular weight of dry air
Atmp = 100; %atmospheric pressure

n_m = str2num(get(handles.edit3,'String')); %
Efficiency of turbine
n_g = str2num(get(handles.edit4,'String'));  %
Efficiency of generator
```

```
pf  = str2num(get(handles.edit5,'String'));  % Pipe
friction losses
ma_d = str2num(get(handles.edit13,'String')); % air
mass flow rate

IsAdiabatic = get(handles.radiobutton2,'Value')
if IsAdiabatic == 1
    fm_d = 0;
    bus = '0';
    set(handles.edit14,'String','0')
else
fm_d = str2num(get(handles.edit14,'String')); %
fuel mass flow rate
end
%--------design objective---------%

power_out = str2num(get(handles.edit15,'String'));
%MW desired power output
duration = str2num(get(handles.edit16,'String'));
%hours
e_gen = duration*power_out; %MWH

%---------check num of vessels-------%
n_vessels = str2num(get(handles.edit1, 'String'));
%Number of vessels
if n_vessels >= 1
else
    f = errordlg('Please enter number of
vessels','Error');
end

%---cavern iterations---%
uplim = str2num(get(handles.edit6,'String'));
lplim = str2num(get(handles.edit7,'String'));
ts2 = str2num(get(handles.edit8,'String'));
%--------Storage---------%
[cps,cvs,ks]=getTemp(ts2);
```

```
%input paramets? or maybe iterate to such values

%---high pressure turbine---%
% cp1 = 1.099; %air heat cap, kJ/kg*K
% cv1 = 0.812; %air heat cap, kJ/kg*K
% k1 = 1.353;
p1 = str2num(get(handles.edit9,'String'));
T1 = str2num(get(handles.edit10,'String'));
[cp1,cv1,k1]=getTemp(T1);
%---low pressure turbine---%
% cp2 = 1.155;
% cv2 = 0.868;
% k2 = 1.331;
p2 = str2num(get(handles.edit11,'String'));
T2 = str2num(get(handles.edit12,'String'));
[cp2,cv2,k2]=getTemp(T1);

alpha = n_m*n_g*cp2*T2*(1+fm_d/ma_d);

beta = cp1*T1/cp2/T2*(1-(p2/p1)^(1-1/k1));


%-----constant turbine inlet pressure----%
Egen_vs = alpha*Mweight*uplim/R/ts2*(beta+1-
(Atmp/p2)^(1-1/k2))...
    *(1-(lplim/uplim)^(1/ks))/3600;


%------variable turbine inlet pressure----%
egenvs_vt = alpha*Mweight*uplim/R/ts2*((beta+1)*(1-
(lplim/uplim)^...
    (1/ks))-(p1*Atmp/p2/pf/uplim)^(1-
1/k2)/ks/(1/ks+1/k2-1)*...
    (1-(lplim/uplim)^(1/ks+1/k2-1)))/3600;

IsConstant = get(handles.radiobutton12,'Value')
if IsConstant ==1
    vfinal = ((1/Egen_vs)*e_gen*1000)/n_vessels
else
```

```
    vfinal = ((1/egenvs_vt)*e_gen*1000)/n_vessels
end
vfinal

vfinalstring = num2str(vfinal)
vs = ((1/Egen_vs)*e_gen*1000)/n_vessels;
vs_t = num2str(vs);
%VOLCALCS
vs_vt = ((1/egenvs_vt)*e_gen*1000)/n_vessels;
vs_vtt = num2str(vs_vt);



vfinal

clc
clear all
close all
% pc = str2num(get(handles.edit1,'String'));
%Compressor power consumption
% temp = str2num(get(handles.edit2,'String'));  %K
ambient input temperature
% [cp1, cv1, y ] = getTemp(temp); % return specific
heat and ratio
% p_input = str2num(get(handles.edit3,'String')); %
atmospheric air
% p_out = str2num(get(handles.edit4,'String')); %
output of machine
%
% m_ain = pc./((cp1*temp)*((p_out/p_input)^((y-
1)/y)-1))
% %----------------Inputs
% Pg = str2num(get(handles.edit5,'String')); %Power
generated (kW)
% T1 = str2num(get(handles.edit6,'String')); %HP
turbine inlet (K)
% T2 = str2num(get(handles.edit7,'String')); %LP
turbine inlet (K)
```

```
% P1 = str2num(get(handles.edit8,'String')); %LP
Pressure
% P2 = str2num(get(handles.edit9,'String')); %HP
Pressure, two turbines
% Pb = str2num(get(handles.edit10,'String'));
%atmospheric pressure in barr also
% m_dot_a_out =
str2num(get(handles.edit11,'String')); %mass rate
out ratio
% % m_dot_fuel =
str2num(get(handles.edit12,'String'));; %fuel rate
% [cp1,cv1,k1]=getTemp(T1);
% [cp2,cv2,k]=getTemp(T2);
% nm = 0.7; %motor efficiency
% ng = 0.8; %generator efficiency
% k = k1;
%
% %---------------calcs
% nnct = ng*nm*cp2*T2;
% zzrg = 1+(m_dot_a_out);
% cp1t1_cp2t2 = cp1*T1/cp2*T2;
% zzrf = 1-(P2/P1)^((k-1)/k);
% zzrd = (Pb/P2)^((k-1)/k);
% full = nnct*zzrg*cp1t1_cp2t2*zzrf*zzrd;
%
% mout = Pg/full;
% %--------------cavernprocess
Tstorage = str2num(get(handles.edit12,'String'));
%time of storage
Vstorage = str2num(get(handles.edit13,'String'));
%volume m^3
Pmin = 3 ;%str2num(get(handles.edit14,'String'));
%LP Pressure
Pmax = 10;%str2num(get(handles.edit15,'String'));
%LP Pressure
m_ain = 0.077;
mout  = 0.28;
MassMax = Pmax*Vstorage/(287.15*Tstorage);%PV=mRT
```

```
Timeinitialcharge = MassMax./m_ain; %seconds
MassMin = Pmin*Vstorage/(287.15*Tstorage);%PV = mRT
Timedischarge = (MassMax-MassMin)/mout; %seconds
Timecharge = (MassMax-MassMin)./m_ain;
% Pbox = [0.1,Pmax,Pmin,Pmax]
% Tbox =
[0,Timeinitialcharge,Timedischarge,Timecharge];
% Tbox = Tbox/3600
Pbox = [0.1,10,3,10]
Tbox = [0,4.7,6.7,10.1];
```

Appendix C – Comsol Output Plots

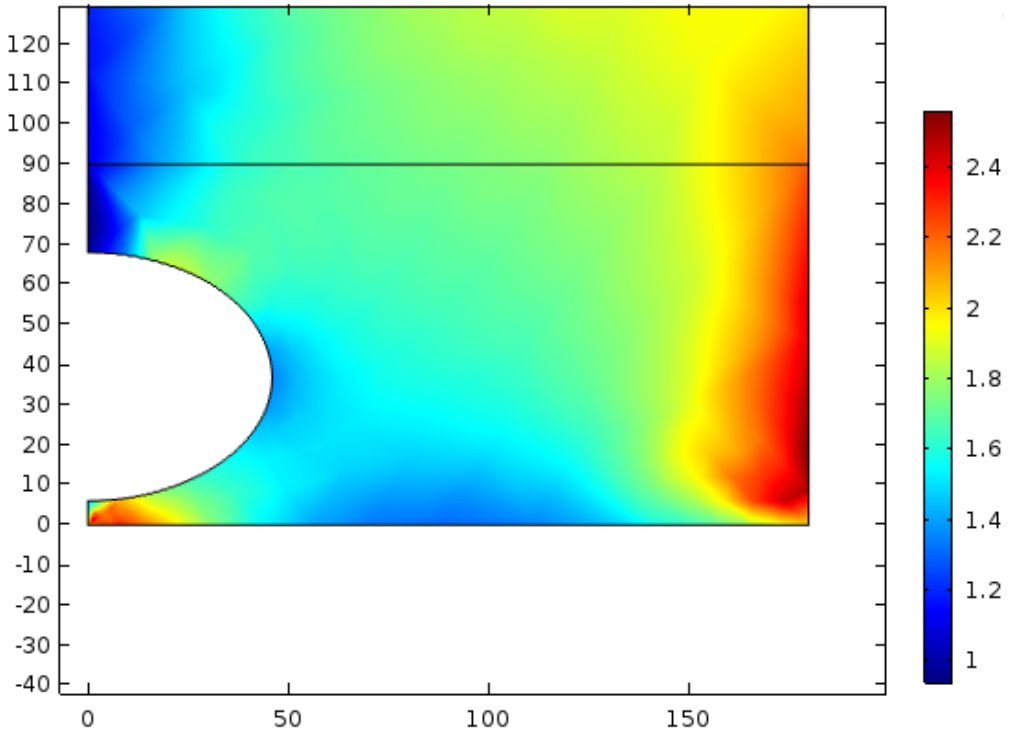

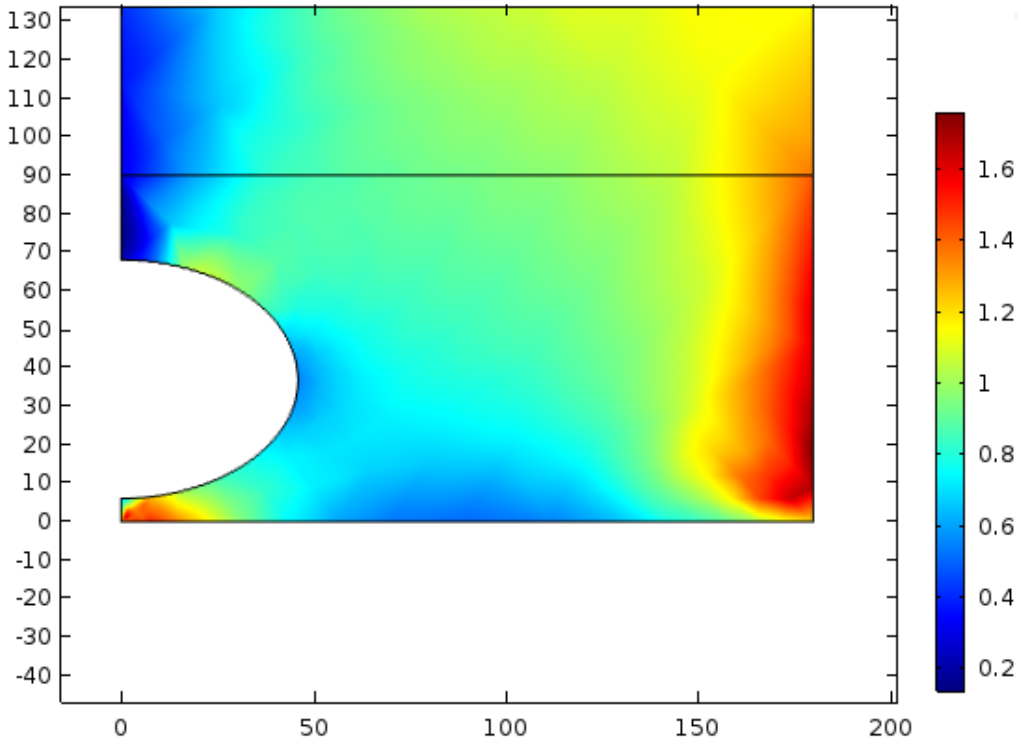

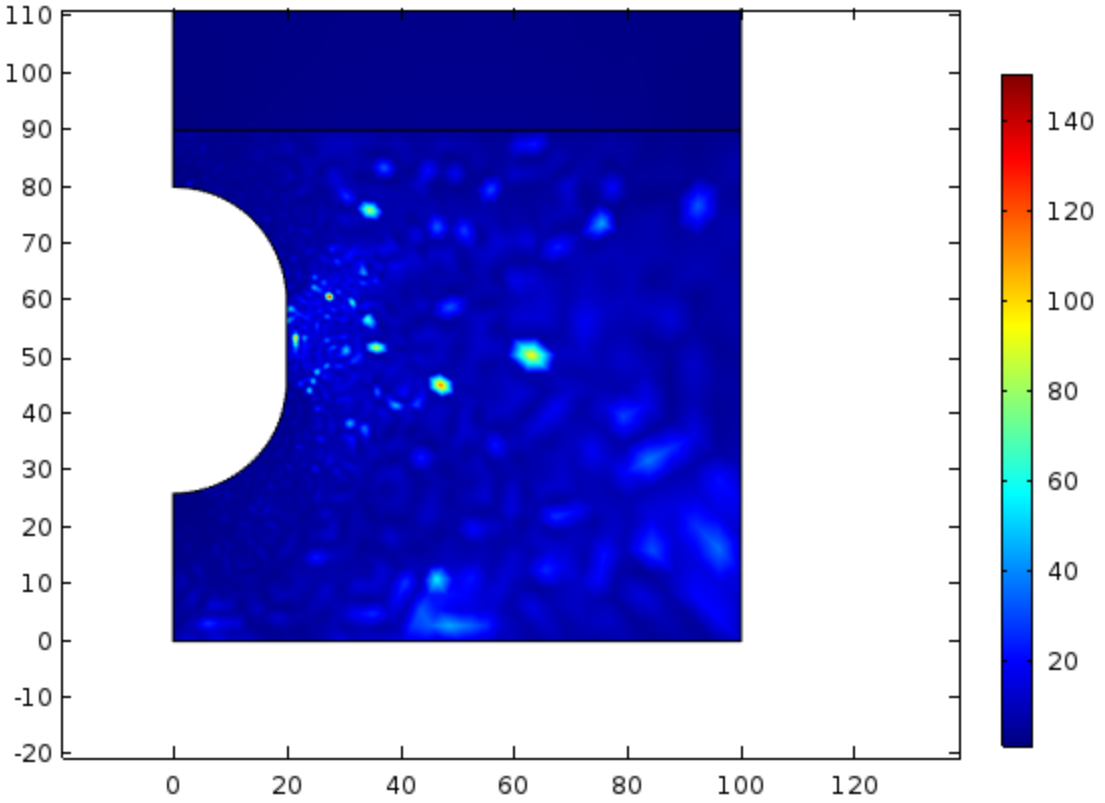

Small cylinder at maximum pressure

Appendix D – Comsol Output Data

Von Mises for Cylindrical Cavern 1

% Model:	chap6_goderich.mph	
% Version:	COMSOL 5.2.1.152	
% Date:	Jul 31 2019, 18:19	
% Table:	Evaluation 2D - Interactive 2D values	
% x	y	Value
9.173805236816406	67.17871856689453	10.649969350632002
8.698284149169922	69.55630493164062	9.68659474975108
4.894130706787109	68.60523986816406	21.24851695311434
83.34930419921875	79.80115509033203	1316496.35886797
2.6885337829589844	81.31281280517578	1429373.9348744994
6.892444610595703	82.51393127441406	1500729.867875864
4.490207672119141	77.1089096069336	2948647.2885590126
4.490207672119141	8.044666290283203	395493.38518555404
6.2918853759765625	2.639636993408203	234492.26125474728
6.2918853759765625	5.642429351806641	254817.74772112447
6.2918853759765625	13.449691772460938	901490.0578428605
0.8868560791015625	23.659191131591797	3973315.874828798
2.0879745483398438	80.71226501464844	1509613.4717343645
7.493000030517578	7.444122314453125	354560.17528206686
2.0879745483398438	12.248588562011719	759070.6668149586
2.0879745483398438	17.053058624267578	1363697.531728259
2.6885337829589844	77.10892486572266	2628503.020762125
0.8868560791015625	71.70389556884766	9310825.807064388
0.5161046981811523	27.166547775268555	1.2015772669191472E7
0.29344844818115234	26.498579025268555	8417610.979422634
1.4067277908325195	22.936080932617188	3454025.7043072367
1.4067277908325195	15.811086654663086	1202104.4490982834
0.29344844818115234	71.25245666503906	1.0150969802961588E7
0.29344844818115234	26.053266525268555	6665897.293968031
1.1840715408325195	22.045455932617188	2732103.5147220274
36.141075134277344	55.44386291503906	3023378.778148351
97.8523941040039	57.511505126953125	757632.856805861
63.783538818359375	52.40117645263672	1443740.8954798935
37.25849151611328	47.0474967956543	3014098.087264185
99.31249237060547	51.42778015136719	683008.1559620125
11.118799209594727	48.24603271484375	5023982.445051907
30.255821228027344	54.625030517578125	3734785.2022115737
10.055631637573242	50.37237548828125	4743996.161473767
4.73979377746582	26.98267364501953	9364368.026199618
33.60595703125	53.540863037109375	3337117.456458685
50.603153228759766	50.46315002441406	1989776.2430382876
27.80044937133789	50.46315002441406	4144054.1154753417
38.34806823730469	33.80880355834961	2488927.5578873856
21.932235717773438	46.63367462158203	4991573.161425676
11.672348022460938	46.63367462158203	5152093.132640174
29.114166259765625	51.25062561035156	3929850.9047287935
15.2633056640625	49.711639404296875	5436242.011068654
26.03619384765625	53.81559753417969	4292661.812649408
51.17292785644531	50.224639892578125	1954795.8419465963
68.10176086425781	49.19864273071289	1323538.1230123306
22.211273193359375	53.23847579956055	662169.687980833
22.211273193359375	53.23847579956055	662169.687980833
15.61859130859375	51.590309143066406	-29394.16067089917
16.717376708984375	51.590309143066406	-3458872.1858161436
9.167558670043945	49.482887268066406	-2983200.083601453
7.92600154876709	49.52164840698242	-2728117.4647661573
9.962203025817871	44.645477294921875	-3233076.5496666343
9.962203025817871	44.645477294921875	-3233076.5496666343
14.838371276855469	48.77146911621094	-3540135.945142959
16.445899963378906	49.14655685424805	-3533007.1503468435

7.175821304321289	50.86125564575195	-2572824.1419731625
7.390158653259277	52.415199279785156	-2640701.118694001
12.768156051635742	48.08064270019531	-3434946.0479614837
14.109476089477539	50.31617736816406	-3494387.3353731814
31.09954833984375	50.76329040527344	-2275701.4583674604
9.19129753112793	48.52775573730469	-2993421.7931838823
13.215261459350586	48.52775573730469	-3462764.9139494
20.368976593017578	48.08064270019531	-3269315.790514525
25.287155151367188	48.08064270019531	-2827839.3866550853
39.14747619628906	48.08064270019531	-1784454.5406320994
42.724334716796875	48.08064270019531	-1581120.0650689597
47.64250946044922	44.950897216796875	-1332909.0877243495
9.517563819885254	45.891937255859375	-3098186.16372278
14.062651634216309	45.802818298339844	-3499867.506571371
7.11134147644043	44.28778839111328	-2663649.3583342275
8.893728256225586	45.089866638183594	-2999147.227747204
9.250205993652344	45.0007438659668	-3074521.7327206917
9.161087036132812	44.911624908447266	-3061692.3967618365
10.497876167297363	44.911624908447266	-3325727.651006942
9.428444862365723	48.11992263793945	-3040979.022529495
12.102025032043457	46.69401168823242	-3415076.3298099935
16.112396240234375	47.317848205566406	-3550551.0560678393
20.12276840209961	46.42665481567383	-3254979.3893235545
11.0325927734375	43.21835708618164	-3403323.5432124874
13.706171989440918	42.05980682373047	-3467910.337481917
16.112396240234375	41.525089263916016	-3231828.353486097
18.518619537353516	42.14892578125	-3111786.8150633615
20.12276840209961	42.505401611328125	-2986293.8188584875
8.893720626831055	45.00074768066406	-3004864.6777318786
10.58698844909668	45.178985595703125	-3329447.6057870165
13.884406089782715	45.268104553222656	-3498824.0394719937
17.716537475585938	45.089866638183594	-3366466.5849132845
22.083389282226562	44.376914978027344	-2960429.240668031
26.62847900390625	43.93131637573242	-2537774.179710729
29.034698486328125	43.84219741821289	-2348413.1564424555
7.735169410705566	46.07018280029297	-2733282.4408883816
9.60667610168457	46.33753967285156	-3106938.5287679457
12.191137313842773	46.33753967285156	-3425296.386297255

Appendix E– Sample Temperature Penetration

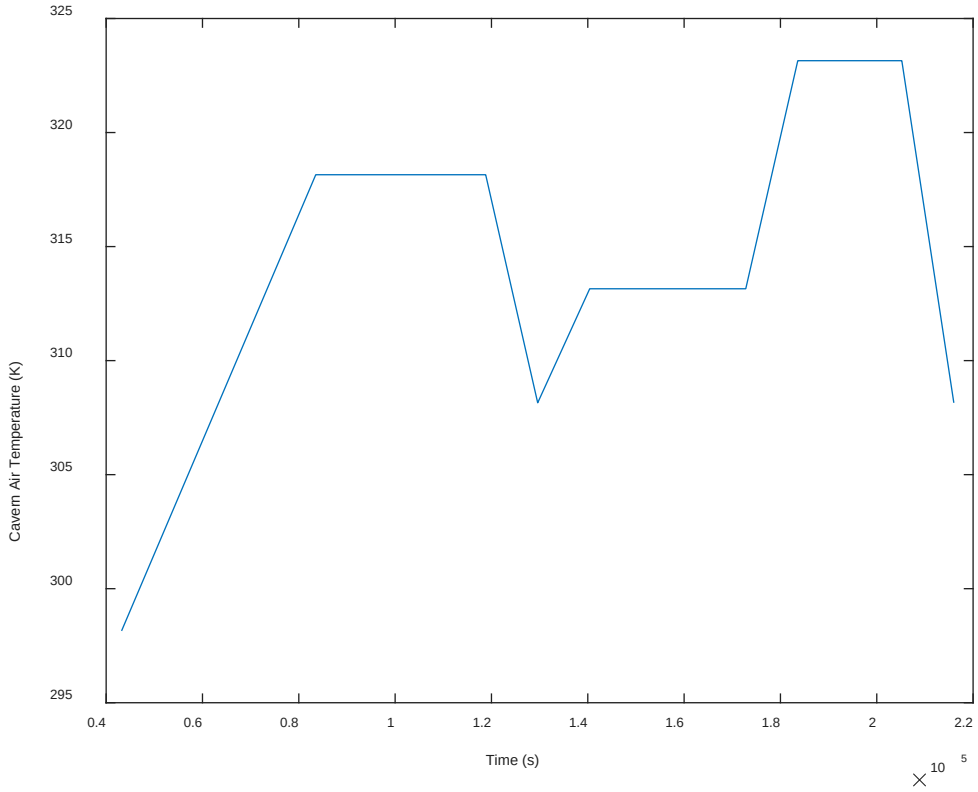

T = 25 C

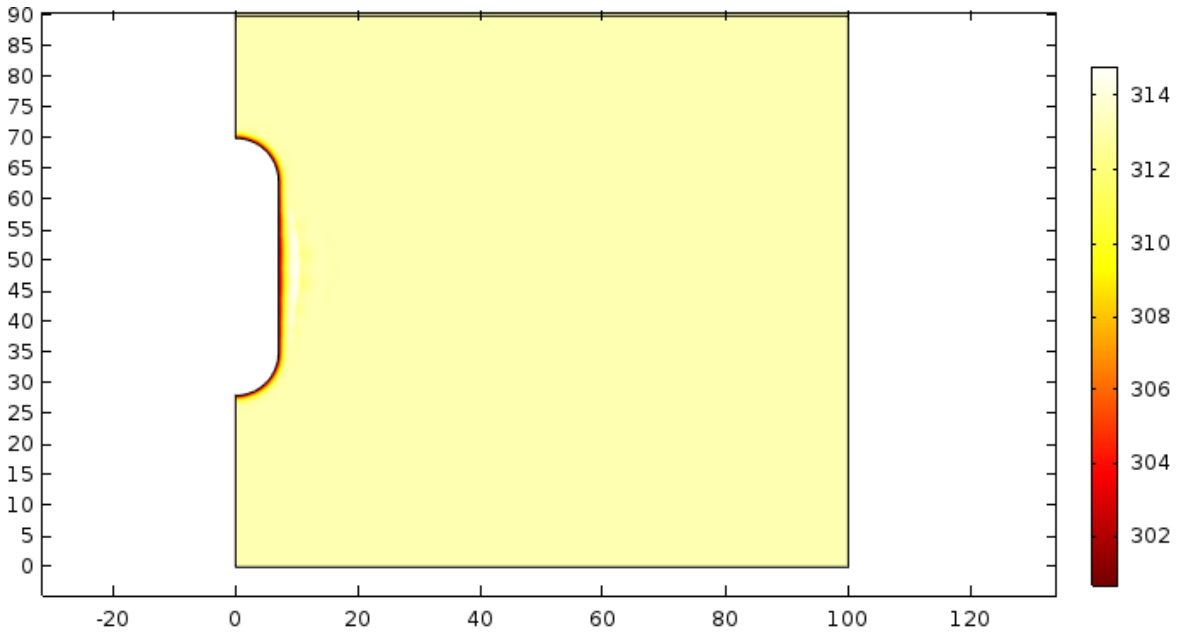

T = 40 C

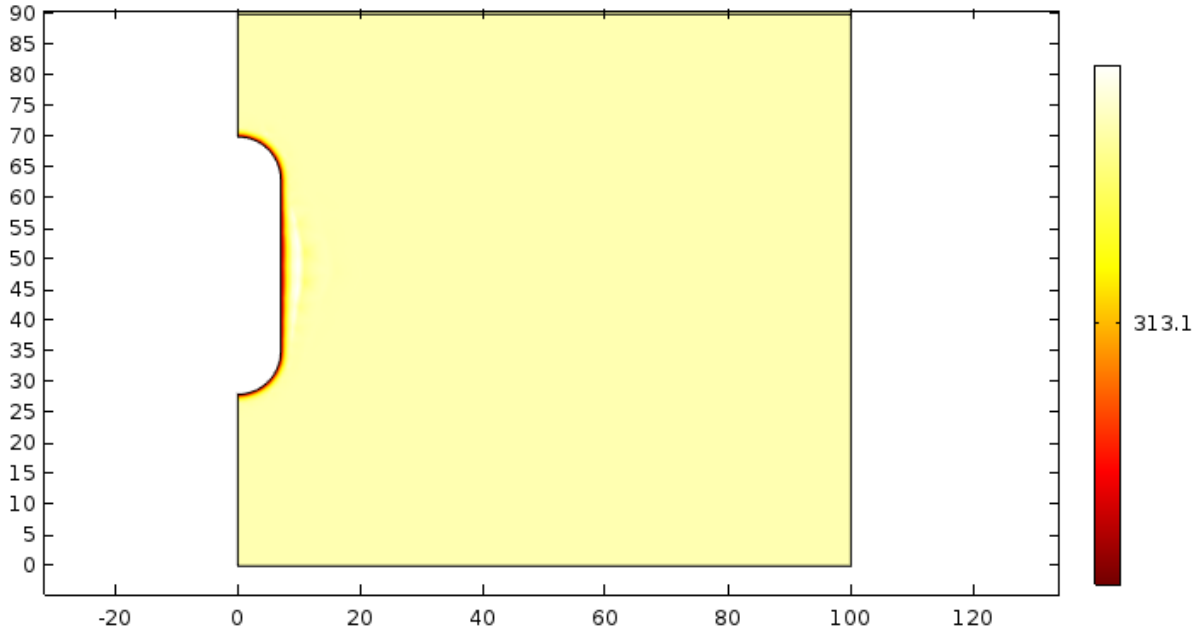
90
85
80
75
70
65
60
55
50
45
40
35
30
25
20
15
10
5
0
-20
0
20
40
60
80
100
120
313.1

T = 50 C

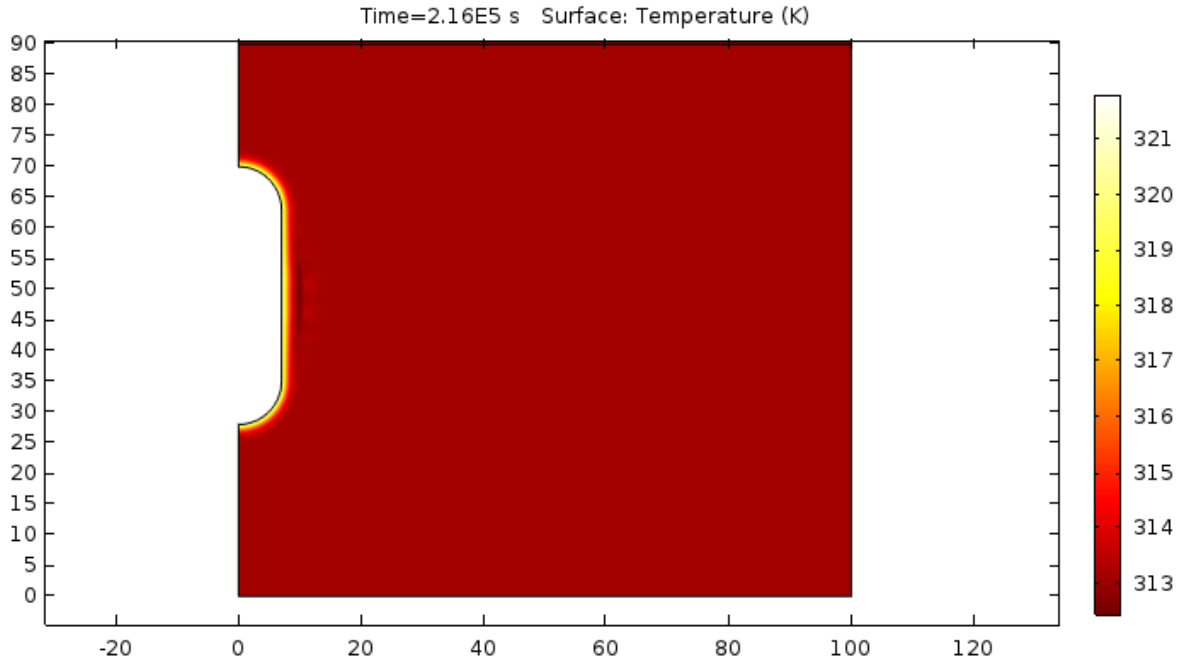
Time=2.16E5 s Surface: Temperature (K)
90
85
80
75
70
65
60
55
50
45
40
35
30
25
20
15
10
5
0
-20
0
20
40
60
80
100
120
321
320
319
318
317
316
315
314
313